Use of phage display technologies for target discovery, antibody generation, and antigen-antibody interaction studies to develop a *Listeria* spp. detection

Von der Fakultät für Lebenswissenschaften

der Technischen Universität Carolo-Wilhelmina zu Braunschweig

zur Erlangung des Grades eines

Doktors der Naturwissenschaften

(Dr. rer. nat.)

genehmigte

D i s s e r t a t i o n

von Gustavo Marçal Schmidt Garcia Moreira
aus Pelotas/RS / Brasilien

1. Referent: apl. Professor Dr. Michael Hust
2. Referent: Professor Dr. Stefan Dübel
eingereicht am: 20.03.2019
mündliche Prüfung (Disputation) am: 25.04.2019

Druckjahr 2019

Vorveröffentlichungen der Dissertation

Teilergebnisse aus dieser Arbeit wurden mit Genehmigung der Fakultät für Lebenswissenschaften, vertreten durch den Mentor der Arbeit, in folgenden Beiträgen vorab veröffentlicht:

Publikationen

Fühner, V., Heine, P.A., Zilkens, K., Meier, D., Roth, K.D.R., **Moreira, G.M.S.G.**, Hust, M. and Russo, G. Epitope Mapping via Phage Display from single gene libraries. Methods Molecular Biology 1904: 353-375 (2019).

Moreira, G.M.S.G., Fühner, V. and Hust, M. Epitope Mapping by Phage Display. Phage display, Ed: Lim, T.S. and Hust, M., Methods Molecular Biology 1701: 497-518 (2018).

Zantow, J., **Moreira, G.M.S.G.**, Dübel, S. and Hust, M. ORFeome Phage Display. Phage display, Ed: Lim, T.S. and Hust, M., Methods Molecular Biology 1701: 477-495 (2018).

Mendonça, M., **Moreira, G.M.**, Conceição, F.R., Hust, M., Mendonça, K.S., Moreira, A.N., França, R.C., Silva, W.P., Bhunia, A.K., Aleixo, J.A. Fructose 1,6-bisphosphate aldolase, a novel immunogenic surface protein on *Listeria* species. 11(8):e0160544 PLoS One (2016)

Tagungsbeiträge

Moreira, G.M. & Hust, M.: A vaccine pipeline: phage display for identification of vaccine candidates, and for the generation of human antibodies for diagnostic and therapy. (Vortrag) III Vaccines R&D, Washington D.C. (2017).

Moreira, G.M. & Hust, M.: Identification of biomarkers of zoonotic pathogens by ORFeome phage display. (Vortrag). National Symposium on Zoonoses Research, Berlin (2017).

Moreira, G.M. & Hust, M.: A vaccine pipeline: phage display for identification of vaccine candidates, and generation of human antibodies for diagnostic and therapy. (Vortrag) TB Congress, London (2016).

Posterbeiträge

Moreira, G.M. & Hust, M.: Identification of novel biomarkers and generation of antibodies for Listeria spp. detection by phage display. (Poster) Seminar for PhD scholars from Brazil, Bonn (2015).

Acknowledgements

To TU Braunschweig, the Biotechnology building, and their professors, for providing a good structure that makes possible to conduct research on high level.

To my mentor Prof. Dr. Michael Hust, for accepting me as a student and guide me sharing his knowledge, which was extremely important for my formation as a PhD.

To Prof. Dr. Stefan Dübel, which contributed with his experience and knowledge through every step of this work.

To the researchers from Brazil Prof. Dr. Fabricio Rochedo Conceição and Prof. Dr. Marcelo Mendonça, which contributed to this work with their scientific input and by providing important material for conducting the present research.

To the remaining researchers from Brazil, especially from the Biotechnology Institute from Universidade Federal de Pelotas, which were always supportive for scientific spreading and consolidating international cooperations.

To the technicians and assistants of the institute: Betina Sandner, Aldeheid Langner, Andrea Walzog, Doris Meier, Marlies Becker, and Wolfgang Grassl, for their competence on laboratory organization, material preparation and equipment installation, which were essential to conduct the present work. A special thanks to the technician Saskia Helmsing for helping with the generation of antibodies that were important for this thesis.

To the secretary Cornelia Oltmann, for her competence in dealing with the documents and the University's paper work.

To my PhD colleagues throughout my PhD: Viola Fühner, Esther Wenzel, Dr. Philip Kuhn, Giulio Russo, Phillip Heine, Kristian Roth, Nora Langreder, Maximilian Ruschig, Ana Flávia Laureano, Siti Ramli, Wieland Fahr, Kai Schneider and my labmate Fabian Oberle. A special thanks to Dr. Tobias Unkauf and Dr. Jonas Zantow, which were essential for my initial adaptation in Germany and were extremely important for the initial part of this work by contributing with their experience.

To all Master students and guest researchers that spent time in our institute, especially Janine Fichtner, and Carolina Georg Magalhães, which were supervised by me. A special thanks to Sarah Mara Stella Köllner, for the organization of events outside the laboratory, and for her effort during her Master thesis, which generated important information for the present work.

To my parents Félix Nedes Moreira (*in memoriam*) and Sirlei Schmidt Garcia, which supported me unconditionally on every moment of the PhD and were strong enough to let me go for a complete new experience far away from home. Love you!

To all my other family members, which were always receptive during my visits to Brazil and helped my parents during difficult moments in my absence.

To my friends from Brazil: Arthur, Bruno, Eduardo, Gabriel, Rafael, and Mohammad for always providing nice conversations and funny moments during my visits to Brazil. A special thanks to Arthur and his wife Jessica for visiting me during my PhD and traveling together in Europe.

To all my friends from the APM group, the dinosaurs, and remaining friends: Alan, Rafaela, Alice, André, Alex, Caroline, Clara, Jenifer, Matheus, Mateus, Igor, Alana, Francisco, Ana, Adriana, Alejandra, Alex, Fernando, Luisa, Fernanda, Bruno, Pablo, Renan, Charlotte, Daisy, Henrique, Daniel, Dieter, Diogo, Fábio, Frederico, Rômulo, Isabela, Juliana, Luisa, Luiza, Manuela, Maria, Murilo, Ramon, Sofia, Sachi, Sarah-Lena, Iara, Kévin, Omar, Marcel, Martyna, Felipe, Raphael, Rafael, Finn, Jessica, Leonardo, Ronaldo, Luis, Diego, João, Giuliana, Gabriella, Renê, Renato, Iago, Rodolfo, Stefânia, Gustavo, Yasmim and many more. Even if a name is not mentioned here, they were extremely important for making the life outside the laboratory much more fun and happy through the 4 years of the PhD. Thanks for the travels, parties, and funny moments. A special thanks to Kamila Yuyama and Thiago Pires for all the help and support during my PhD.

To CNPq and the Brazilian government, for providing my scholarship and funding the research.

Thank you all very much!

“If you can't explain it simply, you don't understand it well enough.”

Albert Einstein

Abstract

The genus *Listeria* comprises bacteria that are ubiquitous and commonly present in food production facilities. Even though *Listeria* monocytogenes is the only *Listeria* species with relevance in causing listeriosis, many new *Listeria* species have been described in the recent years increasing the importance of studies over the genus. In this study, phage display technologies were employed to discover, identify, and characterize novel biomarkers and monoclonal antibodies. In brief, antibody phage display was applied to select antibodies against subcellular fractions of *L. monocytogenes*. Then, the target of the antibodies was identified by ORFeome phage display and confirmed with immunomagnetic separation-mass spectrometry (IMS-MS). Dihydrolipoamide acetyltransferase (pyruvate dehydrogenase complex - enzyme 2, PDC-E2) was identified as the target of the initial antibodies against *Listeria* spp.. Immunoblot and microscopy showed that this protein is present on the bacterial cell surface and is detectable in fluorescent microscopy. In addition, recombinant antibodies were generated against already known targets (internalins A and B, and fructose bisphosphate aldolase). In total, a set of five scFv-Fc against *L. monocytogenes* and 22 against *Listeria* spp. were tested in indirect ELISA against 17 *Listeria* and 15 non-*Listeria* species. All the five scFv-Fc against the pathogenic species showed 100 % sensitivity (CI 88.78-100.0 %) and specificity (CI 88.78-100.0 %), while the two anti-fructose bisphosphate aldolase showed non-optimal diagnostic performance. On the other hand, two antibodies against PDC-E2 (anti-*Listeria* spp.) showed 100 % sensitivity (CI 82.35-100.0 %) and specificity (CI 78.20-100.0 %), confirming PDC-E2 as a suitable detection target for *Listeria* spp.. Furthermore, the binding regions of two hibridoma-derived antibodies and the scFv-Fc against PDC-E2 were defined via single gene phage display, showing that this technique can provide information over the recognized region of a target in a considerable resolution. In addition, it revealed that the two best anti-PDC-E2 antibodies are the only ones to bind a synthetic region composed of two parts of PDC-E2. Hence, through a particular combination of phage display techniques, the biomarker PDC-E2 and two corresponding scFv-Fc against it, as well as scFv-Fc against internalins A and B, are hereby reported as novel promising tools for *Listeria* spp. detection.

Keywords: phage display, monoclonal antibodies, *Listeria* spp., immunodetection, pyruvate dehydrogenase complex

Figures

Figure 1. Representation of antibody structures occurring in higher mammals and humans. 15

Figure 2. Representation of the different structural parts of an antibody. 16

Figure 3. Comparison of non-natural antibody structures to that of IgG. 17

Figure 4. Use of the phagemid system for phage display. 19

Figure 5. Steps of the panning procedure and screening of relevant molecules. 21

Figure 6. Panning formats using antibody libraries. 23

Figure 7. Panning formats using ORFeome libraries. 24

Figure 8. Panning formats using single gene libraries. 26

Figure 9. Use of ORFeome or single gene libraries for protein-protein interaction studies. 28

Figure 10. Process of cell invasion of *L. monocytogenes* and the main proteins involved. 32

Figure 11. Scheme of detection strategies for *Listeria* spp. in food. 35

Figure 12. ELISA of the scFv-Fc antibodies generated against *Listeria* protein fractions. 54

Figure 14. Identification of the target via MS and ORFeome phage display. 58

Figure 15. Fluorescence microscopy of GSM29-D3 (anti InlA) and GSM133-A4 (anti PDC-E2) over alive *L. monocytogenes* 4b DSM 15675. 59

Figure 16. Immunoblot of the scFv-Fc antibodies generated against the purified recombinant PDC-E2. 61

Figure 17. ELISA of the scFv-Fc antibodies generated against the purified recombinant PDC-E2. 63

Figure 18. Reaction profile of the 20 antibodies targeting PDC-E2 in indirect ELISA. 66

Figure 19. Immunoblot and initial indirect ELISA with anti-InlA and anti-InlB scFv-Fc. 69

Figure 20. ELISA of the scFv-Fc antibodies against FBA. 70

Figure 21. Reaction profile of four scFv-Fc against InlA, one against InlB, and two against FBA in indirect ELISA. 71

Figure 22. Summary of the workflow with phage display technologies used in this work compared to conventional techniques. 75

Figure 23. Comparison of 3F8 MSR size between peptide membrane, ORFeome, and single gene phage display. 77

Figure 24. Signal-to-noise ratio of the 20 antibodies targeting PDC-E2 plotted for each strain. 80

Figure 25. Phylogenetic three of the *Listeria* spp. used in indirect ELISA based on PDC-E2 protein sequence. 81

Tables

Table 1. List of the *Listeria* species used for indirect ELISA. 49

Table 2. List of the non-*Listeria* species used for indirect ELISA. 50

Table 3. GenBank codes, identity and similarity of the PDC-E2 sequences from the organisms used in indirect ELISA.....52

Table 4. GenBank codes, identity and similarity of the PDC-E2 sequences from the non-*Listeria* organisms used in indirect ELISA. 53

Table 5. Summary of the hits found by mass spectrometry or ORFeome phage display. 57

Table 6. Diagnostic performance of all the scFv-Fc targeting PDC-E2. 64

Table 7. Epitope mapping results of the anti-PDC-E2 antibodies used in indirect ELISA. 67

Table 8. Diagnostic performance of the scFv-Fc targeting InlA, InlB, and FBA.....70

Table 9. Comparison of the MSR length between ORFeome phage display and single gene phage display. 72

Abbreviations

2xYT – two times yeast extract, tryptone medium
2xYT-A – two times yeast extract, tryptone medium supplemented with ampicilin
2xYT-AK – two times yeast extract, tryptone medium supplemented with ampicilin and kanamycin
2xYT-GA – two times yeast extract, tryptone medium supplemented with glucose ampicilin
ActA – actin polymerization protein
ATCC – American type culture collection
AUC – area under curve
BHI – brain heart infusion
BLAST – basic local alignment search tool
BSA – bovine serum albumin
cDNA – complementary deoxyribonucleic acid
CFU – colony formation unit
DNA – deoxyribonucleic acid
EC_{50} – half-maximal effective concentration
ELISA – enzyme-linked immunosorbet assay
FBA – 1,6-fructose bisphosphate aldolase
HAL – human antibody library
HEK – human embryonic kidney
HRP – horseradish peroxidase
Ig – immunoglobulin
IMS – immunomagnetic separation
InlA – internalin A
InlB – internalin B
IPTG – isopropyl β-D-1-thiogalactopyranoside
LB – Luria-Bertani broth
LD – lipoyl domain
LOD – limit of detection
LPS – lipopolysaccharide
MOI – moiety of infection

MPBS-T – milk with phosphate buffered saline

MRS – Man, Rogosa and Sharpe broth

MS – mass spectrometry

MSR – minimal sequence of recognition

NCIB – national collection of industrial bacteria of Britain

NF – not found

NM – not mapped

NT – not tested

OD_{600} – optical density at 600 nanometers

PAGE – polyacrylamide gel electrophoresis

PBS – phosphate buffered saline

PBS-T – phosphate buffered saline with Tween 20

PCR – polymerase chain reaction

PED – pathogen enrichment device

PDC-E1α – pyruvate dehydrogenase complex, enzyme 1 subunit alpha

PDC-E1β – pyruvate dehydrogenase complex, enzyme 1 subunit beta

PDC-E2 – pyruvate dehydrogenase complex, enzyme 2

PDC-E3 – pyruvate dehydrogenase complex, enzyme 3

PDC-E3BP – binding protein

PEG – polyethylene glycol

PVDF – polyvinylidenfluorid

ROC – receiver operating characteristic

RPA – recombinase polymerase amplification

RPM – rotations per minute

RT – room temperature

RTE – ready-to-eat

scFv – single chain fragment variable

scFv-Fc – single chain fragment variable fused to fragment crystallizable

SDS – sodium dodecyl sulfate

SMART – simple modular architecture research tool

TMB – 3,3′,5,5′-Tetramethylbenzidine

Table of contents

1 INTRODUCTION 14

1.1 Monoclonal antibodies and phage display 14

1.1.1 Antibody structure and formats 14

1.1.2 Kinds of phage display and panning procedures 18

1.2 *Listeria* spp. biology and its importance in food industry 29

1.3 Pathogenic factors of *Listeria monocytogenes* 30

1.4 Targets for pathogenic and non-pathogenic *Listeria* detection 32

1.4.1 Pyruvate dehydrogenase complex (PDC) 33

1.5 Methods for *Listeria* detection 34

2 HYPOTHESIS, AIM, AND OBJECTIVES 37

2.1 Hypothesis 37

2.2 Aim 37

2.3 Objetives 37

3 MATERIAL AND METHODS 38

3.1 Bacteria cultivation and *Listeria* protein fractionation 38

3.2 Expression in *E. coli*, and purification of the targets InlA, InlB, and FBA 39

3.3 Antibody panning over purified InlA, InlB, and FBA and *Listeria* protein fractions 39

3.4 Cloning and production of recombinant antibodies 41

3.5 Immunoblot and ELISA of scFv-Fc generated against recombinant InlA, InlB and FBA 42

3.6 Immunoblot for target location, immunomagnetic separation, and mass spectrometry for target identification 43

3.7 ORFeome phage display for target identification 43

3.8 Immunofluorescence and wide field fluorescent microscopy of *Listeria* cells 46

3.9 Cloning, expression in *E. coli*, and purification of the recombinant target PDC-E2 46
3.10 Antibody panning over recombinant PDC-E2 47
3.11 Indirect ELISA for *Listeria* spp. detection 48
3.12 Single gene phage display for identifying the binding region of hibridoma-derived antibodies against InlA and FBA, and scFv-Fc against PDC-E2 50
3.13 Sequence analysis of PDC-E2 and FBA 51
4 RESULTS 54
4.1 Antibody panning over *Listeria* protein fractions provides useful binders for detection 54
4.2 ORFeome phage display provides similar results to those from mass spectrometry regarding target identification 55
4.3 PDC-E2 target is detectable by fluorescent microscopy, giving more evidence for its location on bacterial cell surface 59
4.4 Antibody panning over purified recombinant PDC-E2 increases the number of generated binders 60
4.5 PDC-E2 target allows the detection of every *Listeria* spp. via indirect ELISA 63
4.6 Most of the generated antibodies against PDC-E2 recognize the lipoyl domains (LD) 66
4.7 scFv-Fc against InlA and InB allow detecting pathogenic *Listeria*, while those against FBA recognize most *Listeria* spp. with reduced diagnostic performance 68
4.8 Single gene phage display results in shorter fragments than ORFeome phage display 72
5 DISCUSSION 73
6 CONCLUSION AND OUTLOOK 84
7 REFERENCES 85
8 CURRICULUM VITAE 98

1 INTRODUCTION

1.1 Monoclonal antibodies and phage display

Currently, mAbs are the most valuable biological molecule, representing the biggest market. Because of that, most of the phage display works are focused on generating antibodies for basic research, diagnostics, and, more importantly, therapeutic applications (Schirrmann et al., 2011; Nixon et al., 2014; Frenzel et al., 2016; Kuhn et al., 2016; Strohl, 2018). Some variations of the technology, such as the ORFeome phage display, can be employed for the discovery of biomarkers, which can further be used for the development of vaccines and diagnostics (Zantow et al., 2016; Zantow et al., 2018). While other variations, like the single gene phage display, can be used to finer characterize epitopes of antibodies (Moreira et al., 2018; Fühner et al., 2019). Considering this, phage display shows to be a flexible technology that allow obtaining both antibodies and biomarkers for product development, as well as having further information regarding their recognition profile.

1.1.1 Antibody structure and formats

In nature, several antibody structures exist, showing different functions in a single organism, or having homologous function but distinct formats between different species. In higher mammals, such as humans, antibodies can be produced as IgA, IgD, IgE, IgG, and IgM (Figure 1). Each of these structures have specific functions in the body, i.e. IgA is mostly present in mucosal tissues, IgD and IgM are the ones firstly produced from B-cells in an immune response, IgE is predominantly involved in allergic responses, and IgG is the most abundant antibody in circulation, responsible for the most specific immune responses (Murphy et al., 2007). Due to its specific recognitions and broad range of functions in the immune response, the IgG is the most studied and applied antibody structure in the immunology field (Chiu & Gilliland, 2016; Elgundi et al., 2017). This way, most of the molecules developed for treatment, research, or other biological applications use this structure or a similar one that keeps its functions. The other antibody formats are also used, but in a much lesser extent.

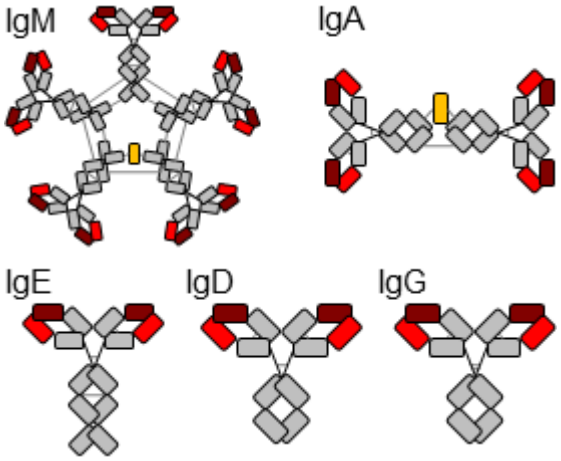

Figure 1. Representation of antibody structures occurring in higher mammals and humans. The binding region of the antibodies is shown in shades of red. The IgM structure (top left panel) is a pentameric protein in which the monomers are connected with disulfide bonds and a J-chain (junction chain, yellow). The IgA (top right panel) is a dimeric antibody also connected with H-bonds and a J-chain. Additionally, this structure contains a secretory protein (not shown) for secretion in mucosal tissues. The IgE structure (bottom left panel) is monomeric and has a longer heavy chain, which is comparable to a monomer of IgM. The IgG and IgD structures (bottom center and right panel) are monomeric, comparable to a single unit of IgA, and differ slightly on their disulfide bond pattern in the constant parts. Among these structures, the IgG is the most common representation of antibodies, especially due to its immunological importance.

Although the antibodies in nature, such as the IgG, show to be the optimal molecules for either therapy or other fields, it is important to consider that they are complex and, thus, may not be applicable in some techniques. The IgG structure is comprised by four chains (two heavy and two light chains), which form a tetrameric structure (Figure 2). Within this structure, there is also the formation of disulfide bonds that increase the stability of the molecule, but also its complexity. Nevertheless, by knowing the function of each region of the antibodies, it is possible to elaborate strategies for reducing its complexity (Frenzel et al., 2016). Its fragment crystallizable (Fc), which is responsible to interact with receptor in effector cells of the immune system, determines the function of each antibody depending on the class of Fc. While the fragment antigen-binding (Fab) is the one promoting the interaction of the antibody with an antigen. In the Fab there are regions with high genetic variability, one in the heavy chain and one in the light chain, that compose the fragment variable (Fv). Within the Fv, the interaction with the antigen occurs though specific amino acid sequences

of the antibody, called complementarity-determining regions (CDR), which are loops that structurally form a region of the antibody called the paratope. The paratope comprises six different loops (three from each heavy and light chains), and are the structural counterpart of the epitope, which in turn is the recognized structure region of an antigen (Schroeder et al., 2010).

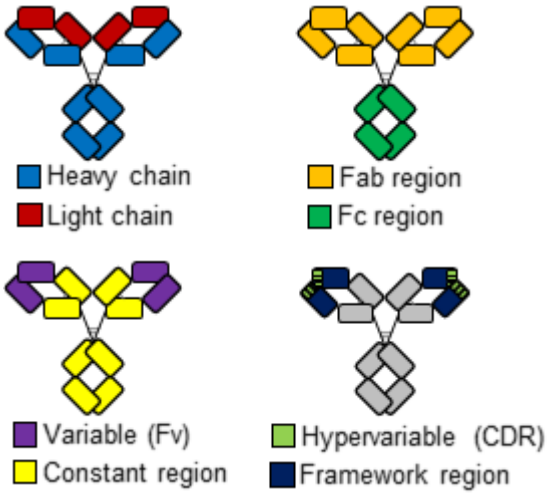

Figure 2. Representation of the different structural parts of an antibody. The antibody structure can be understood regarding its protein assembly (top left panel), which involves two heavy chains (blue) and two light chains (red). It also can be defined regarding the function of the different parts (top right panel), which can be for antigen binding (Fab, golden) or effective responses (Fc, green). The antibody can also be understood regarding its genetic variability (bottom left panel), with variable (Fv, purple) and constant (yellow) regions. Within the Fv (bottom right panel), it is also possible to define hypervariable regions (CDR, light green) and less variable ones, called framework regions (dark blue).

Considering that the CDR promote recognition of a target, it is possible to define a minimal structure of the antibody needed for its binding. Such structure comprises the Fv of the heavy chain (V_H) and light chain (V_L). This way, by connecting both V_H and V_L in the same molecule, it is possible to recreate the minimal structure of a native antibody in a functional manner (Figure 3). The antibody containing connected V_H and V_L is called single chain fragment variable (scFv) and is small enough to be produced in less complex organisms, such as in prokaryotic cells (Bradbury et al., 2011). This way, scFv is nowadays the molecule of choice for most of the display methods that involve selection of antibodies in library scale, such as phage display. Nevertheless, smaller formats can also be studied, such as the single-domain antibody (sdAb). These antibodies comprise only the V_H as binding molecule and were firstly studied in camelid

antibodies (V_HH), which do not possess the V_L counterpart in their structure (Arbabi-Ghahroudi, 2017). In fact, it is known that the major part of the paratope of antibodies relies on the V_H for binding, while the V_L usually has smaller contribution or only stabilizing function (D'Angelo et al., 2018).

Even though it is interesting to have functional and small versions of antibodies, it is important to be able to alter their structure and control their action according to the need. Considering this, a vast amount of antibody formats that are not present in nature have been developed, giving the opportunity to simply transfer the V_H and V_L sequences to a pre-defined scaffold. When considering *in vitro* methods that use recombinant antibodies, it is possible to identify a tendency in which antibodies are selected in smaller formats, and then used in this way or transferred to other formats that suit their application (Jostock et al., 2004; Frenzel et al., 2017). One of the simplest formats that add function to selected scFv, for example, is the scFv-Fc, which comprises the addition of an Fc part to the molecule allowing it to execute its effector functions (Figure 3). Another very common format is the IgG itself, which is used to reconvert the initially selected antibodies to their "similar-to-original" structure. Nevertheless, considering that scFv-Fc and IgG are more complex, they must be produce in other systems, mainly mammalian or other eukaryotic cells (Jäger et al., 2013; Lalonde & Durocher, 2017). In this document, scFv-Fc and IgG will gain more attention, since the list of possible formats, mainly bispecific, is extremely big and is still growing (Brinkmann & Kontermann, 2017).

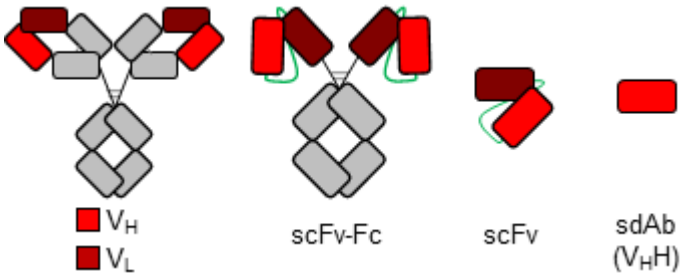

Figure 3. Comparison of non-natural antibody structures to that of IgG. From left to right, the structures of IgG, scFv-Fc, scFv, and sdAb represent the possibility of reducing the structure complexity of antibodies while keeping their binding function. For this, it is noticeable that the VH (red) and VL (burgundy) are the important parts, mainly the former. In case the application of the antibody requires an effector function, the Fc part is usually included or kept.

1.1.2 Kinds of phage display and panning procedures

In the field of proteomics, different technologies have arose to study protein molecules, such as antibodies or antigens, in library scale (Galán et al., 2016). These display methods consist on attaching the genetic information (genotype) to its encoded protein product (phenotype) that, in turn, is displayed on a certain part of the system. In this case, such protein products can be displayed on ribosomes, bacteria, yeasts, mammalian cells, phage, or other biological and chemical components. The main difference between these systems is regarding the amount of different molecules that can be included in the libraries and the capacity of performing posttranslational modifications in the displayed molecules. Among these options, phage display is nowadays the most applied method not only to select antibodies against interesting targets, but also to identify antigens recognized by antibodies (Kügler et al., 2013; Nixon et al., 2014). This way, phage display can be applied for antibody generation, allowing the development of therapeutic molecules and diagnostic tests, as well as for the discovery of biomarkers, which can serve as diagnostic or vaccine targets.

When using the phage display system, different molecules, such as antibodies, antigen fragments, or peptides, can constitute the library. Currently, the filamentous phage M13 system is the most used, since this is a non-lytic phage that can be easily handled though the infection of *E. coli*. In the structure of M13 phage, there are many structural proteins, from which the minor protein III (pIII) can be highlighted (Ledsgaard et al., 2018). This protein is located in one of the extremes of the phage and presented in a fixed amount, limited to five copies per phage. Due to this, pIII is nowadays the molecule of choice to fuse proteins to be displayed on the phage surface (Paschke & Höhne, 2005). The current method for displaying proteins on a phage employs a DNA molecule called phagemid (Figure 4). This molecule is a circular extrachromosomal genetic material similar to a plasmid that contains a packaging signal for M13 phage, a selective marker gene for *E. coli*, and restriction sites that allows the fusion of DNA fragments in-frame with the coding gene for pIII (Breitling et al., 1991). This way, when a phagemid is inserted into *E. coli*, the fusion molecule is produced and used to build the phage particle, resulting in an exposed product of the inserted gene. Other feature of the phagemid is that the molecules produced have the pelB peptide, which directs the protein to the periplasmic space. In case of producing antibodies, this fact is very important considering that this environment is more prone for the formation of disulfide

bonds needed to stabilize the antibody (Skerra & Pluckthun, 1988). A *lac* promoter usually regulates the gene cassette. In addition, the phagemid also contains an Amber stop codon between the inserted gene fragment and the pIII gene. This stop codon can be recognized as a coding codon for Glutamine (Gln, Q) when using Amber-suppressor *E. coli* strains (Krebber et al., 1996). This way, the phagemid allow the production of both the pIII fusion protein and the cloned fragment alone, increasing the possible assays with the same phagemid system.

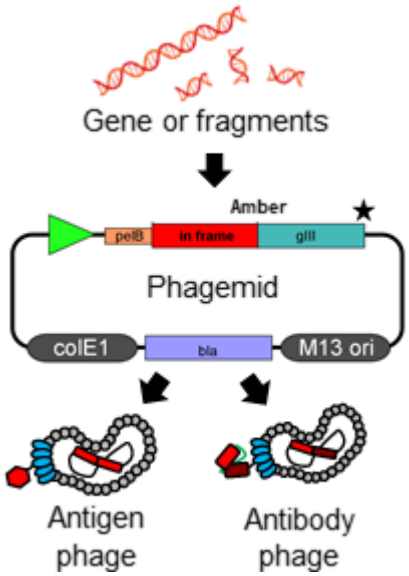

Figure 4. Use of the phagemid system for phage display. Initially, a source of genes or gene fragments is necessary (top panel). This genetic material is then inserted in the phagemid (middle panel) containing a proper cassette, including a promoter (green), a pelB periplasm signal, a cloning site (red), an Amber stop codon, and gIII. If the genetic material is inserted in frame with gIII, the phagemid is able to provide a functional phage displaying the encoded product of it (bottom), e.g. part of an antigen, or a scFv antibody. Other features of the phagemid are an origin of replication in *E. coli* (colE1), a selection marker gene (bla), and a phage packaging signal (M13 ori).

When a phagemid is inserted into *E. coli*, however, it is still not possible to produce infective phage particles. For this, it is necessary to use a so-called helperphage, which is able to infect *E. coli* delivering the other structural genes needed to build a functional phage, including the native pIII gene (Soltes et al., 2007). Nevertheless, the use of this phage also leads to the generation of phage that do not contain the fusion protein target::pIII, once the native pIII has natural preference when building phage. To overcome this problem, a very interesting advance for the phage

display technology was done by using a helperphage with the pIII gene knocked out, the so-called Hyperphage (Rondot et al., 2001). Among the advantages of using Hyperphage is the major production of phage containing only the target::pIII fusion protein, which reduces the amount of “junk phage” (phage displaying wrongly produced fusion proteins, or no fusion protein at all) in the library. Furthermore, since the only source of pIII is the fusion protein, each phage usually presents more than one molecule of the target on its surface (up to five), giving an avidity effect for the components of the library that increases the chance of selecting relevant molecules.

After inserting many different DNA fragments in-frame with pIII and building functional phage displaying the product of the information carried in their phagemids, a phage library is obtained. Considering that many of the phage in the library may not contain relevant molecules for a certain study, an approach for the selection of the interesting ones must be performed. This method is called panning, referring to “gold panning”, which is a procedure of collecting gold using a pan. In this approach, a target molecule is incubated together with the library to promote the interaction between these two parts (Frenzel et al., 2017). This step can be done by immobilizing the target molecule on a surface, e.g. an ELISA plate or magnetic beads, and adding the library afterwards (Figure 5). Then, the non-bound phage is washed away, and the ones that interact with the target are eluted, usually with proteases or chemical changes, such as pH. This eluted phage is used to infect *E. coli*, which is further co-infected with a helperphage, allowing the enrichment of the selected phage. The enriched phage are then used for further rounds of selection through the same procedure, usually one or two more, resulting in molecules with high specificity to the target. Then, the selected phage are screened to confirm the interaction with the target through an immunoassay, usually ELISA. Finally, the phagemids of the clones showing positive reaction in the screening are sequenced, allowing the identification of relevant sequences (Moreira et al., 2018; Zantow et al., 2018; Russo et al., 2018).

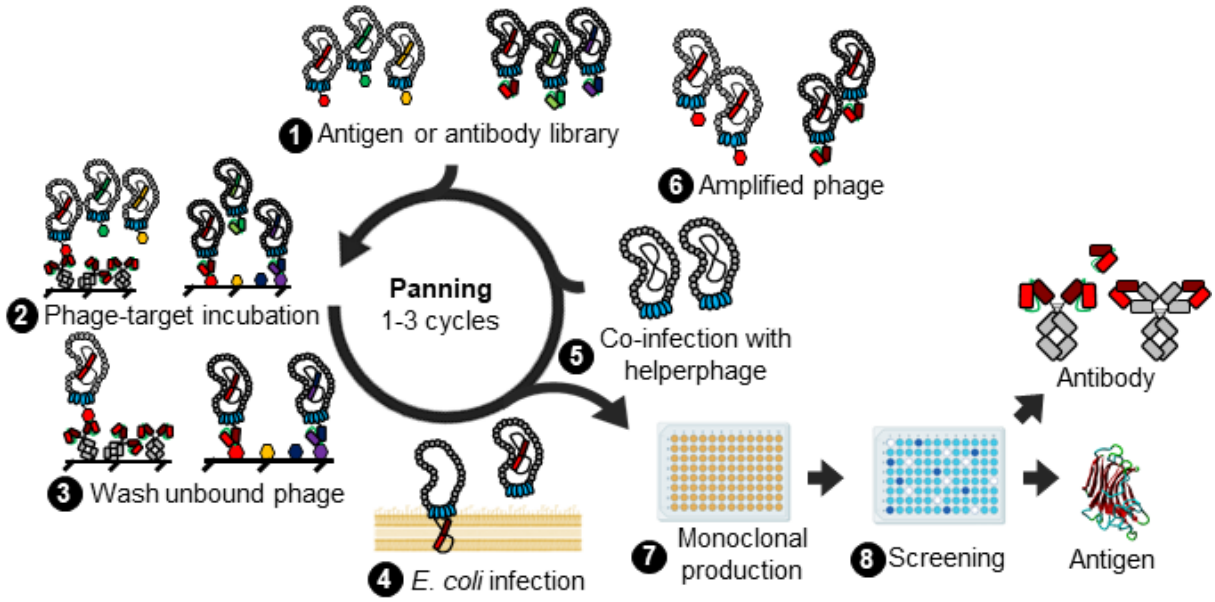

Figure 5. Steps of the panning procedure and screening of relevant molecules. Once the phage library are built containing either antigen or antibody sequences (1), they are further incubated with their targets (2), which can be either an antibody or antigen. The unbound phage from the library is washed away (3), while the bound ones are eluted and used to infect *E. coli* (4). The same cells are co-infected with helperphage (5) and grown for phage amplification of the selected binders (6). After the appropriate number of panning rounds, which can be 1 to 3, the *E. coli* cells infected with the eluted phage are picked individually, grown for the production of the selected molecules (7), and used in screening procedures such as ELISA (8). After sequencing of the positive clones in the screening, it is possible to identify the antigen, or parts of it, as well as antibody sequences for further applications.

When using the phage display technology, the library construction and panning procedures must be performed regardless of the molecules used as target or to build the library. Nevertheless, when using either antibodies or antigens in the library imply some relevant differences on the way the library is build and, more importantly, on the way the panning is performed. On the next paragraphs, the most common kinds of phage display approaches will be addressed.

Antibody phage display

As mentioned previously, the scFv is a structure that contains the binding sequences of antibodies and are simple enough to be produced in prokaryotic systems. This way, this molecule is the mostly applied in phage display, which uses the bacterium *E. coli* as intermediate for the library construction and panning

procedure. To use antibodies in phage display, multiple DNA fragments coding for scFv are inserted in the phagemid and then used to build a library (McCafferty et al., 1990; Kügler et al., 2018). Considering this, it is possible to distinguish different kinds of antibody library regarding the source of the antibody genes.

A very useful kind of antibody phage library can be built by using antibody genes from immature B-cells, which did not yet went through mutations that increase its specificity against a certain target (Vaughan et al., 1996; Kügler et al., 2015). In this library, the V_H genes originated from IgM or IgD from circulating immature B-cells are used together with V_L genes to build a “naïve antibody library”. This kind of library is the most recommended when many different antigens are being studied, since the antibodies contained in it represent the repertoire of immature B-cells and, thus, can bind to virtually every antigen.

Another kind of antibody library is the so called “immune antibody library”. In this case, the genetic information of the V_H is acquired from mature B-cell, i.e. those that were already selected for specificity against a certain target. This way, this kind of library contain sequences mostly derived from IgG and often results in antibodies with higher affinity than those from naïve libraries (Soon Lim & Khim Chan, 2017). The use of this library is indicated when it is possible to induce immune responses against a defined target, allowing later on to acquire the genetic information of the generated antibodies (Kumar et al., 2019).

Differently from the naïve and immune libraries, the “semi-synthetic or synthetic antibody library” does not use sequence directly obtained from B-cells. Instead, the sequences of the antibodies are randomly generated by changing the sequences contained in the CDR, mainly in the CDR3 of the V_H, via PCR, or by shuffling the framework regions (Ponsel et al., 2011). These libraries are indicated when a target is low immunogenic, such as cancer antigens.

When using any of these antibody libraries, the panning procedure is performed in very similar ways. In this case, the antigen is immobilized and the library is used in solution. Regarding the antigens used, they can be of two kinds: complex mixtures, or pure. In the first case (Figure 6A), the selected antibodies can serve as tool to detect new or relevant targets that were not initially separated from a mixture (Paoli et al., 2004; Kuhn et al., 2017). On the other hand, using purified targets (Figure 6B) simply implies a procedure to acquire antibodies to be used as tools for research, detection,

or treatment (Kuhn et al., 2016). Depending on the protocol used for the removal of the unbound phage, binders with better affinity can be selected. Moreover, considering that the library usually contains several millions of different binders, an average of three panning rounds are necessary to ensure the selection of specific antibodies. More rounds may be added depending on the need or application (Moreland et al., 2012). Once the phage are selected, the screening is also conducted with the antibodies in solution, what is possible due to the pelB and Amber stop codon functions.

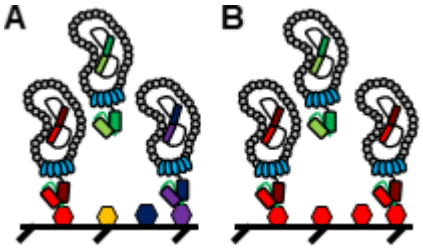

Figure 6. Panning formats using antibody libraries. (**A**) Use of antibody libraries against a complex antigen mixture. Besides allowing the generation of antibodies, this application also allows the discovery of targets that were not previously separated from a mixture. (**B**) Use of antibody libraries against a pure antigen. This represents the most common application of antibody panning, resulting in a panel of different antibodies to be used in different applications.

This kind of phage display can be compared to the classical method of obtaining antibodies, which uses the hibridoma technology. Although many advances have been done to improve hibridoma technology, the research over recombinant antibodies turn the use of phage display much bigger (Debs et al., 2012; Basu et al., 2019). This is because phage display can provide a large number of useful molecules in a short time and, besides this, can avoid the use of animals or biological material from patients. For this reason, antibody phage display is currently the method that mostly provides molecules for clinical applications (Frenzel et al., 2016).

ORFeome phage display

Besides performing selection of antibodies, phage display can be also applied for the selection and identification of antigens. In fact, the initial descriptions of this technique involved the display of antigen peptides that would be further incubated with antibodies (Smith, 1985). In this context, similarly to the case of antibodies, antigen libraries can have different DNA sources. When building libraries of prokaryote

organisms, the genomic DNA can be directly used once they have low amount of non-coding DNA, and do not contain introns (Connor et al., 2016). For eukaryotes, usually the mRNA is used, since it represents a source of genetic material without introns. Nevertheless, the mRNA do not represent the totality of antigens that can be produced by the organism, but the antigens that are specific to the tissue or group of cells employed in the experiment (Becker et al., 2015). In both cases, the genetic material used for the library comprise fragmented genes and, thus, represent a repertoire of ORF from a genome, leading to the name of the technique (Hust et al., 2006).

Although similar to the antibody phage display, the panning procedure with ORFeome phage display has its particularities. One is that the antibodies used as counterpart of the antigens in the library are initially immobilized on a surface. When using polyclonal antibodies (Figure 7A), it is worth to consider that antibodies that are low represented may not be able to be immobilized or provide detectable binders in the screening (Gazarian et al., 2013; Zantow et al., 2016). When using monoclonal antibodies (Figure 7B), however, this effect may not happen (Chikaev et al., 2015; G. Moreira et al., 2018). Regardless of the kind of antibodies used, it is often recommended to perform several panning rounds, similar to what happens for antibody phage display, in order to enrich antigen phage from the initial library. Another particularity is that it is recommended to invert the system during the screening, using the coated antigen (usually in the phage form) and the antibodies in solution in a way to avoid binding problems due to the immobilization of antibodies. This phage display technology is often used for the discovery of immunogenic antigens that can be used as diagnostic tool or vaccine target. When using monoclonal antibodies, it can also be used for target identification, since it gives information about the target of the studied antibody (Kügler et al., 2013; Aghebati-Maleki et al., 2016).

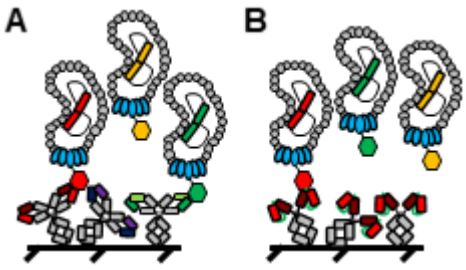

Figure 7. Panning formats using ORFeome libraries. (**A**) Use of ORFeome libraries against polyclonal antibodies. This procedure permits the identification of interesting targets that interact with antibodies from animal or human samples. (**B**) Use of ORFeome libraries against a monoclonal antibody. The

output of this approach gives information about the target of the studied antibody, which is important when the target is previously unknown.

Another technique that can provide results similar to the ORFeome phage display is the two-dimensional polyacrylamide gel electrophoresis followed by mass spectrometry (2D-PAGE/MS) (DelVecchio et al., 2006; Meens et al., 2006). In this technique, a protein extract from a target organism is used to perform a 2D-PAGE. Then, a polyclonal antibody is used to detect immunogenic proteins that are further identified in MS and may be relevant for the application of interest. Nevertheless, the main limitation of this method is regarding the source of protein, which usually relies on *in vitro* cultivation that rarely reproduces the protein profile in the environment. Other techniques for the same purpose can be the peptide/protein array (Schirwitz et al., 2012) or lithic phage display (Lodes et al., 2004; Beghetto et al., 2006). However, the former shows to be a very expensive and laborious method, since it involves the production of several thousands of proteins individually. While the latter shows several practical disadvantages due to the use of lithic phage and has been applied mostly for cancer studies (Minenkova et al., 2003; Chen et al., 2005).

Single gene phage display

Unlike the ORFeome phage display, the single gene phage display is often used when the studied antigen is already known (Cariccio et al., 2016). For example, when a panel of antibodies against one target needs to be analyzed regarding their binding region on the antigen, a single gene library alone can be used to study all the antibodies. It is expected that this procedure result in a higher resolution of the binding site when compared to ORFeome phage display, since the library size is often more than enough to cover a single gene and, thus, results in more different fragments of the same target to be analyzed. Because of that, this approach is also very useful for defining epitopes of antibodies. When monoclonal antibodies are used (Figure 8A), this approach involve a pair of antibody-antigen that are very likely to result in positive hits and, thus, only one panning round is usually needed (Fack et al., 1997; Fühner et al., 2019). On the other hand, when polyclonal antibodies are used (Figure 8B), it may be necessary to perform more rounds in order to confirm the selected clones or enrich

those who are present in lower amounts after selection (Domina et al., 2014). In this latter case, the results might provide regions of the studied antigens that are predominant on generating antibodies.

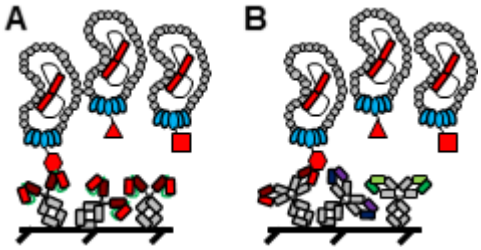

Figure 8. Panning formats using single gene libraries. (**A**) Use of single gene libraries against a monoclonal antibody. The results of this technique allow defining the specific region of an antigen that is bound by an antibody. If the resolution of the output is high enough, it is possible to define the epitope of a panel of antibodies against the same target. (**B**) Use of single gene libraries against polyclonal antibodies. This approach gives information of parts of the antigen that are more prone to stimulate the generation of antibodies by the immune system.

Techniques other than phage display can also give results similar to that of the single gene panning approach. Until the present, X-ray co-crystallography is considered the optimal technique for defining epitopes, since it can give results with atomic resolution (Augustin et al., 2015; Malito et al., 2015). However, not every research facility is able to perform such experiments. Alternatively, methods using MS can be used, although they also employ special equipment. The most common procedures using MS are called “excision” and “extraction” (Opuni et al., 2018). In the former, antigen and antibody interact and are incubated for the digestion of the antigen. Then, the non-interacting parts of the antigen are washed, while the interacting ones are eluted and analyzed in MS. The latter is similar, but involves the incubation of the already digested antigen with the antibody and further analysis of the bound peptides. Approaches using H/De exchange can also be performed by MS with high resolution (Zhang et al., 2014). Other common methods for epitope mapping are site-directed mutagenesis, or peptide arrays. Site directed mutagenesis involve the replacement of amino acids that are considered important for antibody recognition (Liu et al., 2018). This way, this technique requires previous knowledge of the interaction profile and is considered laborious since every antigen mutant has to be produced individually, although advances have been made to turn this option more suitable for high-

throughput studies (Davidson & Doranz, 2014). In its turn, the peptide array method is a good option for defining the epitope with single-amino acid resolution (Vernet et al., 2015). Nevertheless, besides being an expensive method, since every peptide has to be synthetically produced and immobilized on membranes or chips, it may be limited to certain kinds of epitopes. To overcome this drawback, some variations of the method help on increasing the types of epitopes that can be mapped (Amartely et al., 2014).

Considering basic immunology, the epitopes bound by antibodies can be of two kinds: “linear” (also called “continuous” or “consecutive”), or conformational (also called “discontinuous” or “assembled”). The former is defined as amino acids that are close to each other in the sequence and, consequently, in the structure of the antigen. On the other hand, conformational epitopes are defined by sequences that are not close to each other, but are structurally nearby (Hager-Braun & Tomer, 2005). Works also describe information about epitope size, which is often 4-20 amino acids and around 30 Å in diameter, which results in approximately 700 $Å^2$ contact surface area (Sun et al., 2011; Gupta et al., 2013; Rahman et al., 2016). So far, this classification of epitopes can explain most of the cases observed, but they appear to be limited to the analysis of protein loops only, which are 3D structures that resemble the primary structure of proteins. When α-helix or β-sheets are present in the epitope, it becomes more complicated to apply these definitions. Considering this, some works have proposed a third kind of epitope, called “hybrid” (Opuni et al., 2018). This type involves amino acids that are close in sequence, but depend on a secondary structure change to be an epitope; thus, they are understood as a mix between “consecutive” and “assembled” epitopes. Nevertheless, since antigen structures present much more variability than antibodies, it is still complicated to define all possibilities of epitope forms. In this sense, research over paratopes and epitopes, especially those involving sequence and structure data, is of major importance to increase the knowledge over this field.

In a general view, the procedure with biggest resolution for epitope mapping is X-ray co-crystallography. However, since this method require special equipment that is often not available, other techniques may be used according to what is available to the researcher. In many cases, these methods are used in combination either as a way to confirm results or to facilitate the use of further techniques (Rojas et al., 2014). In either case, phage display shows to be a prominent option.

Interactome phage display

Considering that phage display is a technique for protein-protein interaction studies, it is possible to analyze proteins that not necessarily compose an antigen-antibody pair. For this, panning is performed by immobilizing a target antigen and incubating it with a library in order to define other antigens that might interact with the target (Sundell & Ivarsson, 2014; Blikstad & Ivarsson, 2015). When using an ORFeome library (Figure 9A), the output of the panning gives information related to many possible proteins that might interact with the studied target (Di Niro et al., 2010). On the other hand, the use of single gene library can provide detailed information about the interaction partner of the immobilized antigen (Figure 9B). In addition, this approach can be used to increase or decrease the affinity of ligands to their receptors by generating a library with mutants that are incubated with their reaction partners (Rojas et al., 2019).

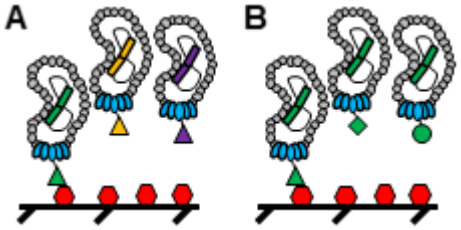

Figure 9. Use of ORFeome or single gene libraries for protein-protein interaction studies. (**A**) Use of ORFeome libraries against an antigen. The output sequences from this technique indicate candidates that may be interaction partners of the immobilized antigen. (**B**) Use of single gene libraries against an antigen. This variation provides information about the specific part of an interaction partner that binds to the studied antigen.

Although these approaches are comparable to the previous ones described, it is important to highlight that protein-protein interactions may show different affinities and behaviors that are harder to deal with when compared to antigen-antibody interactions. Considering this difference on obtaining data, this kind of phage display is often coupled with next-generation sequencing (NGS) instead of the immunoassay screening method (Di Niro et al., 2010).

1.2 *Listeria* spp. biology and its importance in food industry

The genus *Listeria* comprises Gram-positive, facultative anaerobic, non-sporulating, rod-shaped bacteria. After phylogenetic reclassifications, there were 6 *Listeria* species described until 2009, from which the last species was described in 1984 (Seeliger et al., 1984). Later on, 14 new species were described (Graves et al., 2010; Leclercq et al., 2010; Bertsch et al., 2013; Lang Halter et al., 2013; Núñez-Montero et al., 2018; Doijad et al., 2018; Leclercq et al., 2019) resulting in a total of 20 *Listeria* species: *L. monocytogenes*, *L. ivanovii*, *L. innocua*, *L. seeligeri*, *L. welshimeri*, *L. grayi*, *L. marthii*, *L. rocourtiae*, *L. fleischmannii*, *L. weihenstephanensis*, *L. booriae*, *L. newyorkensis*, *L. floridensis*, *L. aquatica*, *L. cornellensis*, *L. riparia*, *L. grandensis*, *L. goaenensis*, *L. costaricensis*, and *L. thailandensis*. This intense description of new species in the recent years shows that research over *Listeria* genus has arising importance. Nevertheless, the main relevant pathogen for humans is still *L. monocytogenes*, while *L. ivanovii* has importance on veterinary medicine (Guillet et al., 2010). There are 13 different serotypes of *L. monocytogenes*, from which three (4b, 1/2a, and 1/2b) are more virulent and responsible for 95-98 % of the human infections (Datta & Burall, 2018).

Listeria genus comprise ubiquitous bacteria, which can be found in many places in the environment, as well as in the microbiota of animals and humans. This fact, summed to its capacity of forming biofilms, elevated resistance to a broad range of pH and temperature, high concentrations of salts, and low amount of oxygen, contributes for the presence of this genus in food production facilities (Moorhead & Dykes, 2004; Zhang et al., 2011; Cruz & Fletcher, 2011). In addition, due to the complex mechanism for gut invasion of *L. monocytogenes*, it is considered a very important food-borne pathogen. The disease caused by these agents is called listeriosis, and affects mostly immunocompromised people, such as transplanted, cancer, and HIV patients, as well as infants, elderly, pregnant and their fetuses. Even though having low incidence (less than 1/100,000 people in most of the countries), the mortality rate worldwide is around 25 % (Noordhout et al., 2015). Because of this, in countries such as USA, laws requiring “zero tolerance” of *Listeria* in ready-to-eat (RTE) foods are applied (Cruz & Fletcher, 2011). In other places, such as in great part of Europe, the laws are less strict, allowing up to 100 CFU/g of in RTE foods (EC Regulations, 2005). In other

countries, there are either few legislation, comprising certain high-risk foods, or no legislation at all, turning *Listeria* contamination an even bigger concern. Therefore, the detection of *Listeria* in produced food or food production environment is essential. The standard method for its detection in food involves microbiological procedures for enrichment, isolation, and chemical characterization (Janzten et al., 2006). Although very specific and precise, the whole procedure is still time-consuming, taking around 7 days from sample collection to result. As an alternative, procedures such as PCR-based techniques, immunological methods, proteomic approaches, and different formats of biosensors have been developed in order to reduce the detection time to around 1 day or less (Jadhav et al., 2012).

Among these technologies, antibody-based assays, such as lateral flow tests, are considered more interesting, since it offers a simple and low-cost detection. Although very attractive for food industry, lateral flow assays, as well as other new methods, still depend on an efficient enrichment step prior detection to increase the amount of detectable cells in the sample. Recently, some works have described significant improvement on the enrichment step, dramatically reducing the time to obtain detectable amounts of bacteria (Hahm et al., 2015). However, although works have been successfully increasing specificity of the lateral flow through the improvement of colorimetric components (Cho et al., 2015), the development of appropriate monoclonal antibodies (mAbs) did not advance the same way, leaving room for improvement.

1.3 Pathogenic factors of *Listeria monocytogenes*

Listeria monocytogenes is an intracellular pathogen that contains diverse mechanisms for invasion, replication, and survival in the host. Once the bacterial cells are inside the host, they promote their own cell invasion via proteins presented on their surface, such as the internalins A (InlA) and B (InlB) (Pizarro-Cerdá et al., 2012). These proteins are able to trigger signals in the host`s cells in order to reorganize the cytoskeleton and promote internalization of the bacteria. Even though InlA and InlB represent the main factors for cell invasion in *L. monocytogenes*, other internalins (e.g. InlF, InlG and InlH) and proteins such as LAP are also involved, but in a lesser extent (Drolia et al., 2018).

Once the bacteria is internalized, it is initially present in a vacuole, isolated from the cytoplasm. At this stage, some proteins are activated by the acidic and reductive environment of the vacuole, and further act to disrupt the vacuole membrane. The main proteins related to this activity are the listeriolysin (LLO), phospholipases (PlcA and PlcB), and metalloprotease (Mpl), resulting in the release of the bacterial cells to the cytosol (Pizarro-Cerdá & Cossart, 2018). Among these proteins, LLO shows to be active in many other parts of the host`s cells, having impact on organelles (e.g. mitochondria and endoplasmic reticulum) protein metabolism, and DNA stability. When the bacterial cells are in the cytoplasm, they possess mechanisms to use metabolites from the host in order to have energy. The main factor described for this purpose is the hexose phosphate transporter (Hpt), which uptake the glucose-6-phosphate from the host`s cells. In addition, the actin assembly-inducing protein (ActA) plays an essential role on the motility of *L. monocytogenes* inside the cells. This protein is responsible to capture actin monomers from the host`s cells and build a tail on the bacterial surface that promotes its motility. This way, the bacterium is able to avoid intracellular defense mechanisms (e.g. autophagosomes), and to promote cell-to-cell spread. Besides these mechanisms for invasion and replication of the bacteria, pathogenic factors can also be responsible to modulate gene expression of the host`s genes. Proteins such as LntA, OrfX, InlC, and even LLO are able to interact with transcriptional factors and inhibit responses of the cell against infection.

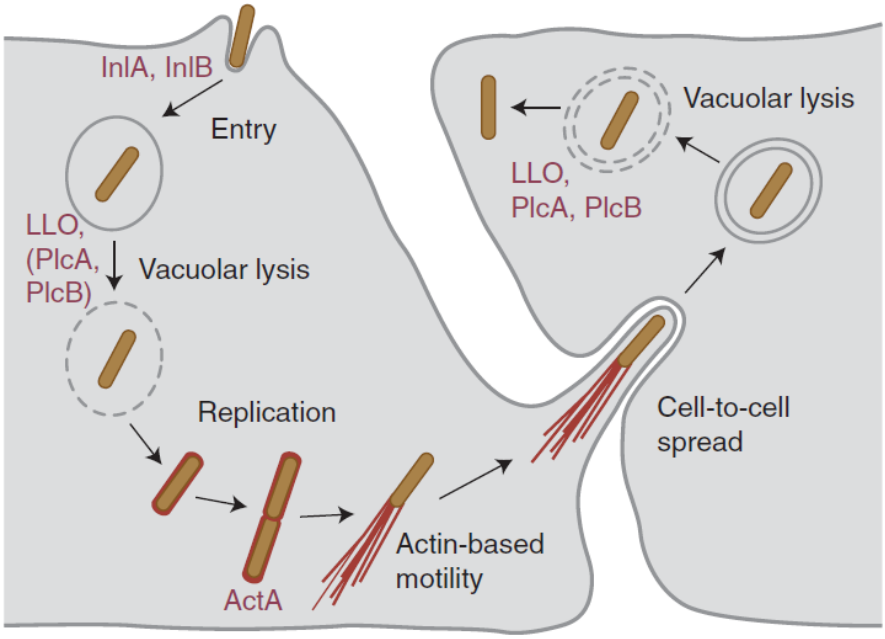

Figure 10. Process of cell invasion of *L. monocytogenes* and the main proteins involved. The bacterial entry in the host`s cells is mainly triggered by the surface antigens InlA and InlB. Once internalized, *Listeria* cells lyse the vacuole using LLO, PlcA, and PlcB. This way, they can reach the cytoplasm, where the bacteria replicated and recruits actin from the invaded cells using ActA. Thereby, *Listeria* cells gain more motility and can spread to adjacent cells, where the process of entry is repeated. This figure is adapted from Pizarro-Cerdá et al. (2012).

1.4 Targets for pathogenic and non-pathogenic *Listeria* detection

The mostly studied detection targets for *Listeria* are related to the detection of *L. monocytogenes*, such as the InlA and InlB (Pizarro-Cerdá et al., 2012; Mendonça et al., 2012). These proteins are involved in the pathogenesis during the intestinal invasion step and are accessible on the cell surface through attachment to the cell wall. In addition to these two proteins, others were described for the detection of pathogenic species, such as ActA (Nanduri et al., 2007), or N-acetyl muramidase (Bhunia et al., 1991; Geng et al., 2006). Besides the detection of the pathogenic species, it is also important to have information about the presence of non-pathogenic ones. This because it has been shown that some non-pathogenic species are able to overgrow the pathogenic ones during the enrichment step, increasing the chance of having false-negative results in detection (Kim & Bhunia, 2008; Oravcová et al., 2008; Besse et al., 2010). This way, the search of biomarkers for the whole genus, such as p60 (Yu et al.,

2004), flagellin (Kim et al., 2005), or 1,6-fructose bisphosphate aldolase (FBA) (Mendonça et al., 2016), became even more interesting.

Besides the surface proteins with defined functions, many others started to be described to have a previously undefined role in the bacteria. This group of proteins that can have more than one function is defined as “moonlighting proteins” (Jeffery, 2016). In many bacteria, several antigens, usually enzymes, have been described to be moonlighting and became more interesting with descriptions of their role in pathogenesis (Jeffery, 2018). In *L. monocytogenes*, the alcohol-acetaldehyde dehydrogenase (also named “*Listeria* adhesion protein”, LAP) is a metabolic enzyme that is also involved in the translocation of bacterial cells through the intestinal cells (Henderson & Martin, 2011). In addition, the fact that *L. monocytogenes* is able to remodel its surface according to the environment by exposing metabolic enzymes that, in principle, should not be located on outer parts of the cell increase the chance of having proteins with yet undescribed moonlighting function in this species (Quereda et al., 2016). In the field of detection, FBA is an example of protein that should not be located on *Listeria* surface, but is detectable in whole cells when using monoclonal antibody (Mendonça et al., 2016). Although not yet described as a moonlighting protein in *Listeria* spp., FBA has been described to have pathogenic role in other microorganisms, such as *Neisseria meningitidis*, *Streptococcus pneumoniae*, *Mycobacterium tuberculosis*, and *Paracoccidioides* spp. (Shams et al., 2014).

1.4.1 Pyruvate dehydrogenase complex (PDC)

The PDC is an enzyme complex that catalyzes the conversion of pyruvate into acetyl-CoA, which is a step that connects glycolysis to the citric acid cycle (CAC). Due to its crucial role for cellular respiration, this complex is conserved among almost every organism, and is composed by three or four different proteins (Patel et al., 2014). Although keeping the same function, the structure of the complex and its enzymes vary among the different forms of life. In eukaryotes, four enzymes often compose the complex, in which a PDC-E3 binding protein (PDC-E3BP) is the additional protein of the complex. In prokaryotes, however, the complex is mostly composed of three enzymes and presents substantial structural difference between Gram-negative and Gram-positive bacteria (Izard et al., 1999). The basic difference between these PDC structures lies on the number of PDC-E2 copies that compose the core of the complex.

In eukaryotes, there are several models proposed for PDC, which can contain 40-60 copies of PDC-E2, together with 12-20 of PDC-E3BP. In Gram-negatives, the core is composed of ≈24 copies of PDC-E2, while in Gram-positives, the core can also have ≈24 copies (forming an octahedral symmetry, cube shape) or get closer to that of eukaryotes with ≈60 copies (forming an icosahedral symmetry, dodecahedron shape).

As to the potential moonlighting role of PDC, it may be a case similar to FBA. As part of the PDC, the enzyme dihydrolipoamide acetyltransferase (also known as pyruvate dehydrogenase complex - enzyme 2, shortly PDC-E2) is responsible for one of the reactions in the conversion of pyruvate to acetyl-CoA, which indicates its presence in the inner parts of the cell. However, other organisms, such as *Mycobacterium pneumoniae* and *Salmonella* Enteretidis, show that components of PDC can also be involved in pathogenesis (Dallo et al., 2002; Pang et al., 2011). This way, it is reasonable that this protein also has its cellular location changed in a way similar to what happens with other metabolic proteins, allowing it to be used as a target for *Listeria* spp. detection as will be further discussed in the present document.

1.5 Methods for *Listeria* detection

The current “gold-standard” method for *Listeria* detection in food samples is based on enrichment, isolation, and biochemical characterization. However, this procedure is considered time-consuming, since it can take up to 7 days for a conclusive result, causing a problem for food industry (Janzten et al., 2006). It is possible to distinguish two main steps in the detection procedures for *Listeria* spp. from food: the enrichment, and the detection itself (Figure 11). Regarding the former, recent works have developed ways to shorten the time needed to acquire detectable amount of bacteria from food, reducing it from 16-30 h to 5-8 h (Hahm et al., 2015). In its turn, the improvement of the detection part is still topic of investigation.

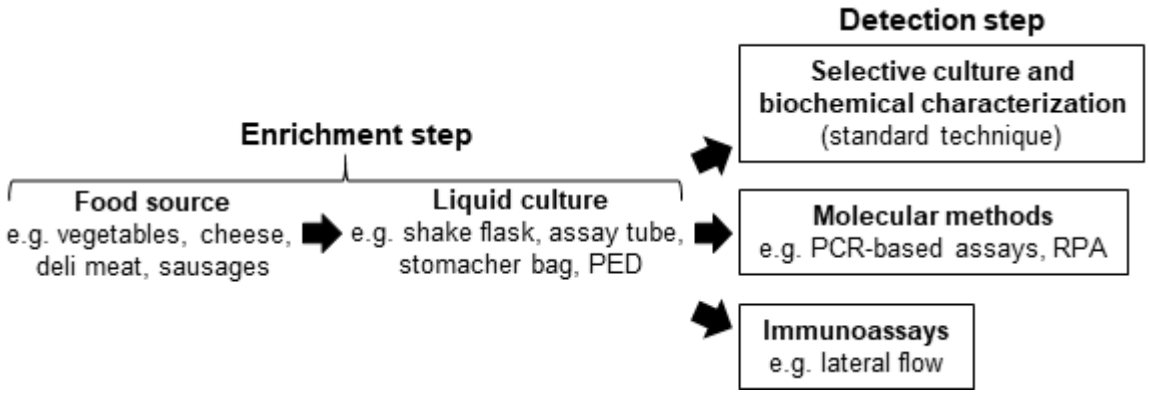

Figure 11. Scheme of detection strategies for *Listeria* spp. in food. The detection method for *Listeria* can be defined in two steps: the enrichment, and the detection. The enrichment is based on allowing the bacteria present in the food sample to grow until a detectable amount is reached. In its turn, the detection can be done directly, as is the case for microbiological methods and immunoassays; or indirectly, as it occurs in assays for detecting the DNA, such as PCR or RPA.

Among the different detection methods that can be used as alternative, the PCR-based techniques and immunoassays are the most attractive ones for accessing the presence of *Listeria* in food samples (Jadhav et al., 2012). PCR-based techniques have the advantage of allowing the detection of low amounts of bacteria, as well as the use of different combination of antigens at the same time via multiplex, increasing the information over the species present in samples. In addition, this technique can show high sensitivity and specificity, reaching a limit-of-detection (LOD) of 10 CFU per gram of food (Hahm et al., 2015), or 1 CFU in 25 mL of milk (Moezi et al., 2019). However, they are considered expensive and less practical since special equipment and material are necessary.

On the other hand, immunoassays, such as lateral flow, show to be a simpler option. This approach do not involve special equipment and presents a much faster time to result. Another point is that the LOD is similar to those of other methods, since the enrichment step is often providing enough cells to be detected regardless of the method used (Jagadeesan et al., 2019). Although presenting relatively good performances, there is still interest on improving the diagnostic methods in order to reduce their time. Most of the works are focused on the detection part, more specifically on the search for new targets and generation of better antibodies that can either reduce the amount of bacteria to be detected (i.e. improve the LOD) or increase the diagnostic

performance (i.e. specificity and sensitivity). Until today, works report LOD around 10^6 CFU/mL (Hahm et al., 2015), which can be improved to 10^4 CFU/mL by using a superparamagnetic lateral flow system (Shi et al., 2015). Other strip tests that do not use antibodies, such those employing recombinase polymerase amplification (RPA) or nucleic acid lateral flow (Liu et al., 2017; Du et al., 2018; Li et al., 2018), show to be an option for improvement, but present similar results as those from previous technologies or still have to be further tested in detection with food samples.

In the present work, a combination of three phage display techniques is applied for the generation of antibodies, discovery/identification of biomarkers, and characterization of antibody-antigen interaction. Using this approach, one target, the PDC-E2, was found to allow the detection of every *Listeria* species tested. In other species, this target has already been used as a molecule for therapy, vaccine, or diagnostic development (Bryk et al., 2013; Devasundaram & Raja, 2017; Sun et al., 2014), and also involved in virulence (Pang et al., 2011; Dallo et al., 2002; Wang et al., 2014). Here, PDC-E2 is described as a target for *Listeria* spp. detection, which allowed to specifically distinguish this genus. The cellular location of the target was accessed, as well as its detectability in fluorescent microscopy. In addition, the already known targets InlA, InlB, and FBA, as well as two hibridoma-derived antibodies, were employed to generate recombinant antibodies for *Listeria* spp. detection, and to test ORFeome and single gene phage display. Finally, the binding region (called “minimal sequence of recognition”, shortly MSR) of the generated antibodies was defined in order to comprehend the detection profile of the antibodies and target.

2 HYPOTHESIS, AIM, AND OBJECTIVES

2.1 Hypothesis

The combination of different phage display techniques allow finding new targets, generating antibodies, and characterizing antigen-antibody interaction in order to develop a detection method for *Listeria* spp..

2.2 Aim

Use different phage display technologies to discover, identify, and characterize PDC-E2 as a new detection target for *Listeria* spp., and generate antibodies against different targets to detect pathogenic and non-pathogenic *Listeria*.

2.3 Objetives

- Employ antibody phage display to discover new targets for *Listeria* spp.;
- Build ORFeome library for *Listeria monocytogenes*;
- Employ ORFeome phage display to identify new targets;
- Build single gene libraries;
- Employ single gene phage display to characterize antibody-antigen recognition;
- Compare different techniques for studying antibody-antigen interaction;
- Generate recombinant antibodies against already known targets for *Listeria* spp. detection;
- Test the applicability of generated antibodies in immunoblot and fluorescent microscopy;
- Access the diagnostic performance of the generated antibodies for *Listeria* spp. detection via indirect ELISA.

3 MATERIAL AND METHODS

3.1 Bacteria cultivation and *Listeria* protein fractionation

The proteins from cell wall, membrane, and cytoplasm from *Listeria* spp. cells were obtained as described elsewhere (Mishra et al., 2011). Briefly, the strains of *L. monocytogenes* ATCC 7644, and *L. innocua* DSM 20649 were grown in 200 mL of BHI medium at 37 °C until OD_{600}=0.8 from an initial OD_{600}=0.1. The cells were harvested by centrifugation (7,000 g; 10 min; 4 °C), suspended in 500 µL of SDS-Tris buffer (0.5% SDS; 10 mM Tris; pH 6.9), transferred to a 1.5 mL tube, and incubated 30 min a 37 °C. The tubes were centrifuged, and the supernatant containing the cell wall fraction was collected. The remaining cell content was mixed with 200 µL of Lysis B solution (100 mM Tris; 100 mM NaCl; 10 mM MgCl2) and submitted to 3 freeze-thaw cycles at -80 °C and 37 °C. The tubes were centrifuged (14,000 g; 15 min), and the supernatant containing the cytoplasm fraction was collected. The remaining cell content was mixed with 200 µL of Sample Solvent buffer (5% SDS, 10% β-mercaptoetanol, 125 mM Tris, 20% glicerol, pH 6.9) and centrifuged (14,000 g; 20 min) to collect the supernatant containing the membrane fraction.

Each protein fraction was tested by ELISA regarding the presence of the proteins InlA (which must be present mainly in the cell wall) and FBA (which must be present on every fraction, but mainly in the cytoplasm and membrane). For this, the cell wall, cytoplasm, and membrane fractions were diluted in PBS 1:100, 1:100, and 1:400, respectively, and coated on ELISA Costar plates (Corning). The plates were blocked with 2 % MPBS-T (PBS-T with 2 % (w/v) of skimmed milk powder), and incubated with monoclonal antibodies 2D12 (anti-InlA, 1 ng/mL) and 3F8 (anti-FBA, 1 µg/mL). Finally, the plates were incubated either with anti-mouse Fc specific (Sigma), for 2D12, or anti-mouse IgA, G, M (Antibodies Online), for 3F8, both HRP conjugated. After each step, the wells were washed three times with 300 µL PBS-T. The reaction was developed with TMB solution (TMB-A: 50 mM citric acid, 30 mM potassium citrate, pH 4.1; TMB-B: 90% (v/v) ethanol, 10% (v/v) acetone; 10 mM tetramethylbenzidine; 1 mL 30% H2O2; mix 19 parts of TMB-A with 1 part of TMB-B), stopped with 1 N H_2SO_4, and plates were read at 450 nm, using 620 nm as reference.

3.2 Expression in *E. coli*, and purification of the targets InlA, InlB, and FBA

The genes for InlA, InlB, and FBA were cloned and described in previous works (Mendonça et al., 2012; Braun et al., 1997; Mendonça et al., 2016). Briefly, the plasmids pAE-*inlA*, pET21b-*inlB*, and pAE-*fba* were transformed into *E. coli* BLR(DE3). For the expression, the cells containing the respective plasmids were grown in 10 mL LB-A for 16 h at 37 °C, 250 RPM. Then, 200 mL of LB-A was inoculated until OD_{600}=0.1 and grown under the same conditions until OD_{600}=0.6-0.8, when it was induced with IPTG to a final concentration of 125 µM and incubated for more 4 h. The cells were harvested by centrifugation (10,000 xg; 10 min; 4 °C) and frozen at -20 °C for 16 h. Later, the cells were suspended in 20 mL binding buffer (5 mM imidazole, 0.5 M NaCl, 20 mM Tris-HCl, pH 7.9) before sonication (3x 2 min of pulsed cycles). The suspension was centrifuged (16,000 xg; 10 min; 4 °C) and the supernatant transferred to a new tube. A SDS-PAGE 12 % and immunoblot with anti-6xHis (Dianova) was performed to confirm the expression of the recombinant protein. Finally, the purification was made with His-tag purification sepharose (GE Healthcare) in a gravity-flow column using washing (60mM imidazole, 0.5M NaCl, 20mM Tris-HCl, pH 7.9) and elution buffers (1M imidazole, 0.5M NaCl, 20mM Tris-HCl, pH 7.9). The proteins were dialyzed directly against PBS at 4 °C for 16 h, and further checked on SDS-PAGE 12 %, and immunoblot anti-6xHis.

3.3 Antibody panning over purified InlA, InlB, and FBA and *Listeria* protein fractions

For antibody generation against the recombinant proteins, 1 µg of each protein was diluted in 150 µL of PBS and coated onto an ELISA Costar plate well overnight at 4 °C. In parallel, one additional well coated with Panning Block (BSA 1% (w/v), dried skim milk 1% (w/v), PBS-T) solution was also made for pre-incubation. The libraries HAL9 and HAL10 were mixed for pannings against InlA and InlB, and used separately against FBA, always $5x10^{10}$ CFU from each. The pre-incubation was done for 30 min at RT on a well coated with Panning Block.

The *Listeria* protein fractions were used to perform four different panning strategies as following: 1) *L. monocytogenes* ATCC 7644 cell wall fraction, with pre-

incubations on *B. subtilis* (1x) and Panning Block (2x); 2) *L. monocytogenes* ATCC 7644 cytoplasm fraction, with pre-incubations the same way; 3) *L. monocytogenes* ATCC 7644 membrane fraction, with pre-incubations the same way; 4) same as the first strategy, but with a pre-incubation on *L. innocua* DSM 20649 cell wall in place of one of the Panning Block. For each strategy, the according subcellular fractions were coated the same way as described in the previous topic, and the pre-incubation was made sequentially in three ELISA wells. The first was coated with either heat-inactivated *Bacillus subtilis* 168 NCIB 10106 or *L. innocua* DSM 20649 cell wall. While the second and third were coated with Panning Block. The preparation of heat-inactivated *B. subtilis* cells was performed by growing the strain in BHI overnight at 37 °C, 250 RPM. The cells were harvested (2,600 g, 7 min, 4 °C), suspended in Carbonate-Bicarbonate buffer until OD_{600}=1.0, and stored at -20 °C until use. Libraries HAL9 and HAL10 were used separately the same way as for FBA.

The remaining panning procedure was done as described elsewhere (Russo et al., 2018). Briefly, after transferring the libraries to the wells containing the targets, they were incubated 1.5 h at RT, the wells were washed 20x with PBS-T, the bound phage was eluted with Trypsin 10 µg/mL and used to infect *E. coli* TG1 (Lucigen). The infected cells were grown at 37 °C up to OD_{600}=0.5, infected with M13K07 phage, and grown for 16 h at 30 °C. This procedure was repeated two more times, and on the last time, however, the eluted phage were used to infect *E. coli* XL1-Blue MRF', which were directly plated on 2xYT agar with 100 mM glucose and 100 µg/mL ampicillin (2xYT-GA) and grown for 16 h at 37 °C.

The screening of individual clones was also performed by picking colonies from the plates of each strategy were pick, which were transferred to 96-well plates containing 2xYT-GA and grown for 16 h, at 37 °C, 800 RPM. From these plates, 20 µL were transferred to another plates containing 180 µL of the same medium, and grown at 37 °C for 1.5 h. Then, the plates were centrifuged (3,200 xg; 10 min; RT), the medium was removed, 2xYT-A with 50 µM IPTG was added, and the plates were incubates for 16 h at 30 °C, 800 RPM. The plates were centrifuged the same way and the supernatant was used to perform ELISA against: the respective purified recombinant proteins (200 ng/well diluted in PBS) or the *Listeria* subcellular fractions used for scFv selection; live *Listeria* cells, and live *B. subtilis* (negative control). The ELISA plates

containing the protein fractions were prepared as described on the previous topic. The plates containing live cells were prepared by growing *L. monocytogenes* ATCC 7644, as well as *L. innocua* DSM 20649 and *B. subtilis* 168 NCIB 10106 in BHI at 37 °C, for 16 h, 250 RPM. Then, the cells were centrifuged (2,600 xg; 4 °C; 7 min), washed 2 times with PBS, and suspended in carbonate-bicarbonate buffer 150 mM, pH 9.7, until OD_{600}=1.0 (≈ 10^9 cells/mL). From this solution, 100 µL/well was added on each plate for coating for 16 h at 4 °C. Each plate was blocked with 2 % MPBS-T for 30 min, 25 µL of the *E. coli* culture supernatants containing the scFv were diluted on 75 µL of 2 % MPBS-T into the wells, and incubated 1 h at RT. Later, mouse 9E10 anti-myc-tag IgG (1:50), and goat anti-mouse Fc specific HRP-conjugated (1:40,000; Sigma) were sequentially added, both diluted in 2 % MPBS-T and incubated for 1 h at RT. After each step, the wells were washed three times with 300 µL PBS-T. The reaction was developed with TMB solution, stopped with 1 N H_2SO_4, and the plates were read at 450 nm, using 620 nm as reference.

3.4 Cloning and production of recombinant antibodies

The scFv genes selected against purified InlA, InlB, FBA, and subcellular protein fractions on the previous step were subcloned into pCSE2.6 vectors with mouse IgG2a Fc for scFv-Fc production (Miethe et al., 2014). In the case of GSM133-E2, it was also produced as human IgG1 using the vectors pCSEH and pCSL. For this, *E. coli* XL1-Blue MRF' containing the selected phagemids were grown in LB for 16 h at 37 °C and used for plasmid extraction with NucleoSpin Plasmid EasyPure kit (Macherey-Nagel). After being checked by sequencing, the unique scFv sequences were subcloned to pCSE2.6, or to the IgG vectors (using *Bss*HI and *Nhe*I for pCSEH, or *Age*I and *Dra*III for pCSL), by making digestion of the phagemids with *Nco*I and *Not*I (NEB) followed by ligation reaction with T4 DNA ligase (Promega) following the manufacturer's instructions. The ligation reaction was used to transform *E. coli* XL1-Blue MRF' via heat shock and the cells were spread onto 2xYT-GA agar plates for 16 h at 37 °C. The resulting colonies on the next day were screened by colony PCR, had their plasmids extracted the same way as before, and the possible positive colonies were confirmed by sequencing.

The resulting pCSE2.6 vectors, or the combination of pCSEH and pCSL, containing the scFv-Fc sequences were used to transfect Expi293 HEK cells. The transfection is made with polyethylenimine “Max” 40 kDa (Polysciences) using 25 µg of PEI with 10 µg of plasmid mixed in 0.5 mL. This volume is then transferred to 5 mL of Expi293 HEK cells containing ≈2 × 10^6 cells/mL. The cells are grown in FreeStyle F17 medium (Gibco) supplemented with 8 mM L-glutamine (Biochrom) and 0.1 % Pluronic F-68 (PAN-Biotech) for 7 days, and on day 3 they are fed with 5 mL of HEK-TF and 1 mL of HEK-FS media (Xell). On day 7, the cultures were centrifuged (1,000 xg, 5 min, RT) and the supernatant used on a 24-well Protein A purification plate followed by buffer exchange to PBS using Zeba Spin Desalting 7K columns (Thermo Scientific). After purification, the binding of every scFv-Fc on *Listeria* spp. cells was checked by ELISA in a format similar to the one for scFv screening. For that, *L. monocytogenes*, *L. innocua*, and *B. subtilis* cells were coated the same way. However, the antibodies added were serially diluted √10-fold and incubated 1 h at RT, followed by goat anti-mouse Fc specific HRP-conjugated (1:40,000; Sigma) was added, both diluted in 2 % MPBS-T. After each step, the wells were washed three times with 300 µL PBS-T. The reaction was developed with TMB solution, stopped with 1 N H_2SO_4, and the plates were read at 450 nm, using 620 nm as reference.

3.5 Immunoblot and ELISA of scFv-Fc generated against recombinant InlA, InlB and FBA

The immunoblots by running 1 µg of the purified recombinant protein into each lane of a 12 % SDS-PAGE gel and subsequently transferred to a methanol-activated polyvinylidenfluorid (PVDF) 0.45 µm membrane (Roth). The membrane was blocked with 2 % MPBS-T for 16 h at 4 °C, and further incubated with 1 µg/mL of each of the scFv-Fc for 1 h at RT. Goat anti-mouse Fc specific HRP-conjugated (1:40,000; Sigma) was used as secondary antibody, and DAB solution (6 mg 3.3-diaminobenzidine tetrahydrochloride; 10 µL 30 % H_2O_2; 9 mL PBS; 1 mL $NiSO_4$ 250 mM) solution was finally added for 15 min. The membrane was washed three times with PBS-T after each step. As positive control antibody, a mouse anti-6xHis monoclonal (1:500 in 2 % MPBS-T, Dianova) was used. The ELISA was performed by coating 200 ng/well of the recombinant target diluted in PBS overnight at 4 °C. After blocking the wells with 2 %

MPBS-T, each of the produced antibodies were diluted √10-fold 8 times starting with 10 µg/mL and incubated 1 h at RT. In both assays, goat anti-mouse Fc specific HRP-conjugated (1:40,000; Sigma) was used as secondary antibody, while SuperSignal West Pico (Thermo Scientific) and TMB solution substrates were used for immunoblot and ELISA, respectively.

3.6 Immunoblot for target location, immunomagnetic separation, and mass spectrometry for target identification

The produced scFv-Fc against *Listeria* subcellular protein fractions were used for the identification of possible new targets via immunoblot. The protein fractions from the cell wall and cytoplasm of *L. innocua* DSM 20649 were run in a 12 % SDS-PAGE and subsequently transferred to a methanol-activated PVDF 0.45 µm membrane (Roth). The remaining steps for the immunoblots were done the same way as described in the previous topic.

In order to isolate the target from the protein fractions, immunomagnetic separation (IMS) was performed with 100 µL of SureBeads Protein A magnetic beads (Bio-Rad), which were coated with 10 µg of each antibody for 10 min at RT. Then, the preparation of *L. innocua* DSM 20649 cytoplasm was diluted 1:2 in PBS in a total of 200 µL and incubated with the beads for 1 h at RT. Then, the elution was made with glycine buffer 20 mM, pH 2.0, for 5 min at RT, to which 10 % (v/v) Na-phosphate buffer 1 M, pH 7.4, was added. The elution samples were used in 12 % SDS-PAGE, from which the proteins referring to the target were excised for further mass spectrometry (MS) analysis. The immunoblot was performed the same way as described in the previous paragraph, using the same scFv-Fc used for the IMS as primary antibody.

3.7 ORFeome phage display for target identification

The library used (named *L. monocytogenes* ATCC 7644) is described in a previous work (Mendonça et al., 2016), as well as the panning procedure performed for two hibridoma-derived antibodies, 2D12 against InlA (Mendonça et al., 2012) and 3F8 against FBA (Mendonça et al., 2016). Recombinant antibodies against purified InlA, InlB, and FBA were not included. In summary, 2D12 or 3F8 were diluted in Panning

Block and coated on two wells of a Costar ELISA plate (Corning, Wiesbaden, Germany). Two additional wells were coated with Panning Block only, and the plate was incubated for 16 h at 4 °C. The *L. monocytogenes* ATCC 7644 library (≈1 × 10^{10} CFU/mL) was diluted in Panning Block and added to the panning solution well for pre-incubation for 30 min at RT, while the wells containing the mAbs were blocked with the same solution. The library was further transferred to the wells containing the antibody and incubated 1.5 h at RT. Then, the wells were washed and eluted with trypsin. The eluted phages were used to infect *E. coli* TG1, which was further infected with helperphage M13K07 (MOI 1:20) and grown 16 h at 30 °C, 500 rpm. On the next day, the cultures were centrifuged and the supernatant containing phage used instead of the library. In total, three panning rounds were done, and the phage eluted after the 2^{nd} and 3^{rd} rounds were used to infect *E. coli* XL1-Blue MRF', which were diluted, plated on 2xYT-GA agar plates, and grown for 16 h at 37 °C. The resulting plates were used to acquire individual colonies, which were transferred to a 96-well culture plate containing 2xYT-GA. The plate was grown for 16 h at 34 °C and then 20 µL was used to inoculate another plate with 180 µL/well of the same medium, which was incubated 2 h at 37 °C. Then, clones in each well were infected with *Hyperphage* (MOI 1:20) and had the medium changed to 2xYT-AK; the plate was then incubated 16 h at 30 °C, 800 rpm. On the next day, the plate was centrifuged again and the supernatant transferred to another plate, in which PEG solution was added and incubated 1 h at 4 °C. The plate was centrifuged, the pellet suspended in PBS and centrifuged again. Finally, 50 µL of each supernatant was added to 50 µL of PBS in a Costar ELISA plate (Corning, Wiesbaden, Germany), which was incubated overnight at 4 °C for coating. Afterwards, the plate was blocked with 2 % MPBS-T and further incubated with 2D12 or 3F8 antibody (1 µg/mL) for 1 h at RT. Then, goat anti-mouse IgA, M, G HRP-conjugated antibody (AntibodiesOnline, Prod. ABIN376851, 1:4,000) was incubated 1 h at RT. A well with anti-M13 (pVIII) HRP-conjugated (1:40,000) served as positive control for phage production. The reactions were developed with TMB solution for 15 min and read at 450 nm. Reactive clones had their phagemids extracted and sent for sequencing.

As to the recombinant antibodies against subcellular fractions, they were used in ORFeome phage display in parallel to MS analysis. The panning procedure was

conducted in a similar was as for the hibridoma-derived antibodies with few modifications. In this case, $2x10^{11}$ CFU of the library was pre-incubated 20 min at RT on each of 3 different wells: the first coated with Panning Block; the second coated with a non-related scFv-Fc; and the third coated the same way as the second, but with additional 10 µg of the non-related scFv-Fc in solution. The remaining steps of panning and screening were done the same way as described in the previous paragraph. Only one panning round was conducted, and after identifying reactive clones by ELISA, they were sequenced and analyzed with BLASTn. In order to confirm and validate the results obtained with the screening ELISA, some of the positive hits were produced as monoclonal phage in a larger scale. For this, the positive hits were grown in 2xYT-GA medium for 16 h at 37 °C. Later, the cultures were inoculated in 5 mL of the same medium and grown until OD_{600}≈0.5, when Hyperphage was added to the cultures (MOI 1:20, ≈$1x10^{10}$ CFU). They were incubated 30 min at 37 °C, followed by 30 min at 37 °C, 500 RPM, and transferred to a 100-mL shake flask with 2xYT-AK, which was incubated 24 h at 30 °C, 250 RPM. The cultures were centrifuged (16,000 xg; 10 min; 4 °C), the supernatants transferred to 50-mL tubes and mixed with PEG-NaCl solution (20 % (w/v) PEG 6,000; 2.5 M NaCl) to a final concentration of 20 % (v/v), and incubated at 4 °C for 1 h. Then, they were centrifuged (3,200 xg; 1 h; 4 °C), the pellet containing phage suspended in 500 µL of PBS and transferred to a 2-mL tube, which was again centrifuged (16,000 xg; 1 min; RT), and the liquid transferred to a new tube. This solution containing the produced phage was titrated by infecting *E. coli* XL1-Blue MRF' at OD_{600}≈0.5 in different dilutions. The produced monoclonal phage were then used in indirect ELISA to confirm the binding of each antibody. For this, different amounts of phage were coated onto ELISA wells, starting with 10^9 CFU/well and diluting 8 times √10-fold. Then, each antibody against the respective monoclonal phage was used diluted in 2 % MPBS-T to 2 µg/mL, and incubated 1 h at RT. The, goat anti-mouse Fc specific HRP-conjugated (1:40,000; Sigma) was added, followed by TMB solution and 1 N H_2SO_4, as described in previous paragraphs. After each step, the wells were washed three times with 300 µL PBS-T, and plates were read at 450 nm, using 620 nm as reference.

3.8 Immunofluorescence and wide field fluorescent microscopy of *Listeria* cells

The strain *L. monocytogenes* ser. 4b DSM 15675 was grown in BHI (16 h; 37 °C, 110 RPM), 2 mL were centrifuged (2,500 xg; 2 min), washed 2 times with PBS, and incubated with three different antibodies: 1) GSM29-D3 scFv-Fc (anti-internalin A) as positive control; 2) a non-related scFv-Fc as negative control; and 3) GSM133-A4 scFv-Fc (anti-PDC-E2, as experiment molecule). These antibodies were diluted in 2 % MPBS-T to 5 µg/mL and incubated 1 h at RT. The cells were then washed three times with PBS-T and incubated 1 h at RT with anti-mouse Alexa 647 secondary antibody (Thermo Scientific), diluted 1:500 in 2 % MPBS-T. The cells were washed the same way and suspended in a corresponding volume of DAPCO (1,4-diazabicyclo[2,2,2]octane) containing mounting medium. Sample preparation was performed as described before (Boedeker et al., 2017). Briefly, 2 µL of the suspension were added to 1 % (w/v) agarose pads to reduce cell movement, which were surrounded with grease (Vaseline, Lenhart Kosmetik) and covered with high-precision coverslip (LH24.1, Roth). Imaging was performed with a Nikon Eclipse Ti inverse microscope with Fm4–64 (650/13-705/72) filters. Fluorescence z-stacks and bright-field images were taken using a Nikon N Plan Apochromat l λx100/1.45 oil objective and the ORCA FLASH 4.0 HAMMATSU camera. Images were processed using the NIS-elements imaging software V4.3 (Nikon) together with the 3D Landweber Deconvolution algorithm.

3.9 Cloning, expression in *E. coli*, and purification of the recombinant target PDC-E2

The gene (AL596167.1:98629-100260) and protein (WP_010990728.1) sequences were obtained from GenBank and used to design primers for the subcloning. Primers containing the restriction sites *Nde*I and *Not*I were ordered as following: forward 5’-AATTCCATATGGCATATTCATTTAAATTACCGGATATCG-3’, and reverse 5’-ATTGCGGCCGCCACCTCCATTAGTAATAATTCTG-3'. The PCR was conducted with Phusion High-Fidelity DNA Polymerase (Thermo Scientific), according to the manufacturer’s instructions, and using the genomic DNA of *L. monocytogenes* ATCC 7644 as template with the following thermocycler program: 98 °C, 30 s + 98 °C,

10 s; 56.5 °C, 30 s; 72 °C, 40 s (x30) + 72 °C, 5 min. The amplified gene was checked in an agarose gel 0.8 % and digested with *Nde*I and *Not*I (NEB), as well as the expression vector pET21a(+) (Novagen). Then, a T4 DNA Ligase (Promega) was performed and used to transform *E. coli* XL1-Blue MRF' via heat shock. The cells were spread onto a 2xYT-GA agar plate and grown at 37 °C for 16 h. Recombinant clones were screened by PCR and confirmed by sequencing. One correct clone was propagated and used to obtain plasmid to transform the expression strain *E. coli* BLR(DE3) also via heat shock.

For the expression, the same procedure made for InlA, InlB and FBA was performed. Briefly, *E. coli* BLR(DE3) containing pET21a(+)/PDC-E2 was grown LB-A, transferred to 200 mL of of the same medium until OD_{600}=0.1 and grown under the same conditions until OD_{600}=0.6-0.8, when it was induced with IPTG and incubated for more 4 h. The cells were harvested and frozen at -20 °C for 16 h, suspended in 20 mL binding buffer and sonicated before sonication. The suspension was centrifuged and the supernatant transferred to a new tube. Analysis with SDS-PAGE 12 % and immunoblot, as well as the purification were done the same way as before. The dialysis was made against elution buffer diluted with PBS to gradually decrease the concentration of NaCl (reduction of 50 mM every 1-2h), followed by a dialysis against only PBS (Moreira et al., 2016).

3.10 Antibody panning over recombinant PDC-E2

For antibody generation against recombinant PDC-E2, the same procedure made for InlA and InlB was done. Briefly, 1 µg of the protein was diluted in 150 µL of PBS and coated onto an ELISA Costar plate well overnight at 4 °C. In parallel, one additional well coated with Panning Block solution was also made for pre-incubation. Libraries HAL9 and HAL10 were mixed in the same panning well and three rounds were performed. The screening of the scFv was also performed the same way, using *L. monocytogenes* ATCC 7644, as well as *L. innocua* DSM 20649 and *B. subtilis* 168 NCIB 10106. A plate coated with 200 ng/well of the recombinant protein diluted in PBS was prepared as positive control.

3.11 Indirect ELISA for *Listeria* spp. detection

The employed strains (Tables 1 and 2) were from the German Collection of Microorganisms and Cell Cultures ("Leibniz-Institut DSMZ, Deutsche Sammlung von Mikroorganismen und Zellkulturen"). Each bacterium was recovered from lyophilized stocks with BHI, grown in 10 mL BHI, and streaked onto BHI-agar plates. The exception was *L. paracasei*, which was always grown in MRS or MRS-agar. The bacteria were grown at 30 or 37 °C according to their need, under 110 or 80 RPM, respectively. When needed, microaerobic condition was created with the use candle jars.

For the ELISA, a single colony of each bacteria was taken from the plates and grown in 10 mL of the corresponding medium, and under the described conditions. As previously described in this work, all cells were centrifuged, washed twice with PBS, and suspended in carbonate-bicarbonate buffer until OD_{600}=1.0. Then, ELISA plates were prepared by coating 100 µL/well of the cell suspension 16 h at 4 °C. Plates were blocked with 2 % MPBS-T for 1 h at RT, and further incubated 1 h at RT with the different antibodies diluted in 2 % MPBS-T in three different concentrations: a) the estimated EC_{50} (named "EC_{50}"); b) a √10 dilution above the EC_{50} (named "EC_{50}+"); and c) a √10 dilution below the EC_{50} (named "EC_{50}-"). Then, goat anti-mouse IgG Fc specific HRP-conjugated (1:30,000; Jackson ImmunoResearch Laboratories) was diluted in 2 % MPBS-T and incubated 1 h at RT. As controls, wells with a non-related scFv-Fc, diluted √10-fold starting with 10 µL/mL, and only the secondary antibody were used. After each step, the wells were washed two times with 300 µL PBS-T. The reaction was developed with TMB solution, stopped with 1 N H_2SO_4, and the plates were read at 450 nm, using 620 nm as reference. Every combination of antibody concentration and bacterial strain was performed in a single well that was repeated twice in independent plates. Thus, only one of the repetitions was selected to perform the statistical analysis.

To determine the diagnostic value for each antibody, a signal-to-noise ratio was calculated with every read divided by the average of three wells from the secondary antibody control of each plate. The resulting values for each antibody dilution and bacterial strain combination were used in a Receiver Operating Characteristic (ROC) analysis using GraphPad software (Prism, v 5.01), in which the sensitivity and

specificity, as well as the confidence intervals (CI), was calculated. To facilitate description of these results, the area under the ROC curve (AUC) value was also used for representing this data instead of the ROC curve itself.

Table 1. List of the *Listeria* species used for indirect ELISA.

Species	Serovar	DSM nº	Temperature (°C)/condition
L. monocytogenes	4b	15675	37/aerobic
	1/2a	102976	37/aerobic
	1/2b	19094	37/aerobic
L. innocua	6a	20649	37/aerobic
L. marthii	NI	23813	37/aerobic
L. welshimeri	1/2b	20650	37/aerobic
L. ivanovii	5	20750	37/aerobic
L. seeligeri	1/2b	20751	37/aerobic
L. floridensis	NI	26687	37/aerobic
L. fleischmannii subsp. fleischmannii	NI	24998	37/aerobic
L. aquatica	NI	26686	37/aerobic
L. grayi	NI	20601	37/aerobic
L. cornellensis	NI	26689	30/aerobic
L. rocourtiae	NI	22097	30/aerobic
L. booriae	NI	28860	37/aerobic
L. riparia	NI	26685	37/aerobic
L. weihenstephanensis	NI	24698	30/aerobic
L. grandensis	NI	26688	30/aerobic
L. newyorkensis	NI	28861	37/aerobic

NI, not informed.

Table 2. List of the non-*Listeria* species used for indirect ELISA.

Species	Serovar	DSM nº	Temperature (°C)/condition
Salmonella enterica	Typhimurium	17058	37/aerobic
Escherichia coli	O157:H7	17076	37/aerobic
Pseudomonas aeruginosa	NI	50071	37/aerobic
Klebsiella pneumoniae	3	30104	37/aerobic
K. aerogenes	NI	30053	30/aerobic
Enterobacter cloacae	NI	30054	30/aerobic
Staphylococcus aureus	3	20231	37/aerobic
Jonesia denitrificans	NI	20603	37/aerobic
Bacillus subtilis	NI	10	30/aerobic
B. thuringiensis	NI	2046	30/aerobic
B. cereus	NI	31	30/aerobic
Enterococcus faecium	D, 11	20477	37/microaerobic
E. faecalis	D	20478	37/microaerobic
E. lactis	NI	23655	37/microaerobic
Lactococcus lactis	N	20481	30/microaerobic
Lactobacillus paracasei	NI	5622	30/microaerobic

NI, not informed.

3.12 Single gene phage display for identifying the binding region of hibridoma-derived antibodies against InlA and FBA, and scFv-Fc against PDC-E2

A single gene library was built with the genes coding for InlA, FBA, and PDC-E2 following procedures already described (Moreira et al., 2018; Fühner et al., 2019). Briefly, the gene was amplified via PCR with Phusion DNA polymerase (Thermo Scientific), fragmented with sonication using Bioruptor Plus (Diagenode), and cloned into pHORF3 phagemid after DNA end repair reaction with Fast DNA End Repair (Thermo Scientific). After ligation with T4 DNA ligase (Promega), the reaction product was purified with Ultracel-0.5 mL Ultracel-30K columns (Amicon) and used to transform *E. coli* SS320 (Lucigen) via electroporation. The transformed cells were spread onto 2xYT-GA agar 25-cm plates, and onto 10-cm plates for titration and library checking. Some colonies were picked from the latter plates and amplified via colony PCR to

check the insert rate of the ligation. While from the former plate, the cells were taken and used to perform library packaging with Hyperphage. For this, the bacteria were scraped out of the plates with 2xYT-GA, grown until OD_{600}=0.5, and infected with Hyperphage. After growing for 24 h at 30 °C, the packaged library was precipitated from the supernatant with PEG/NaCl solution and titrated using *E. coli* XL1-Blue MRF'. From the titration plates, some clones were sent for sequencing to check the in-frame rate of the library.

The panning was performed in a way similar to the ORFeome panning for target identification. Briefly, 1 µg of each antibody was coated on a well of and ELISA plate, and the pre-incubation with three wells was done the same way. In this case, 10^9 CFU were used per panning well, and only the first panning round was conducted. The screening was done the same way, once reactive clones were sent for sequencing and the resulting sequences were aligned with ClustalOmega software to define the minimal sequence of recognition (MSR, defined as the shortest sequence present on every clone sent for sequencing).

3.13 Sequence analysis of PDC-E2 and FBA

The protein sequences of the target PDC-E2 detected with MS and ORFeome phage display, as well as of the FBA (Mendonça et al., 2016), were compared to sequences of the related protein from the species used in the indirect ELISA (Table 3 and Table 4). The identity and similarity were calculated with the online tool EMBOSS Needle (Li et al., 2015). The sequence of PDC-E2 (GenBank code: WP_107899613.1) was also analyzed with SMART online software (Letunic & Bork, 2018), which allowed defining the different regions of the protein.

Table 3. GenBank codes, identity and similarity of the PDC-E2 sequences from the organisms used in indirect ELISA.

Organism	GenBank code	Identity (%)	Similarity (%)	Gaps (%)
Listeria monocytogenes[a,*]	WP_107899613.1	100.0	100.0	None
L. innocua[b]	WP_010990728.1	99.3	99.4	None
L. marthii[c]	EFR88158.1	98.2	98.9	None
L. welshimeri	WP_011701854.1	98.2	98.7	None
L. ivanovii	WP_014092472.1	97.1	98.2	None
L. seeligeri	WP_012985326.1	96.1	97.6	None
L. floridensis	WP_036096782.1	83.2	89.6	1.8
L. fleischmannii subsp. fleischmannii	WP_007472784.1	83.0	89.4	2.7
L. aquatica	WP_036071619.1	82.7	89.6	2.6
L. grayi	WP_036106310.1	82.4	88.5	2.2
L. cornellensis	WP_036077440.1	82.0	89.5	2.5
L. rocourtiae	WP_036070034.1	82.0	89.3	2.2
L. booriae	WP_036086614.1	81.9	89.5	3.2
L. riparia	WP_036098974.1	81.9	89.5	3.2
L. weihenstephanensis	WP_036063351.1	81.9	89.3	2.9
L. grandensis	WP_036067464.1	81.9	89.1	2.9
L. newyorkensis	WP_059140683.1	81.9	88.9	2.9
Salmonella enterica	WP_073877127.1	36.3	54.7	10.6
Escherichia coli	WP_057699170.1	35.4	53.3	11.1
Pseudomonas aeruginosa	WP_042930711.1	35.0	53.5	6.9
Klebsiella pneumoniae	KMH79087.1	34.6	53.4	10.6
K. aerogenes	WP_058655303.1	34.9	52.9	10.6
Enterobacter cloacae	WP_023480469.1	30.7	47.2	21.4
Staphylococcus aureus[d]	WP_061644423.1	51.8	60.8	24.8
Enterococcus faecalis	WP_010827359.1	62.9	73.9	5.2
E. faecium	WP_104674310.1	60.7	73.2	5.2
E. lactis	NF	NF	NF	NF
Lactobacillus paracasei	WP_003598571.1	55.7	70.7	6.6
Bacillus cereus	WP_078181369.1	52.3	62.6	23.4
B. thuringiensis	WP_000863429.1	51.7	63.3	23.4
B. subtilis	WP_060398546.1	50.4	61.9	24.6
Lactococcus lactis	WP_011675116.1	44.4	62.1	4.7
Jonesia denitrificans	WP_015772709.1	26.3	39.7	30.9

[a] Sequence found with MS.

[b] Sequence found via ORFeome phage display followed by BLASp.

[c] Sequence is “partial”.

[d] *S. aureus* was not included in the indirect ELISA experiments due to protein A-related background on every well.

NF, not found with BLASTp.

* *L. monocytogenes* sequence was used as reference in the alignment.

Table 4. GenBank codes, identity and similarity of the PDC-E2 sequences from the non-*Listeria* organisms used in indirect ELISA.

Organism	GenBank code	Identity (%)	Similarity (%)	Gaps (%)
Listeria monocytogenes	WP_003729264.1	100.0	100.0	None
Salmonella enterica	WP_023200272.1	40.1	57.5	2.1
Escherichia coli	WP_053287829.1	52.1	70.5	1.7
Pseudomonas aeruginosa	WP_065278711.1	32.5	49.0	21.3
Klebsiella pneumoniae	WP_115196261.1	51.6	67.2	1.4
K. aerogenes	WP_023312727.1	50.9	66.9	1.4
Enterobacter cloacae	WP_063624399.1	42.2	58.8	6.1
Staphylococcus aureus [a]	WP_001662541.1	65.6	78.6	0.4
Enterococcus faecalis	WP_010818782.1	51.5	68.4	3.1
E. faecium	WP_002345564.1	50.9	68.4	3.1
E. lactis	NF	---	---	---
Lactobacillus paracasei	WP_128538748.1	47.1	64.6	2.7
Bacillus cereus	WP_098682829.1	70.2	80.7	0.4
B. thuringiensis	WP_042969964.1	70.2	80.7	0.4
B. subtilis	WP_014481411.1	60.7	74.5	2.1
Lactococcus lactis	WP_075525349.1	48.0	65.7	6.0
Jonesia denitrificans	WP_015772663.1	28.8	44.4	22.2

[a] *S. aureus* was not included in the indirect ELISA experiments due to protein A-related background on every well.

NF, not found with BLASTp.

* *L. monocytogenes* sequence was used as reference in the alignment.

4 RESULTS

4.1 Antibody panning over *Listeria* protein fractions provides useful binders for detection

Antibodies were generated against *Listeria* protein fractions by phage display and, after screening of monoclonal binders, four scFv-Fc were validated by titration ELISA over alive bacterial cells (Fig. 1). These four antibodies allowed the detection of both pathogenic (*L. monocytogenes*) and non-pathogenic (*L. innocua*) species of *Listeria*, while showing practically no reaction with the non-related species *B. subtilis*. Even though just a small number of strains was used, it is possible to affirm that the target is accessible on the surface of the coated cells.

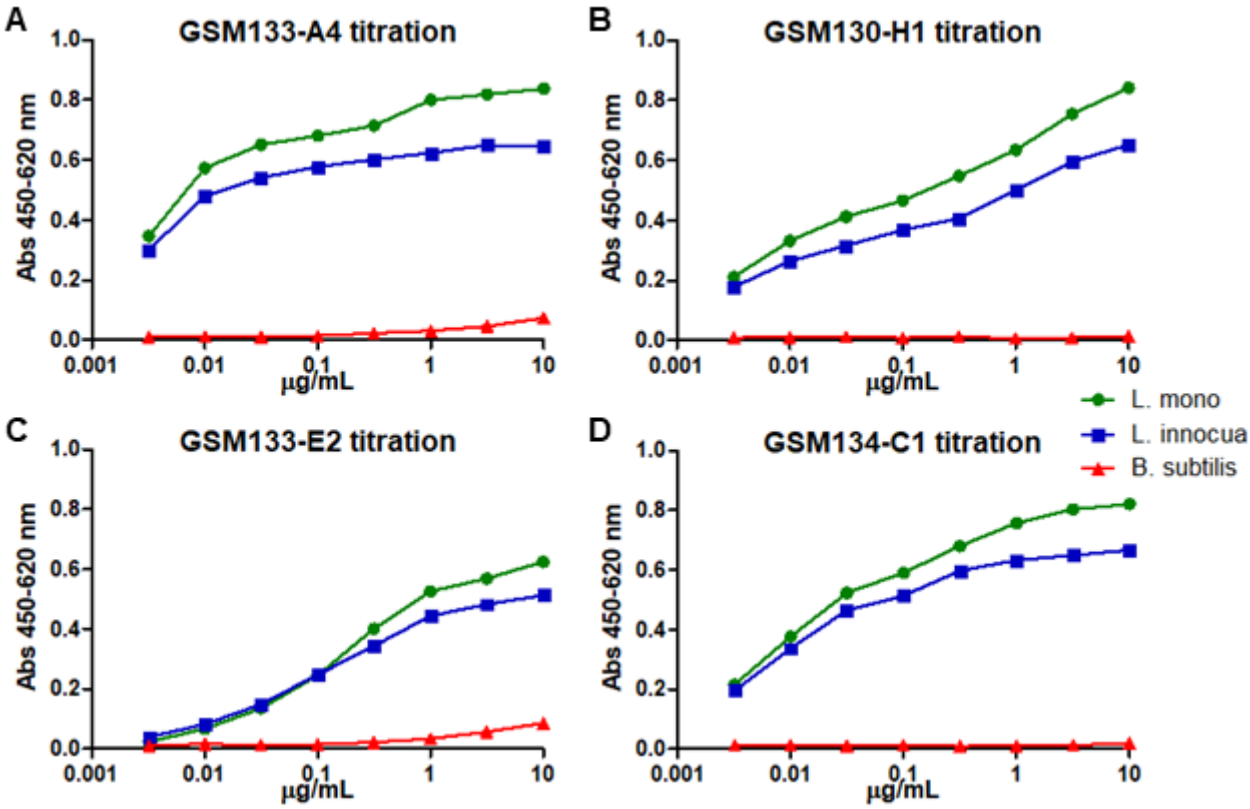

Figure 12. ELISA of the scFv-Fc antibodies generated against *Listeria* protein fractions. The monoclonal scFv-Fc GSM133-A4 (**A**), GSM130-H1 (**B**), GSM133-E2 (**C**), and GSM134-C1 (**D**) were diluted √10-fold from 10 µg/mL until 3.2 ng/mL. Then, they were tested against three strains coated alive onto ELISA plates: *L. monocytogenes* ATCC 7644 (L. mono), *L. innocua* DSM 20649 (L. innocua), and *B. subtilis* 168 NCIB 10106 (B. subtilis).

In addition to the ELISA, these initial four antibodies were tested in immunoblot against cell wall and cytoplasm fractions of *L. innocua*. The results indicate that the

target protein is present on both fractions with apparent more concentration in the cytoplasm (Figure 13). This way, it was possible to explain the ELISA results, in which alive cells were detected when coated on a plate, indicating its actual location on the cell surface. Although the EC_{50} could not be precisely determined, GSM133-A4 showed the best binding, since the highest dilution presented about 2-fold higher signal when compared to the other antibodies. Thus, this antibody was chosen for further initial characterization of the target.

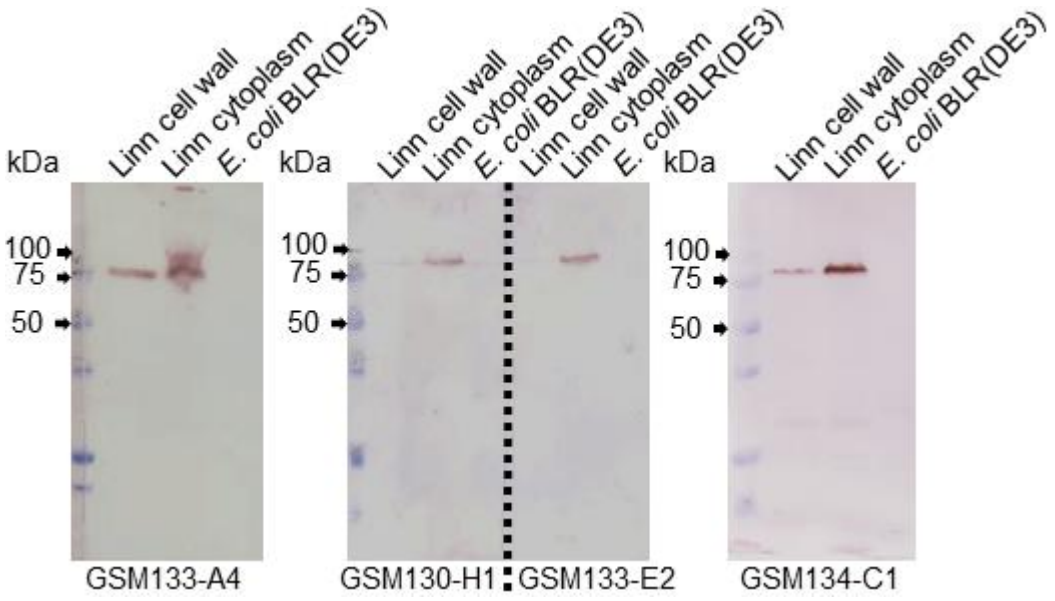

Figure 13. Immunoblot of the scFv-Fc antibodies generated against *Listeria* protein fractions. The monoclonal scFv-Fc GSM133-A4, GSM130-H1, GSM133-E2, and GSM134-C1 were diluted and tested against protein fractions from cell wall and cytoplasm of *L. innocua* DSM 33090 (Linn). The strain *E. coli* BLR(DE3) was used as negative control.

4.2 ORFeome phage display provides similar results to those from mass spectrometry regarding target identification

After generating antibodies against protein mixtures of *Listeria*, the target was identified by either IMS-MS and ORFeome phage display. In order to have samples suitable to MS, IMS was made using GSM133-A4 to isolate the target from the cytoplasmic protein mixture. This procedure led to the proper isolation of the target, as confirmed by SDS-PAGE and immunoblot (Fig. 2A). In addition to the target, other proteins (named as “unknown” 1-3) were also detected in SDS-PAGE. This way, all proteins were cut from the gel and analyzed by MS, which identified the protein

dihydrolipoamide acetyltransferase (GenBank: WP_010990728.1), also known as pyruvate dehydrogenase complex - enzyme 2 (PDC-E2), as the target. While the unknown proteins 2 and 3 were detected as PDC-E1α (GenBank: WP_072572643.1) and PDC-E1β (GenBank: WP_038409535.1). Considering this information, it is possible to assume that the “unknown 1” protein would refer to PDC-E3, meaning that the whole complex was captured in the procedure, but it was not properly detected due to its close proximity with the scFv-Fc. The MS analysis was done in by the Proteomics group of Helmholtz-Zentrum für Infektionsforschung (HZI) under the supervision of Prof. Dr. Lothar Jänsch.

In parallel to the MS analysis, ORFeome phage display was performed to identify the target of the four initial antibodies (GSM130-H1, 133-A4, 133-E2, and 134-C1) using an antigen library built with the genome of *L. monocytogenes* ATCC 7644. With this approach, the identified target was also PDC-E2 (GenBank: WP_107899613.1, Table 5). Out of the four antibodies used, only GSM134-C1 did not allow to identify the target (Fig. 2B). Moreover, the panning with GSM133-A4 resulted in two hits: one referring to PDC-E2, and another to a non-related protein that was discarded due to low reactivity (data not shown).

Table 5. Summary of the hits found by mass spectrometry or ORFeome phage display.

Technique	Antibody used	GenBank code	Protein information [a]
Mass spectrometry	GSM133-A4	WP_010990728.1	dihydrolipoamide acetyltransferase, *Listeria innocua* (target)
		WP_072572643.1	pyruvate dehydrogenase (acetyl-transferring) E1 component subunit alpha, *Listeria monocytogenes* (unknown 2)
		WP_038409535.1	alpha-ketoacid dehydrogenase subunit beta, *Listeria monocytogenes* (unknown 3)
ORFeome phage display	GSM130-H1, GSM133-A4, GSM133-E2	WP_107899613.1 [b]	dihydrolipoamide acetyltransferase, *Listeria monocytogenes*

[a] For mass spectrometry, the protein information also contain the protein identification used in Figure 3 of the main article in parenthesis. For ORFeome phage display, the antibody used for target identification, also shown in Figure 3, is in parenthesis.

[b] This code refers to the cloned sequence used in further steps, which was present in the BLASTx results of the output sequences for the mentioned antibodies.

To confirm that the isolated antigen fragments were actual correct targets, some were produced as monoclonal phage and tested by ELISA against the respective antibodies. This showed that every antibody-peptide phage combination was correct, presenting higher reactions then the negative control in a concentration-dependent way (Fig. 2C). In addition, since the isolated fragments of the 3 antibodies are close related to each other in the protein sequence, some were tested with GSM134-C1, which did not select any fragment on panning. The result showed that this scFv-Fc can recognize the peptides isolated from panning with other antibodies, indicating that it may bind to a similar region. Furthermore, it is important to mention that the reactions of GSM133-E2 was lower than other antibodies, indicating a different behavior of this scFv-Fc.

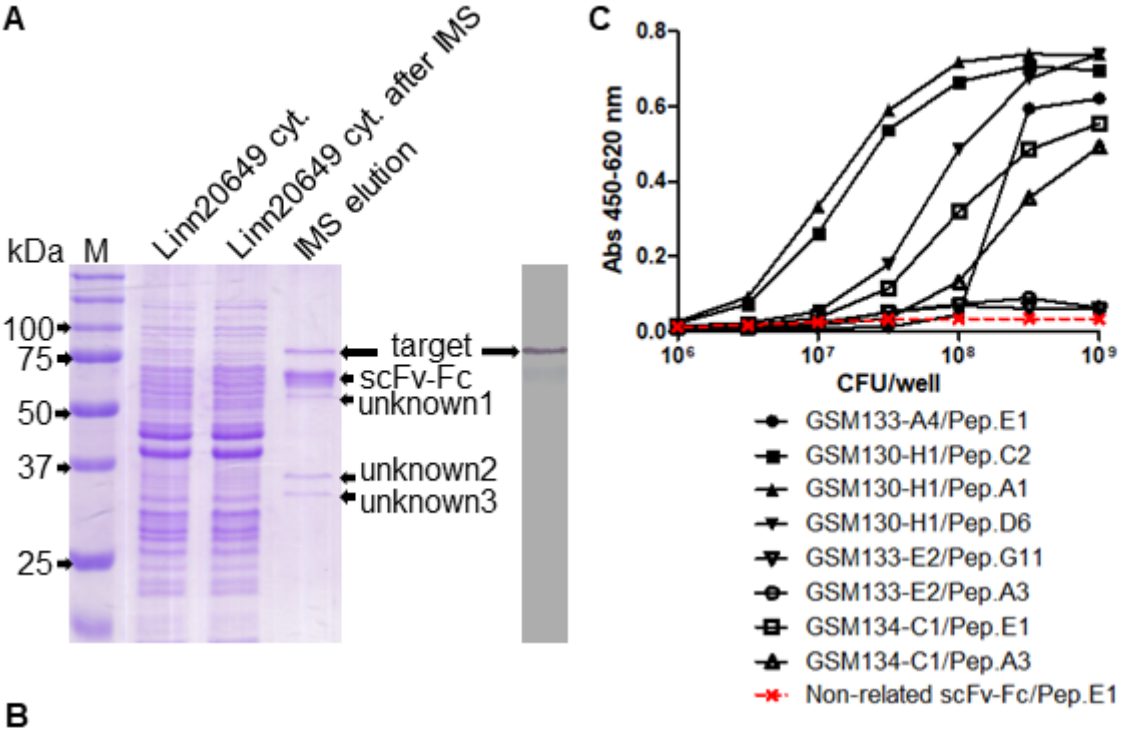

B

```
WP_107899613.1    1   MAYSFKLPDIGEGIHEGEIVKWFVQPGDKIEEDESLFEVQNDKSVEEITSPVSGTIKEIK   60
GSM130-H1             ------------------------------------------------------------
GSM133-A4         3   ---SFKLPDIGEGIHEGEIVKWFVQPGDKIEEDESLFEVQNDKSVEEITSPVSGTIKEIK   60
GSM133-E2             ------------------------------------------------------------

WP_107899613.1    61  VAEGTVATVGQVLVTFDGVEGHEDDAEEESAAPKAESTESTPAPAQASGKGIFEFKLPDI   120
GSM130-H1         113 ------------------------------------------------FEFKLPDI   120
GSM133-A4         61  VAEGTVATVGQVLVTFDGVEGHEDDAEEESAAPKAESTESTPAPAQASGKGIFEFKLPDI   120
GSM133-E2         98  ----------------------------------TESTPAPAQASGKGIFEFKLPDI   120

WP_107899613.1    121 GEGIHEGEIVKWFIQPGDKVEEDQSIFEVQNDKSVEEITSPVDGTVKDILVSEGTVATVG   180
GSM130-H1         121 GEGIHEGEIVKWFIQPGDKVEEDQSIFEVQNDKSVEEITSPVDGTVKDILVSEGTVATVG   180
GSM133-A4         121 GEGIHEGEIVKWFIQPGDKVEEDQSIFEVQNDKSVEE----------------------   142
GSM133-E2         121 GEGIHEGEIVKWFIQPGDKVEEDQSIFEVQNDKSVEEITSPVDGTVKDILVSEGTVATVG   180

WP_107899613.1    181 QVLVTFEGDFEGEASHESTPESPAEEAEL   209
GSM130-H1         181 QVLVTFEGDFEGEA--------------   194
GSM133-A4             ----------------------------
GSM133-E2         181 QVLVTFEGDFEGEASHESTPESPAEEAEL   209
```

Figure 14. Identification of the target via MS and ORFeome phage display. (**A**) SDS-PAGE and immunoblot after IMS with GSM133-A4. (**B**) Alignment of the first 209 amino acids of a reference PDC-E2 sequence (WP_107899613.1) with the MSR of scFv-Fc GSM130-H1, GSM133-A4, and GSM133-E2 after ORFeome phage display. (**C**) Titration curves of the 4 initial scFv-Fc against different amounts of monoclonal phage isolated in the ORFeome phage display for target identification.

4.3 PDC-E2 target is detectable by fluorescent microscopy, giving more evidence for its location on bacterial cell surface

In order to check the accessibility of PDC-E2 on the bacterial surface and the ability of the PDC-E2 target in being recognized by antibodies in microscopy, GSM133-A4 was also employed to stain *L. monocytogenes* ser. 4b DSM 15675 in fluorescence microscopy (Fig. 3B). The negative control with a non-related scFv-Fc shows imperceptible fluorescence in Cy5 channel. On the other hand, the positive control using a scFv-Fc anti-InlA, which is a well-characterized target that is linked to the cell wall and displayed on the surface of *L. monocytogenes*, showed better visible fluorescence. In its turn, the Cy5 fluorescence of GSM133-A4 showed to be much clearer, demonstrating that the target is actually accessible on *Listeria* cell surface and likely laying on *Listeria* cell wall. This procedure was done together with Dr. Christian Boedeker in DSMZ.

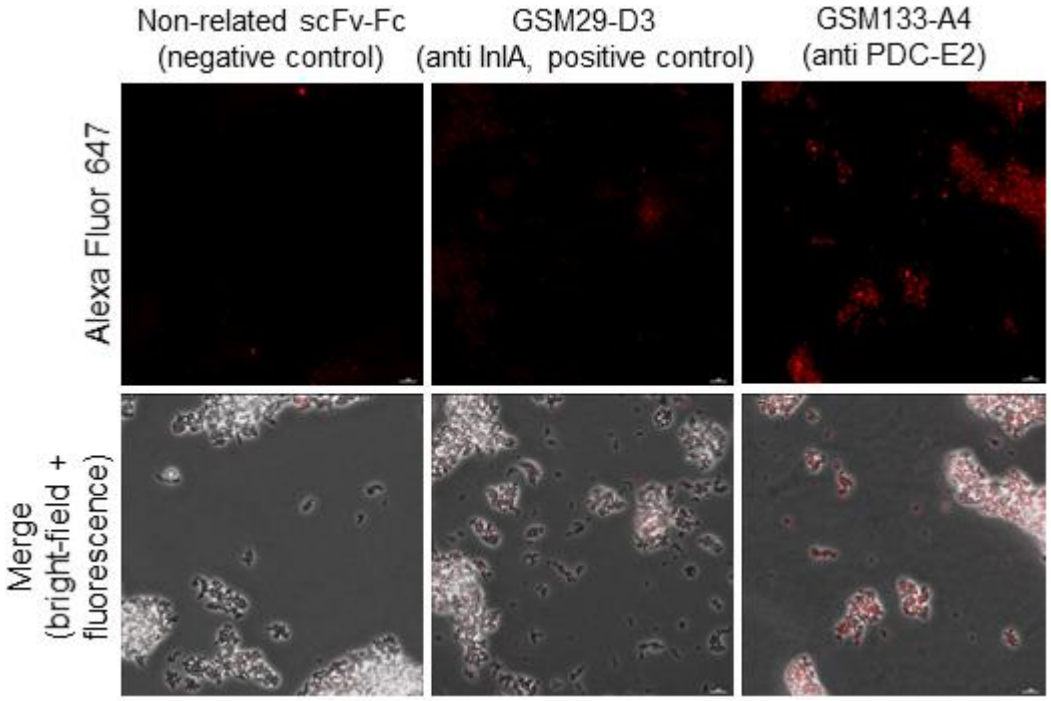

Figure 15. Fluorescence microscopy of GSM29-D3 (anti InlA) and GSM133-A4 (anti PDC-E2) over alive *L. monocytogenes* 4b DSM 15675. When comparing the signals of both scFv-Fc with those from the negative control with a non-related antibody, it is possible to confirm that they are applicable for fluorescent microscopy. Moreover, the experiment indicates that the target of GSM133-A4 is accessible on *Listeria* cell surface, more likely laying on the cell wall.

4.4 Antibody panning over purified recombinant PDC-E2 increases the number of generated binders

In order to increase the set of antibodies against PDC-E2, a second antibody panning was performed, this time, over the recombinant protein. For this, PDC-E2 gene was cloned and expressed as a recombinant protein in *E. coli*. Then, the purified protein was used to select antibodies from HAL9 and HAL10 libraries, which were now mixed in the same panning well. With this approach, other 16 binders were identified and produced as scFv-Fc. Initial tests showed that they bind specifically to *Listeria* spp. when using 4 strains for an initial screening and are all able to recognize recombinant PDC-E2 in immunoblot and ELISA (Fig. 4 and Fig. 5). This way, antibody panning over the purified antigen could increase the number of useful binders, allowing the generation of approximately 4 times more antibodies when compared to the panning on subcellular fractions.

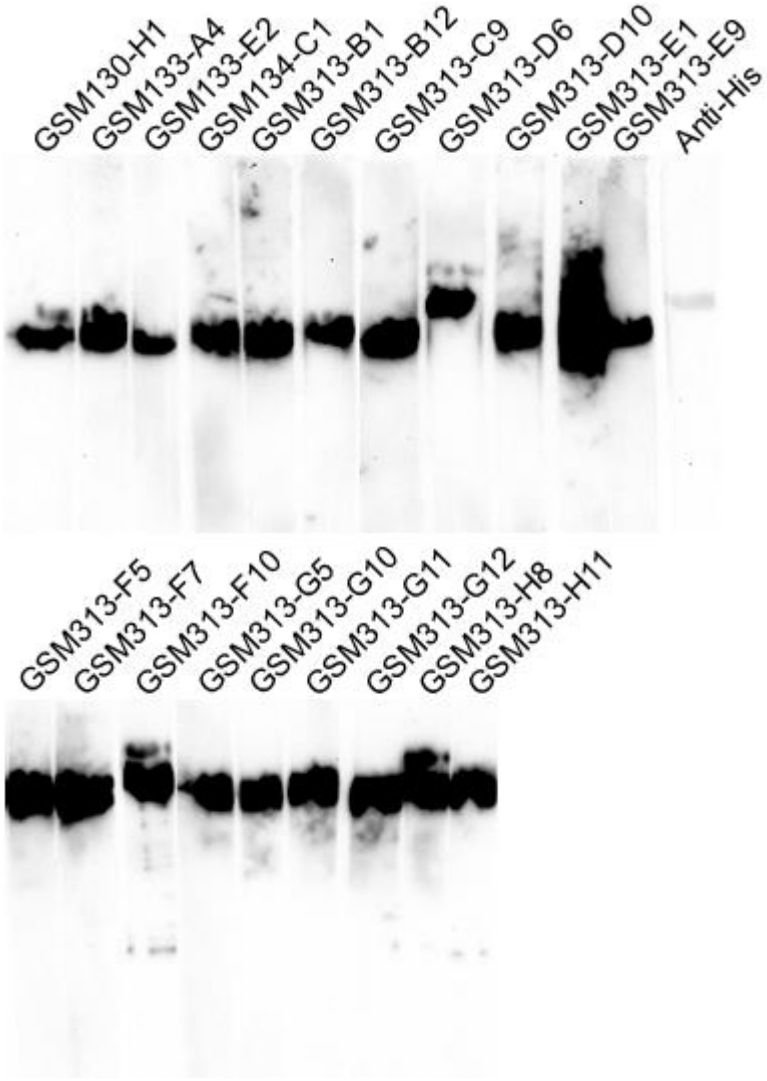

Figure 16. Immunoblot of the scFv-Fc antibodies generated against the purified recombinant PDC-E2. The 20 newly generated scFv-Fc were diluted to 1 µg/mL and tested against 1 µg of the recombinant PDC-E2.

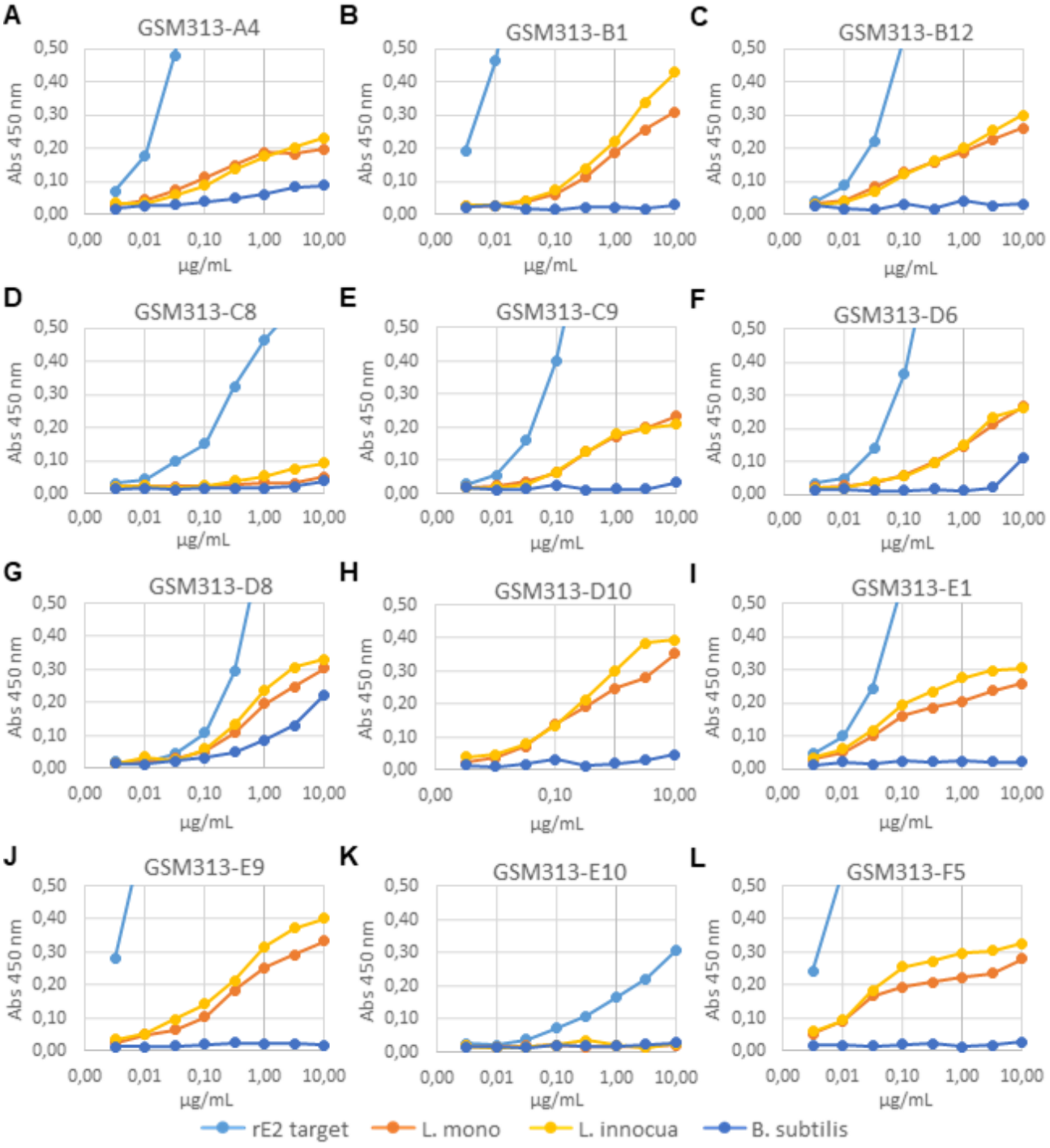

Figure 5 continues on the next page.

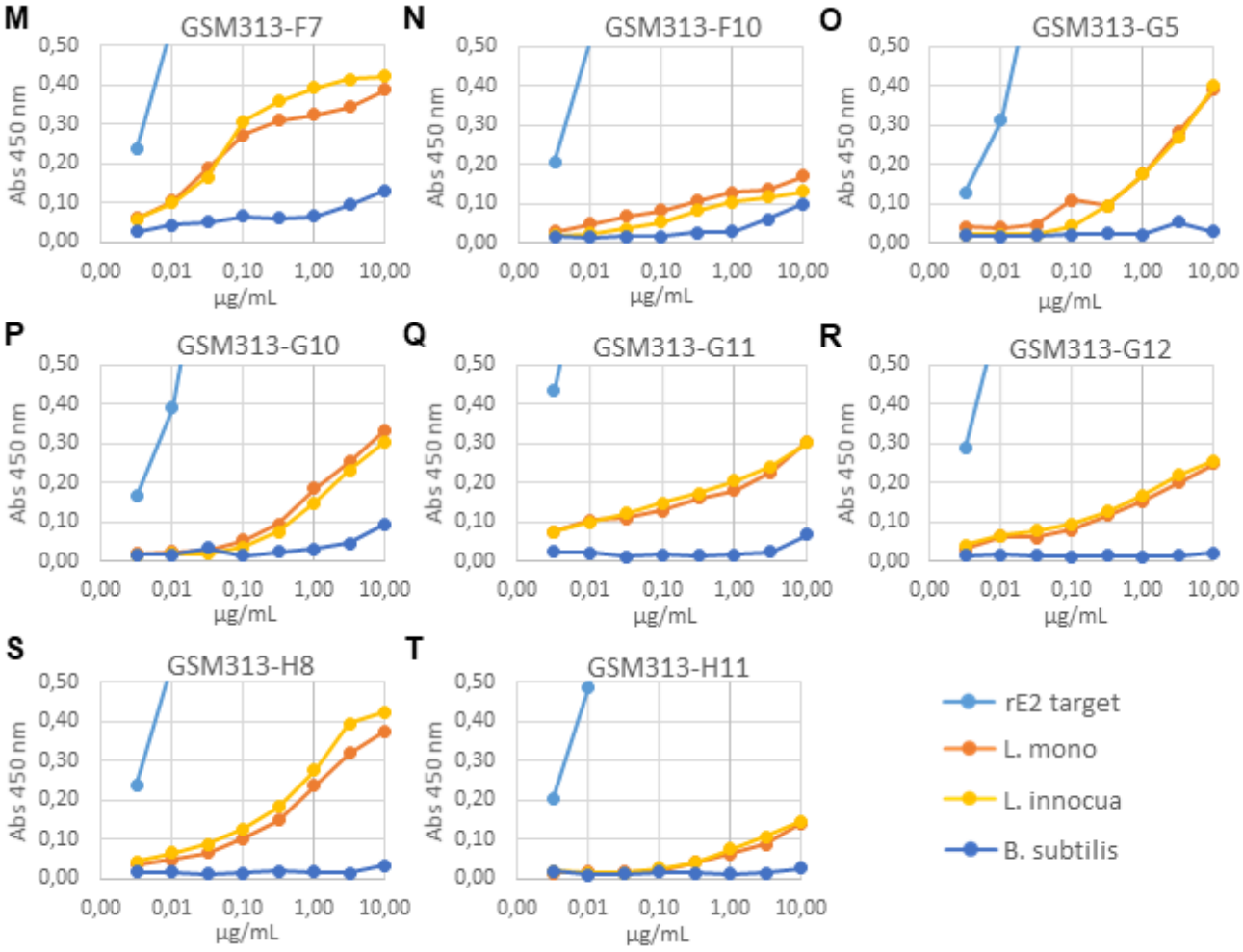

Figure 17. ELISA of the scFv-Fc antibodies generated against the purified recombinant PDC-E2. The 20 newly generated scFv-Fc (**A-T**) were diluted √10-fold from 10 µg/mL until 3.2 ng/mL. Then, they were tested against the recombinant PDC-E2 (rE2 target) and three strains coated alive onto ELISA plates: *L. monocytogenes* ATCC 7644 (L. mono), *L. innocua* DSM 20649 (L. innocua), and *B. subtilis* 168 NCIB 10106 (B. subtilis).

4.5 PDC-E2 target allows the detection of every *Listeria* spp. via indirect ELISA

In total, 20 scFv-Fc against PDC-E2 were used in indirect ELISA for *Listeria* spp. detection. When performing the ROC analysis, the concentrations showing the best AUC were used to estimate the best equilibrium of sensitivity and specificity. Out of this antibody set, two scFv-Fc (GSM313-E9, and GSM313-H8) showed to discriminate *Listeria* spp. from other tested species with 100 % sensitivity and specificity, with AUC=1.0 (Table 6). Thus, these two were considered the most suitable for detection. The next three antibodies with best performance are GSM313-F5,

GSM313-G12, and GSM130-H1, from which it is interesting to observe that GSM130-H1 is the only one derived from the panning over *Listeria* protein fractions.

Table 6. Diagnostic performance of all the scFv-Fc targeting PDC-E2.

Antibody	Best concentration [a]	Sensitivity % (CI)	Specificity % (CI)	AUC (CI)
GSM313-E9	EC_{50}+	100.0 (82.35-100.0)	100.0 (78.20-100.0)	1.0 (1.0)
GSM313-H8	EC_{50}+	100.0 (82.35-100.0)	100.0 (78.20-100.0)	1.0 (1.0)
GSM313-F5	EC_{50}+	94.74 (73.97-99.87)	100.0 (78.20-100.0)	0.993 (0.9746-1.011)
GSM313-G5	EC_{50}-	100.0 (82.35-100.0)	93.33 (68.05-99.83)	0.993 (0.9745-1.011)
GSM130-H1	EC_{50}+	94.74 (73.97-99.87)	93.33 (68.05-99.83)	0.9895 (0.9663-1.013)
GSM313-G12	EC_{50}+	89.47 (66.86-98.70)	100.0 (78.20-100.0)	0.986 (0.9574-1.014)
GSM313-D10	EC_{50}+	94.74 (73.97-99.87)	93.33 (68.05-99.83)	0.9789 (0.939-1.019)
GSM313-C9	EC_{50}+	89.47 (66.86-98.70)	100.0 (78.20-100.0)	0.9579 (0.8904-1.025)
GSM313-D6	EC_{50}	84.21 (60.42-96.62)	100.0 (78.20-100.0)	0.9439 (0.8705-1.017)
GSM313-G11	EC_{50}+	89.47 (66.86-98.70)	86.67 (59.54-98.34)	0.9439 (0.8693-1.018)
GSM313-B1	EC_{50}-	100.0 (82.35-100.0)	80.0 (51.91-95.67)	0.9404 (0.8646-1.016)
GSM134-C1	EC_{50}-	94.74 (73.97-99.87)	80.0 (51.91-95.67)	0.8965 (0.7803-1.013)
GSM133-A4	EC_{50}	94.74 (73.97-99.87)	80.0 (51.91-95.67)	0.8947 (0.7815-1.008)

GSM313-H11	EC_{50}+	89.47 (66.86-98.70)	86.67 (59.54-98.34)	0.8596 (0.7135-1.006)
GSM313-E1	EC_{50}+	94.74 (73.97-99.87)	80.0 (51.91-95.67)	0.8246 (0.6465-1.003)
GSM313-F7	EC_{50}	73.68 (48.80-90.85)	73.33 (44.90-92.21)	0.7895 (0.618-0.9609)
GSM133-E2	EC_{50}-	78.95 (54.43-93.95)	73.33 (44.90-92.21)	0.7789 (0.5889-0.969)
GSM313-B12	EC_{50}+	73.68 (48.80-90.85)	66.67 (38.38-88.18)	0.7789 (0.6205-0.9374)
GSM313-F10	EC_{50}+	94.74 (73.97-99.87)	66.67 (38.38-88.18)	0.7158 (0.5034-0.9282)
GSM313-G10	EC_{50}-	63.16 (38.36-83.71)	66.67 (38.38-88.18)	0.6632 (0.4727-0.8536)

[a] As mentioned in the material and methods section, the antibody concentrations used were: the EC_{50}; a √10-fold concentration above the EC_{50} (EC_{50}+); and a √10-fold concentration below (EC_{50}-).

When analyzing the reaction of the antibodies against the tested strains, it is possible to observe some important aspects of recognition. One of them is that the species *L. aquatica*, *L. grayi*, and *L. cornellensis* were difficult to be recognized, since 11, 8, and 7, respectively, out of the 20 antibodies were not able to detect these species (Fig. 6). Other important observation is that most of the reactions with non-*Listeria* species were against *Enterococcus* (11/20) and *Bacillus* (8/20) genus, sometimes with more than one species of each. This fact may imply that the recognition of these antibodies are not unspecific, but undesired, since it appears that Gram-positives may have a preference on the recognition of PDC-E2. In accordance to this, PDC-E2 sequences from both *Enterococcus* and *Bacillus* are the ones showing to be closer related to the one from *L. monocytogenes*, around 50-60 % identity, while the other strains, except *L. paracasei* (55.7 %), did not surpass 45 % (Table 3).

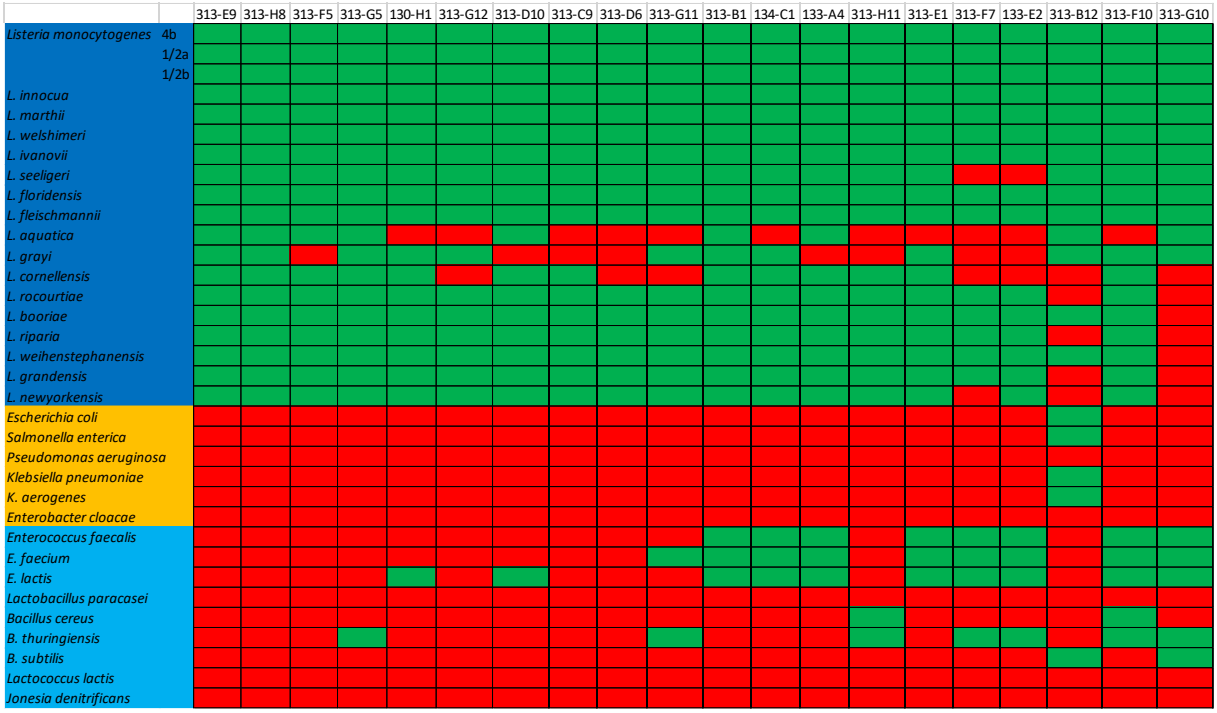

Figure 18. Reaction profile of the 20 antibodies targeting PDC-E2 in indirect ELISA. Indirect ELISA was done with 19 *Listeria* strains (dark blue background) and 15 non-*Listeria* strains, including Gram-negative (golden background) and Gram-positive (light blue background). After performing a ROC curve analysis, the cut-off value for each antibody was used to determine positive (green) and negative (red) reactions.

4.6 Most of the generated antibodies against PDC-E2 recognize the lipoyl domains (LD)

To further analyze the anti-PDC-E2 antibodies, their MSR was determined with single-gene phage display using a library displaying fragments of PDC-E2. This way, the 18 of the 20 antibodies used for the indirect ELISA had their binding region defined. Interestingly, all but one of the mapped antibodies showed to bind the same region, which was either the 1st or 2nd LD (Table 7). Besides this, some cases are worth to be mentioned. One is that 4 out of 18 antibodies (GSM133-A4, GSM313-D10, -F7, and -G10) are able to recognize both LD domains, although one is preferred. Another case is with GSM133-E2, which initially showed very low reactions, resulted in one clone that was not initially defined as its binding region and one nonsense clone. Thus, this antibody was tested in IgG format, which was then able to reproduce the results from ORFeome phage display, although other binding regions that are not related to each

other were also detected. The last and most intriguing observation of the mapped MSR is regarding GSM313-E9 and -H8. As aforementioned, these antibodies were the only ones to show 100 % sensitivity and specificity in the indirect ELISA experiments. Likewise, these two antibodies were also the only ones to bind a synthetic sequence, composed by a mixture of the 1st and 2nd LD. The data for MSR of the scFv-Fc against PDC-E2 is part of the Master thesis of Sara Mara Stella Köllner.

Table 7. Epitope mapping results of the anti-PDC-E2 antibodies used in indirect ELISA.

Antibody	AUC	MSR location	MSR length (amino acids)	Domain (nº of sequences)
GSM313-E9	1.0	115-185	71	2nd (12/13), synthetic (1/13) LD
GSM313-H8	1.0	104-188	85	2nd (10/12), synthetic (2/12) LD
GSM313-F5	0.993	115-185	68	2nd LD (14/14)
GSM313-G5	0.993	103-188	86	2nd LD (11/11)
GSM130-H1	0.9895	113-188	76	2nd LD (23/23)
GSM313-G12	0.986	108-187	80	2nd LD (11/11)
GSM313-D10	0.9789	5-79, 115-188	74, 74	1st (12/15), 2nd (3/15) LD
GSM313-C9	0.9579	5-79	74	1st LD (13/13)
GSM313-D6	0.9439	109-191	83	2nd LD (4/4)
GSM313-G11	0.9439	108-188	81	2nd LD (11/11)
GSM313-B1	0.9404	108-188	81	2nd LD (11/11)
GSM134-C1	0.8965	106-192	87	2nd LD (14/14)
GSM133-A4	0.8947	108-188	81	1st LD (3/21), 2nd LD (18/21)
GSM313-H11	0.8596	232-305	73	PDC-E3 binding domain (12/12)
GSM313-E1	0.8246	NM	NM	NM
GSM313-F7	0.7895	3-77, 115-187	73, 75	1st (9/11), 2nd (2/11) LD
GSM133-E2	0.7789	402-424	23	catalytic domain (1/2), nonsense (1/2)

GSM133-E2 (IgG)	NT	113-145, 301-359, 526-543	32, 58, 18	2nd LD (9/11), catalytic domain (2/11, different parts)
GSM313-B12	0.7789	5-81	77	1st LD (14/14)
GSM313-F10	0.7158	NM	NM	NM
GSM313-G10	0.6632	3-78, 113-191	79, 76	1st (6/11), 2nd (5/11) LD

NM, not mapped.

NT, not tested.

4.7 scFv-Fc against InlA and InB allow detecting pathogenic *Listeria*, while those against FBA recognize most *Listeria* spp. with reduced diagnostic performance

The scFv-Fc produced against recombinant InlA or InlB were able to recognize the recombinant targets in immunoblot (Fig. 7A), as well as, the three pathogenic *Listeria* tested initially tested (Fig. 7B-F). In indirect ELISA, these antibodies reacted only with the three pathogenic *L. monocytogenes* strains tested, resulting in 100 % sensitivity and specificity, with AUC=1.0 (Table 8). On the other hand, the antibodies against FBA showed slight distinction between the *Listeria* spp. and *B. subtilis* (Fig. 8). In accordance to this, the diagnostic performance was reduced, since GSM309-G5 and GSM310-B12 showed AUC=0.807 and 0.8842, respectively.

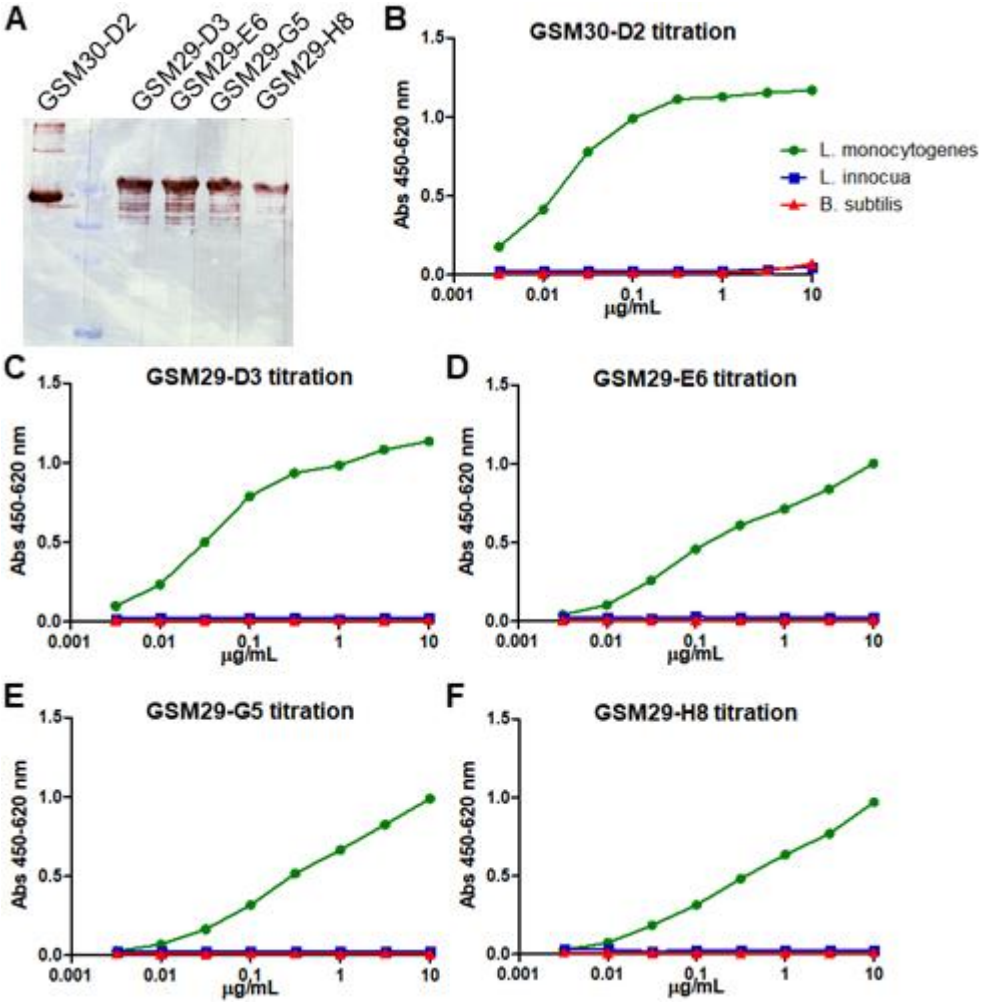

Figure 19. Immunoblot and initial indirect ELISA with anti-InlA and anti-InlB scFv-Fc. (**A**) Immunoblot of GSM30-D2 (anti-InlB) and GSM29-D3, -E6, -G5, and -H8 (anti-InlA) against the recombinant targets. (**B-F**) Titration ELISA with the respective antibodies diluted √10-fold from 10 µg/mL until 3.2 ng/mL. Then, they were tested against three strains coated alive onto ELISA plates: *L. monocytogenes* ATCC 7644 (L. mono), *L. innocua* DSM 20649 (L. innocua), and *B. subtilis* 168 NCIB 10106 (B. subtilis).

Table 8. Diagnostic performance of the scFv-Fc targeting InlA, InlB, and FBA.

Target	Antibody	Best concentration[a]	Sensitivity % (CI)	Specificity % (CI)	AUC (CI)
InlA	GSM29-D3	All tested	100.0 (29.24-100.0)	100.0 (88.78-100.0)	1.0 (1.0)
	GSM29-E6	All tested	100.0 (29.24-100.0)	100.0 (88.78-100.0)	1.0 (1.0)
	GSM29-G5	All tested	100.0 (29.24-100.0)	100.0 (88.78-100.0)	1.0 (1.0)
	GSM29-H8	All tested	100.0 (29.24-100.0)	100.0 (88.78-100.0)	1.0 (1.0)
InlB	GSM30-D2	All tested	100.0 (29.24-100.0)	100.0 (88.78-100.0)	1.0 (1.0)
FBA	GSM309-G5	EC_{50}+	84.21 (60.42-96.62)	66.67 (38.38-88.18)	0.807 (0.6627-0.9513)
	GSM310-B12	EC_{50}+	94.74 (73.97-99.87)	80.00 (51.91-95.67)	0.8842 (0.76-1.008)

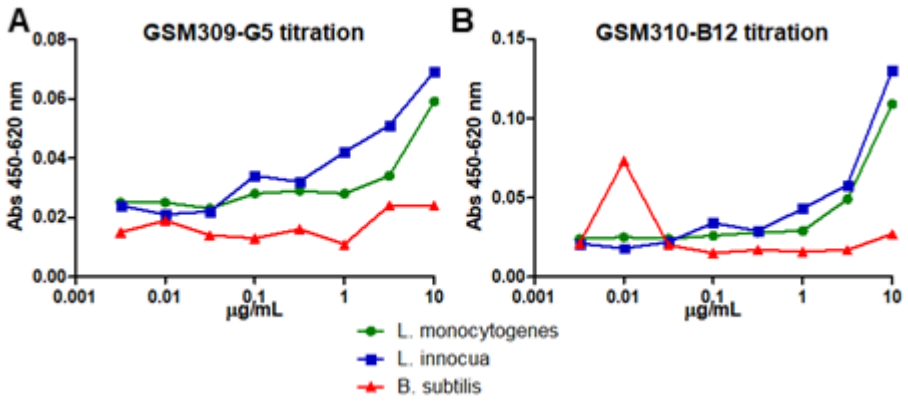

Figure 20. ELISA of the scFv-Fc antibodies against FBA. The monoclonal scFv-Fc GSM309-G5 (A), and GSM310-B12 (B) were diluted √10-fold from 10 µg/mL until 3.2 ng/mL. Then, they were tested against three strains coated alive onto ELISA plates: *L. monocytogenes* ATCC 7644 (L. mono), *L. innocua* DSM 20649 (L. innocua), and *B. subtilis* 168 NCIB 10106 (B. subtilis).

The recognition profile of scFv-Fc against FBA shows a similar behavior to that from scFv-Fc against PDC-E2. In this case, GSM309-G5 is not able to recognize *L. aquatica*, *L. grayi*, and *L. cornellensis*, while reactions against *E. faecium*, *E. lactis*, and *B. cereus* were considered positive. In addition, this antibody also shows positive reactions against the Gram-negative bacteria *P. aeruginosa* and *K. aerogenes* (Fig. 9). Similarly, GSM310-B12 did not detect *L. aquatica*, while showed positive reaction with the three *Enterococcus* species. This way, it is likely that the homology of the target has also an influence on the detectability of the strains, since FBA from all strains detected as positive, except *K. aerogenes*, show high homology to *Listeria* FBA (>50% identity).

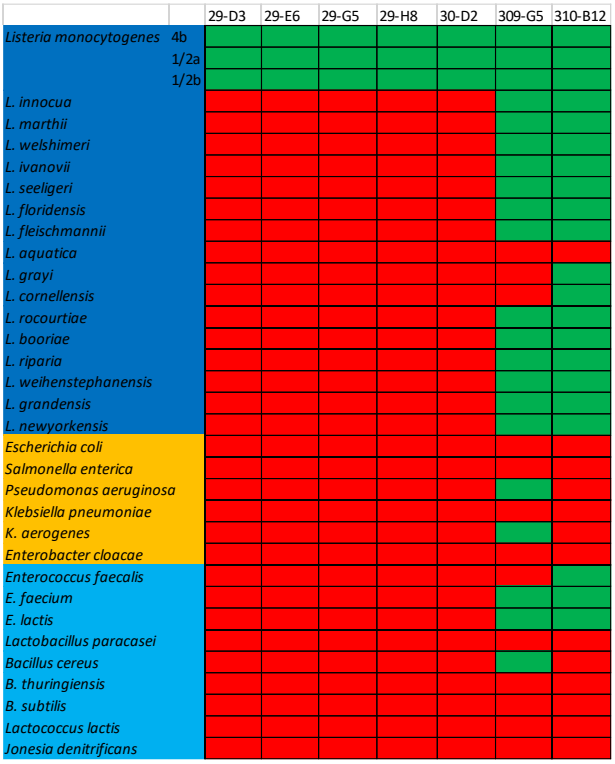

Figure 21. Reaction profile of four scFv-Fc against InlA, one against InlB, and two against FBA in indirect ELISA. Indirect ELISA was done with 19 *Listeria* strains (dark blue background) and 15 non-*Listeria* strains, including Gram-negative (golden background) and Gram-positive (light blue background). After performing a ROC curve analysis, the cut-off value for each antibody was used to determine positive (green) and negative (red) reactions.

4.8 Single gene phage display results in shorter fragments than ORFeome phage display

It is also worth to note that the size of the isolated fragments with the 4 antibodies used for ORFeome phage display could be reduced when using epitope mapping phage display (Table 9). The scFv-Fc antibodies GSM130-H1 and GSM133-A4 showed 7.32 and 47.40 %, respectively, smaller MSR in single gene phage display. While the IgG GSM133-E2 showed 70.54 % reduction in MSR size. In the case of GSM134-C1, the single gene phage display resulted in reactive sequences to determine the MSR, what could not be done with ORFeome phage display. The data for MSR length of the scFv-Fc against PDC-E2 is part of the Master thesis of Sarah Mara Stella Köllner.

Table 9. Comparison of the MSR length between ORFeome phage display and single gene phage display.

Antibody	**MSR length (amino acids)**		**MSR reduction (%)** [a]
	ORFeome phage display	**Single gene phage display**	
2D12	162	98	39.51
3F8	18	10	44.44
GSM130-H1	82	75	8.54
GSM133-A4	154	79, 88	48.70, 42.86
GSM133-E2	112	32 [b]	71.43
GSM134-C1	NH	87	---

NH, no hits.

[a] The MSR reduction indicates how much the fragments from single gene phage display are smaller in comparison to those from ORFeome phage display.

[b] This sequence refers to the MSR in the 2nd LD domain of the IgG molecule, since GSM133-E2 showed multiple MSR.

5 DISCUSSION

Phage display is an important technique to study proteins in a library scale, making it easier to analyze a vast amount of different molecules at the same time. Since antibodies represent the biggest market for biological products, this method is nowadays mostly applied to generate antibodies against interesting targets for diagnostic and treatment purposes (Frenzel et al., 2017). Nonetheless, phage display can also be applied for the study of antigens in order to find biomarkers to be used in diagnostics or vaccines (Kügler et al., 2013). In this case, libraries presenting fragments of antigens are employed, allowing the automatic detection of interesting proteins for application as bioproducts and, thus, giving information about antibody-antigen recognition. Taking this in consideration this, phage display is a versatile technique that allows the generation of antibodies and the discovery of antigens for different applications. In this study, however, an unusual combination of the different phage display techniques was employed. Initially, antibody phage display was used for the discovery of new biomarkers instead of the usually described antigen phage display. For this, subcellular fractions from the target species to be detected (*L. monocytogenes*) was used as target at first. This approach resulted in 4 antibodies useful for detection, showing that the generation of antibodies against complex protein mixtures can also give relevant results. Other works involving viruses, such as Porcine Epidemic Diarrhea Virus (Zhang et al., 2019) and Yellow Fever (Daffis et al., 2005), and the Gram-negative bacteria *Legionella pneumophila* (Kuhn et al., 2017), also describe the generation of antibodies against multiple proteins as a target. However, in the case of viruses, the targets are usually known and their number is diminished compared to subcellular fractions. In the case of *L. pneumophila*, a panning over whole cells would represent a much more complex pool of targets. Nevertheless, in this case, the *Legionella* cells were previously treated with formaldehyde, what could have impaired the availability of protein targets in the sample and, thus, explaining the acquirement of antibodies against lipopolysaccharide (LPS). A similar study employed antibody phage display to generate scFv specifically against *L. monocytogenes* (Paoli et al., 2004). The protocol employed live cells as target, and included two different strategies with four or seven panning rounds, which resulted in the same binder. Another work with *L. monocytogenes* isolated binders from a peptide library that was able to distinguish the pathogenic species (Morton et al., 2013). In this case, the

procedure also involved negative and positive selections and 5 panning rounds, showing the complexity of the procedure. In accordance to this, even though resulting in different antibodies, the present study also reported that the same target was found with different panning strategies, showing a possible technical limitation when using complex protein mixtures. In summary, this data supports the idea that complex protein mixtures, such as whole cells or subcellular fractions, allow the acquisition of useful binders in phage display, but in a limited way.

Conversely, most of the works regarding antibody generation via phage display describe the use of purified antigens, indicating that this approach may be more successful in providing high-quality antibodies (Rangnoi et al., 2011; Eliyahu et al., 2018; Fühner et al., 2018; Jalilzadeh-razin et al., 2019; Liu et al., 2019). Thus, after identifying the target of the initial four antibodies as PDC-E2, the recombinant version of this protein was produced in *E. coli* and used for another set of antibody panning strategies. In fact, more antibodies were generated with this strategy, which resulted in 16 new scFv-Fc, compared to 4 from the initial strategy. In accordance with the hypothesis that panning over purified antigens can provide higher-quality antibodies, four out of the 16 new antibodies showed better diagnostic performance than the best of the initial 4 (see Table 6). This way, it is possible to confirm that a “2-step antibody phage display” (one against a complex protein mixture, and then against a purified target) is recommended when using antibody phage display as an approach for biomarker discovery (Fig. 10).

Another atypical application of a phage display method in this work was regarding ORFeome phage display. This technique, which employs a library built with antigen fragments from bacterial genomes or cDNA, is often used for the discovery of biomarkers that are tested against sera from patients or other source of polyclonal antibodies (Connor et al., 2016; Zantow et al., 2016; Zantow et al., 2018; Ramli et al., 2019). In the present work, however, this technique was employed for a target identification purpose, which is usually made or confirmed with MS-based techniques. This way, besides the IMS-MS approach to identify the target after the first antibody panning, ORFeome phage display was also applied for the identification of the target. In this approach, 3 out of the 4 antibodies showed the same target as the IMS-MS (Table 5). Only GSM134-C1 showed no positive hit, and GSM133-A4 showed a

reaction with a not-related peptide that was further discarded due to low reaction in screening ELISA. Considering this, it is possible to affirm that ORFeome phage display could provide similar information as IMS-MS regarding target identification, allowing a “phage display-only” approach (Fig. 10, right panel). One limitation, however, is that more than one antibody may be necessary in case some do not present positive hits in screening ELISA, as it was the case of GSM134-C1.

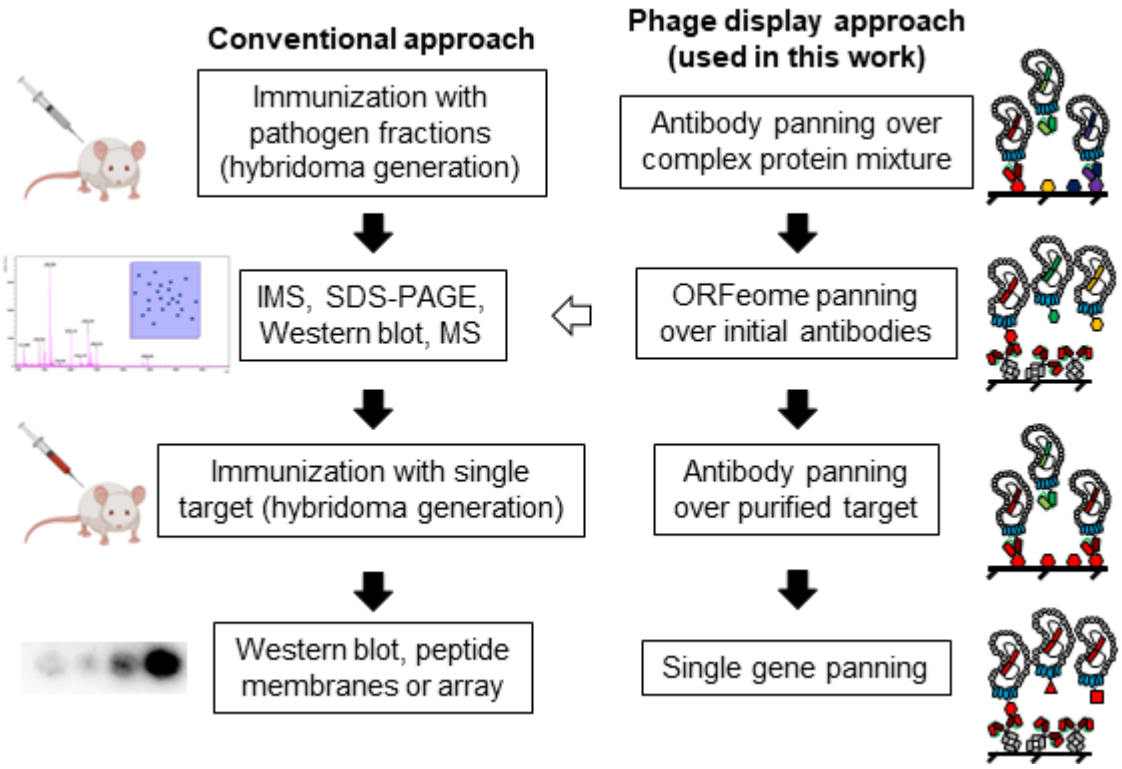

Figure 22. Summary of the workflow with phage display technologies used in this work compared to conventional techniques. In studies aiming to develop antibodies and find new biomarkers, some standard steps must be followed to characterize either the generated antibodies or the discovered antigen. These steps can be achieved with conventional techniques (left workflow), such as hybridoma technology, IMS, MS, and peptide membranes or arrays, which have been successfully applied. In the present study, the conventional techniques could be replaced by the corresponding phage display technique accordingly to the purpose (right workflow). In this phage display approach, IMS-MS was used as validation of the results from ORFeome phage display (empty arrow).

After performing the single gene phage display, it was possible to observe that most of the scFv-Fc against PDC-E2 showed MSR length ranging from 71 and 87 amino acids, referring to the approximate size of one of the LD. This indicates that the

structure of the domain is essential for recognition. More interestingly, the resulting fragments from single gene phage display were smaller than those obtained with ORFeome phage display when using the same antibodies. In the present study, the size of the MSR from single gene panning showed a reduction of 7-70 % depending on the antibody (Table 9). This implies that single gene libraries can in fact give better resolution of binding regions when the target of a set of antibodies is already known. Besides this, single gene phage display allowed to better characterize the antibodies, since it was possible to determine that GSM133-A4 actually recognized both LD of PDC-E2 and to determine the MSR of GSM134-C1, which could not be done with ORFeome. In an already published work, ORFeome allowed to define the MSR of the mAb 3F8 (anti-FBA, hybridoma-derived) as a 25-amino-acid sequence, which fits the size of a normal linear epitope (Mendonça et al., 2016). Moreover, the combination of ORFeome with peptide membrane immunoblot allowed reducing the size of the epitope to 14 amino acids. In the present study, single gene panning was able to reduce the MSR length of 3F8 to 10 amino acids (compared to 18 from ORFeome, 44.44% reduction), making it comparable to other methods, such as the use of peptide membranes (Fig. 11). Regarding 2D12 (anti-InlA, hybridoma-derived) and the recombinant antibodies against PDC-E2, only protein fragments with 75-162 amino acids were able to be detected with either techniques (see Table 9), indicating that phage display procedures allow the study of conformational epitopes. Nevertheless, the consistency of this difference between these two techniques may be subject of further works. Finally, a combination of antibody, ORFeome, and single gene phage display (Fig. 10) allowed generating antibodies, identifying a novel biomarker, and characterizing antibody-antigen interactions that are useful for *Listeria* spp. detection.

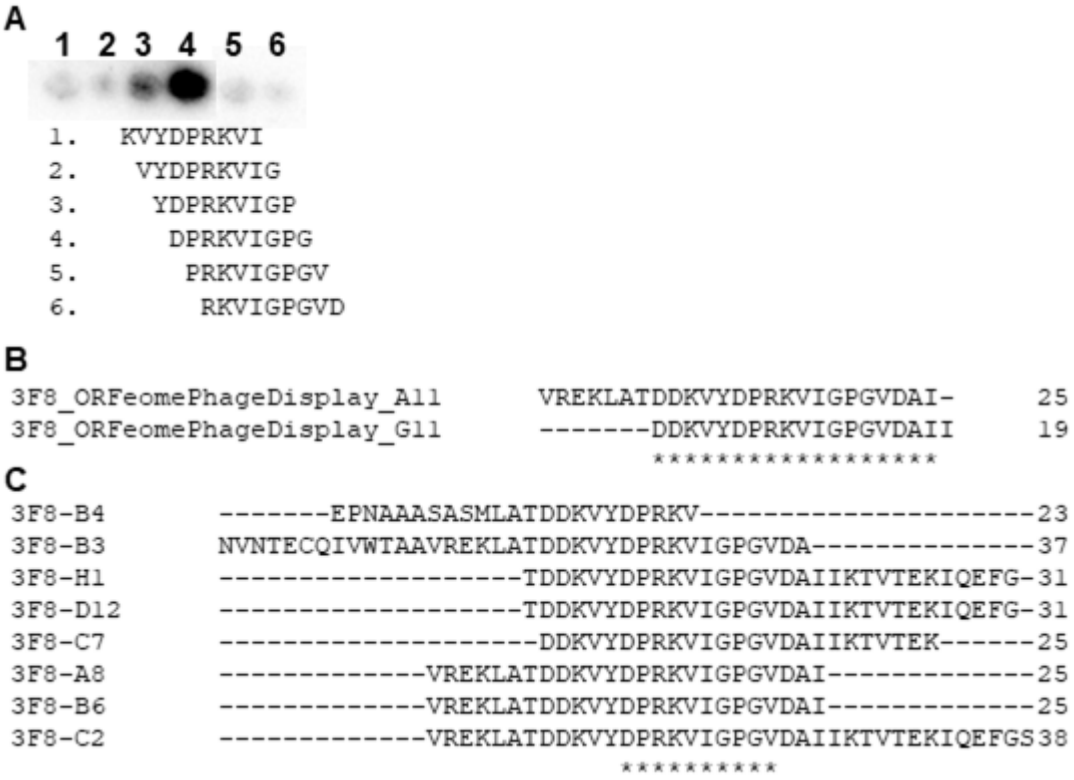

Figure 23. Comparison of 3F8 MSR size between peptide membrane, ORFeome, and single gene phage display. (**A**) In the already published work (Mendonça et al., 2016), a peptide membrane allowed reducing the MSR for mAb 3F8 from 25 to 14 amino acids. (**B**) In this study, ORFeome phage display allowed the definition of 3F8 MSR as an 18-amino acid sequence. (**C**) In the present work, single gene phage display allowed defining a region of the MSR of 10 amino acids as the MSR of 3F8.

Considering the structural information of PDC, mainly for PDC-E2, and the indirect ELISA results showed in this study, it is possible to observe some correlations. The Gram-negative species used in the present work showed no reaction with most of the tested antibodies (only GSM313-B12 showed cross-reactivity), supporting the already known structural difference of the between Gram-negatives and Gram-positives. Additionally, the already determined structures of *E. faecalis* (species used in this study) and *Geobacillus stearothermophilus* present icosahedral symmetry; and since *Enterecoccus* was one of the genus showing most of the cross-reactivity in indirect ELISA, it suggests that *Listeria* spp. possess the same kind of PDC symmetry.

As to the cellular location, the PDC in eukaryotes acts in the mitochondrial matrix after the transport of pyruvate from the cytosol. However, the exact location of the complex in the matrix is not fully described and, thus, its proximity to membranes in

mitochondria is not clear. Similarly, the PDC in Gram-negatives, as well as in Gram-positives, is mostly found in the cytosol. Nevertheless, other metabolic proteins, such as FBA, are described to be mainly cytoplasmic or attached to the membrane, but are also present in the cell wall and, thus, accessible on the bacterial cell surface (Ramnath et al., 2003; Mendonça et al., 2016). Likewise, PDC-E2, the core protein of PDC, is known to be mainly cytoplasmic, but, in the present study, it was detected in the cell wall fraction and showed to be accessible on the bacterial surface, as shown in immunoblot, fluorescent microscopy, and indirect ELISA. This indicates that, at least in *Listeria* genus, PDC-E2 behaves similarly to FBA as a protein that is mainly present in the cytoplasm but makes its way through the membrane reaching the cell wall and surface. Considering this, further studies could address whether other metabolic proteins have the same behavior in Gram-positive bacteria.

Although the metabolic function of PDC is well defined, the importance of this protein in some organisms may not have the relevance completely defined in other fields. In *Mycobacterium tuberculosis*, PDC-E2 was found to induce strong cellular response in immunocompetent infected population, as well as contributing for the resistance of the bacteria against host reactive nitrogen intermediates (Nguyen et al., 2018). Moreover, it is being studied as a target for antibiotic treatment (Bryk et al., 2010; Bryk et al., 2013). In *Mycobacterium bovis*, PDC-E1β was identified as an immunodominant antigen in infected cattle, allowing the development of an indirect ELISA diagnostic test with better performance than commercial assays (Sun et al., 2014). The PDC-E1β of *Mycobacterium pneumoniae* was described to possess fibronectin binding activity, allowing the definition of this protein as a moonlighting protein (Dallo et al., 2002). In another study, PDC-E1 of *Salmonella* Enteretidis was described as a virulence factor, once mutants with deletions or without the gene showed to be less capable of causing important symptoms of the disease (Pang et al., 2011). Characteristics such as slower growth and increased membrane fluidity also occur in PDC-deficient *S. aureus*, indicating a structural impact of the enzyme (Singh et al., 2018). Up to date, no study has shown the impact of PDC from *Listeria* spp. in any of these aspects. Nevertheless, since other metabolic enzymes, such as LAP (Jagadeesan et al., 2011), show moonlighting role in *Listeria*, the possibility of PDC presenting additional functions should be further investigated.

Regarding the recognition profile of the antibodies against PDC-E2 in indirect ELISA, it is possible to observe that some *Listeria* species show reduced reactions, while some non-*Listeria* species present elevated reactions (Fig. 12). The species *L. grayi*, *L. aquatica*, and *L. cornellensis* showed the lowest reactions among the *Listeria* species, with signal-to-noise ratio barely above 1. Although many factors not investigated in this study may contribute to the difference in the reactivity, some possibilities and observations may be worth of mentioning. Regarding *L. grayi*, it is known that this species is genetically classified in an independent phylogenetic subgroup (called Murraya), indicating special characteristics for this bacterium that may affect protein expression profile and composition of cell surface (Orsi & Wiedmann, 2016). In accordance to this, when analyzing the phylogeny based on sequences of PDC-E2, *L. grayi* also appear isolated from other species of the genus, showing the highest genetic change (Fig. 13). In its turn, *L. aquatica* is part of another subgroup (called Mesolisteria) together with *L. fleischmannii* and *L. floridensis*. Nevertheless, it shares some characteristics with *L. grayi*, as both are the only two species of the genus known to produce acetonin out of glucose metabolism (den Bakker et al., 2014). Additionally, both species show similar genetic change and the highest when compared to the other species using 325 single-copy genes for analysis (Orsi & Wiedmann, 2016). This behavior is also noticed when using PDC-E2 sequences for phylogeny, once both *L. grayi* and *L. aquatica* have the highest genetic change (Fig. 13), partially explaining the lower reactivity. As to *L. cornellensis*, it is grouped in a different subgroup (called Paenilisteria). It is worth to highlight that the optimal growth of this species in the present study was achieved with 30 °C, instead of 37 °C for most of the other species. Curiously, all the species grown under 30 °C in this study are part of this subgroup and show to be in the same phylogenetic cluster (Orsi & Wiedmann, 2016). In addition, *L. cornellensis* is the only species that does presents a low lactose acidification, although this fact alone may not explain the lower reactivity (den Bakker et al., 2014).

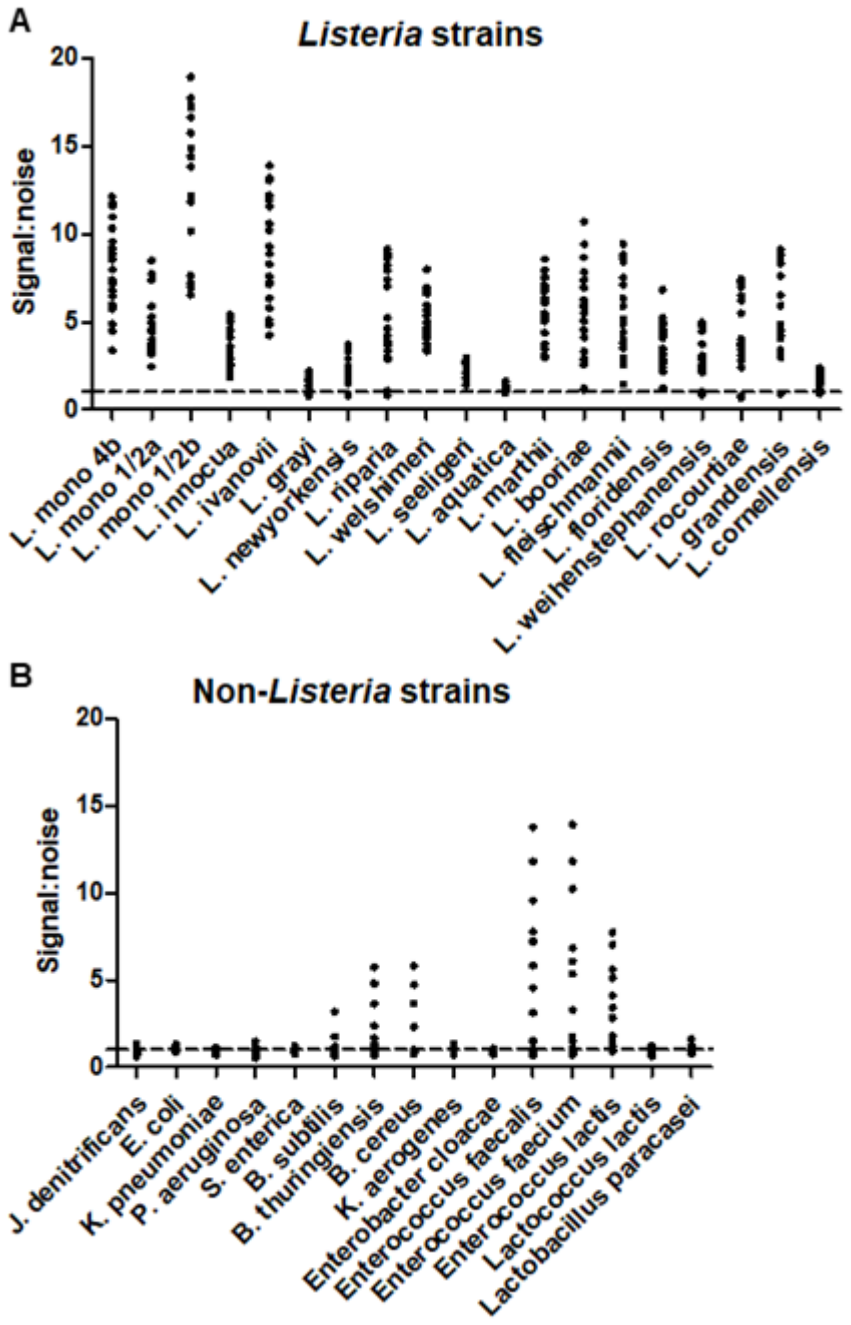

Figure 24. Signal-to-noise ratio of the 20 antibodies targeting PDC-E2 plotted for each strain. (**A**) The 19 Listeria strains were employed to test the sensitivity of the test. Among them, it is important to observe that the species *L. grayi*, *L. aquatica*, and *L. cornellensis* were the ones with lowest signal:noise ratio, being slightly above the value of 1 (dashed line). (**B**) The 15 non-Listeria strains were used to determine the specificity of the test. Most of them showed low signal:noise ratio, being basically on the value of 1 (dashed line). Interestingly, the species from genus *Bacillus* and *Enterococcus* were the only ones presenting considerable reaction with some antibodies, what may indicate that PDC-E2 is also accessible on the surface of the cells, and that the protein shows considerable similarity to that one of Listeria. Each point of the graphic represent one of the antibodies, which were tested against every strain identified in the x-axis.

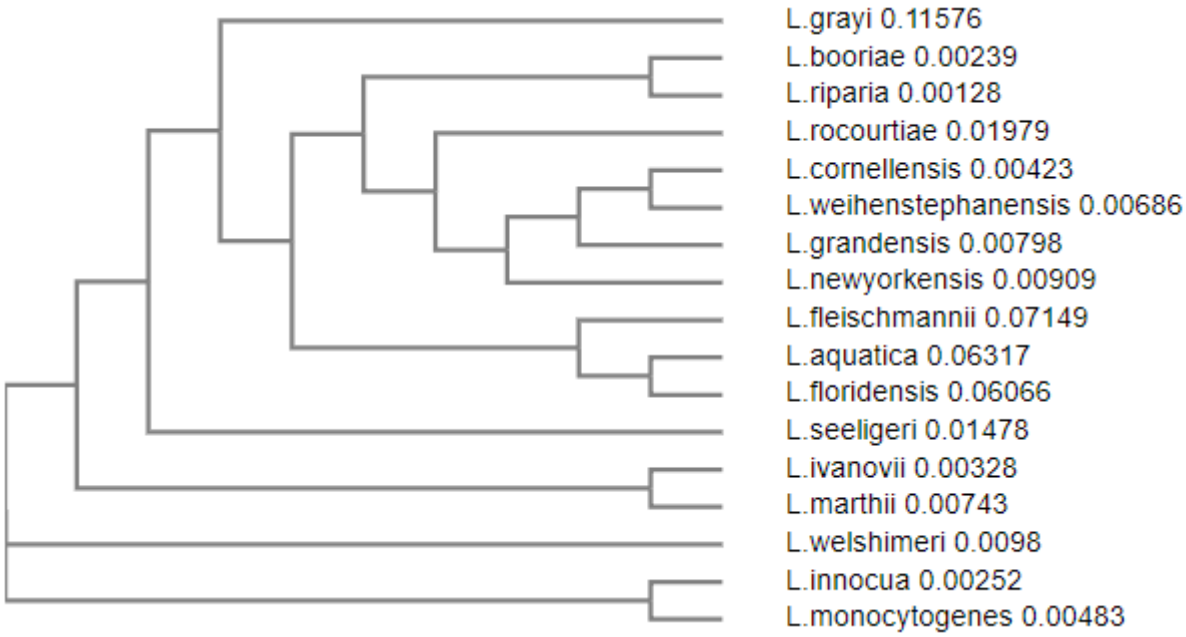

Figure 25. Phylogenetic three of the *Listeria* spp. used in indirect ELISA based on PDC-E2 protein sequence. The GenBank protein codes are described in Table 3. The numbers after the species name represent the level of genetic change.

When analyzing the pattern of reactivity of the non-*Listeria* strains, it is clear that species from *Bacillus* and *Enterococcus* genus show high reactivity with some of the antibodies against PDC-E2. In accordance to this, many works describe *Bacillus* as closely related to *Listeria*, what strongly indicates phenotypic similarity (Hain et al., 2006; Chiara et al., 2015). Although phylogenetic comparisons between *Listeria* and *Enterococcus* are not often made, these organisms may be related enough to share a phenotype that can explain the high reactions with some antibodies (Franz et al., 1999). In addition, PDC-E2 of *Bacillus* and *Enterococcus* show considerable identity to that of *L. monocytogenes* (>50 %), what can be also important to determine this recognition. The fact that only Gram-positive species showed such reactions may indicate that there is a higher tendency of PDC-E2 to be exposed on the cell surface, what can be a consequence of the similar structure of PDC in this group of bacteria (Izard et al., 1999). In summary, the recognition of PDC-E2 by the antibodies shown in this study may depend on multiple factors, such as cellular location of the target (phenotype), identity to *Listeria* PDC-E2, and the overall structure of the complex. Regarding FBA recognition, similar effect of homology was observed, once non-

Listeria species having >50 % identity tend to be recognized by the two tested antibodies. More details about this target were part of a previous work (Mendonça et al., 2016).

As to the PDC-E2 region that is recognized by the antibodies used in indirect ELISA, it is interesting to notice that the recognition of both LD of PDC-E2 are actually not beneficial for the diagnostic performance. Intuitively, if an antibody is able to recognize both LD in the same molecule, a higher signal, which can lead to higher sensitivity, is expected since twice more antibodies could be bound. Nonetheless, although GSM313-F7 shows higher reactions than most of the antibodies, the increase on reactivity seems not to be a trend of the antibodies that recognize both LD and does not contribute for the sensitivity. Moreover, the recognition of both LD may be associated with reduced specificity, since 2 out of the 4 scFv-Fc with this pattern of recognition show elevated reactions with non-*Listeria* species and AUC<0.8 (0.7895 for GSM313-F7, and 0.6632 for GSM313-G10), putting them in the bottom five in diagnostic performance, including the bottom one (see Table 6). The other two antibodies were GSM313-D10 and GSM133-A4, which showed AUC=0.9789 and 0.8947, respectively, but the reasons for their better diagnostic performance were not accessed in this study.

Other interesting pattern of recognition occurred with the best two scFv-Fc in diagnostic performance. Both GSM313-E9 and GSM313-H8 recognized the 1st LD and a synthetic LD formed by the fusion of the two LD of PDC-E2, which was probably a result of the random fragmentation and ligation during the library construction. Unfortunately, the reason of the correlation between reactivity with this synthetic sequence and improvement of diagnostic performance cannot be addressed with the results in the present work. Thus, it may be object of investigation of further studies. The case of GSM133-E2 is also worth of mentioning, since this antibody is specific for PDC-E2, but presents multiple binding sites, possibly exemplifying a case of multispecificity. Multispecific antibodies are known to recognize more than one epitope with the same CDR with high specificity (James & Tawfik, 2003; James et al., 2003; Mariuzza, 2006). Although most of the cross-reactions are explained to occur due to hydrophobic interactions, which lead to unspecificity, multispecificity is composed of strong interactions such as hydrogen bonds. In fact, the detected peptides out of the

LD regions show higher hydrophobic composition (45-55 % of the amino acids, compared to ≈40% in the LD regions), although it is not excessively elevated considering that highly hydrophobic peptides present >50 % of hydrophobic amino acids and <25 % acidic composition (Hoofnagle et al., 2017). Besides this, although peptide properties can be rather complex (Malavolta et al., 2006), all peptides represent regions of the protein surface that may be mostly soluble in aqueous solution. This way, it is probable that GSM133-E2 is not intrinsically unspecific, but shows a multispecificity that lowers its diagnostic performance. If this were the case, it would be the first reported multispecific antibody generated from a human naïve antibody phage display library that binds different parts of the same target. However, similar to the cases of GSM313-E9 and GSM313-H8, further investigation is necessary to determine the cause and details of such event.

As aforementioned, InlA and InlB are the main studied targets when it comes to detecting *L. monocytogenes*. Previous studies characterized monoclonal antibodies against, including a scFv against InlB, by showing their application in fluorescence-based detection (Tully et al., 2006). Other works used an aptamer against InlA for the detection of the pathogenic species using a biosensor (Ohk et al., 2010). In this case, the method was able to selectively recognize *L. monocytogenes* from artificially contaminated food In its turn, InlB was used as a target to generate an VHH (variable domain of the heavy chain) antibody from *Camelidae* libraries (MacKenzie et al., 2014). However, this antibody was not extensively tested regarding its diagnostic performance, since only recombinant InlA was used as negative control for cross-reaction. In the present work, although the panel of *L. monocytogenes* strains was not big, since it included three strains representing the three more prevalent serovars in clinical cases (Orsi et al., 2011), no reaction against the other 31 species tested, indicating its high applicability for detection. As to the limit of detection (LOD), commercial lateral flow tests are able to detect 10^4-10^6 CFU/mL, while efforts to reduce this number were not completely successful (Shi et al., 2014). In this work, the LOD for each antibody was not investigated once the final assay would involve the use of lateral flow assays or biosensors that could not be accessed at the moment of the research.

6 CONCLUSION AND OUTLOOK

The genus *Listeria* has gained more attention in the past years due to the description of new species, what led to an increase on the number of studies over its genetics and phenotypes. Summed to this, the pathogenic species *L. monocytogenes* is still a major concern over the public health once it is still the agent of many food contamination outbreaks around the world. This way, studies over *Listeria* spp. and how to detect it are of interest to help defining the new characteristics of the bacteria and to avoid problems with food contamination. In the present work, a novel target for the detection of *Listeria* spp. (i.e. PDC-E2) is described, increasing the list of enzymatic targets that can be used for the detection of such bacteria. This may open new research over the applicability of PDC-E2 in biological products. Besides this, two antibodies against this target showed to bind specifically the genus *Listeria*, allowing further studies over the target and the generation of immunodetection methods for increasing food safety. In addition, different combinations of phage display techniques were applied in order to perform biomarker discovery and identification, antibody generation, and epitope mapping, opening way to new applications of phage display technology. The comparison between ORFeome and single gene phage may still be topic of further works, which will help to elucidate the complete application of such technologies, especially on the field of antigen-antibody interaction. As to the antibodies generated against PDC-E2, it is expected to further investigate the reason why the best antibodies are the only ones able to recognize a synthetic fragment of PDC-E2. In addition, the GSM133-E2 case may receive more attention since it can provide further knowledge over the output of antibody phage display. Finally, it is expected that the biological tools generated in this study, mainly the antibodies against PDC-E2, InlA, and InlB, will be used in diagnostic assays that can generate a biological product, such as lateral flow assays.

7 REFERENCES

AGHEBATI-MALEKI, L., BAKHSHINEJAD, B., BARADARAN, B., MOTALLEBNEZHAD, M., AGHEBATI-MALEKI, A., NICKHO, H., YOUSEFI, M. & MAJIDI, J. (2016). Phage display as a promising approach for vaccine development. *Journal of biomedical science*. 23(1). p. 66.

AMARTELY, H., IOSUB-AMIR, A. & FRIEDLER, A. (2014). Identifying protein-protein interaction sites using peptide arrays. *Journal of visualized experiments : JoVE*. (93). p. E52097.

ARBABI-GHAHROUDI, M. (2017). Camelid Single-Domain Antibodies: Historical Perspective and Future Outlook. *Frontiers in immunology*. 8. p. 1589.

AUGUSTIN, T., CEHLAR, O., SKRABANA, R., MAJEROVA, P. & HANES, J. (2015). Unravelling viral camouflage: approaches to the study and characterization of conformational epitopes. *Acta virologica*. 59(02). p. 103–116.

DEN BAKKER, H.C., WARCHOCKI, S., WRIGHT, E.M., ALLRED, A.F., AHLSTROM, C., MANUEL, C.S., STASIEWICZ, M.J., BURRELL, A., ROOF, S., STRAWN, L.K., FORTES, E., NIGHTINGALE, K.K., KEPHART, D. & WIEDMANN, M. (2014). Listeria floridensis sp. nov., Listeria aquatica sp. nov., Listeria cornellensis sp. nov., Listeria riparia sp. nov. and Listeria grandensis sp. nov., from agricultural and natural environments. *International journal of systematic and evolutionary microbiology*. 64(Pt 6). p. 1882–9.

BASU, K., GREEN, E.M., CHENG, Y. & CRAIK, C.S. (2019). Why recombinant antibodies — benefits and applications. *Current Opinion in Biotechnology*. 60. p. 153–158.

BECKER, M., FELSBERGER, A., FRENZEL, A., SHATTUCK, W.M.C., DYER, M., KÜGLER, J., ZANTOW, J., MATHER, T.N. & HUST, M. (2015). Application of M13 phage display for identifying immunogenic proteins from tick (Ixodes scapularis) saliva. *BMC biotechnology*. 15. p. 43.

BEGHETTO, E., GARGANO, N., RICCI, S., GARUFI, G., PEPPOLONI, S., MONTAGNANI, F., OGGIONI, M., POZZI, G. & FELICI, F. (2006). Discovery of novel Streptococcus pneumoniae antigens by screening a whole-genome Î»-display library. *FEMS Microbiology Letters*. 262(1). p. 14–21.

BERTSCH, D., RAU, J., EUGSTER, M.R., HAUG, M.C., LAWSON, P.A., LACROIX, C. & MEILE, L. (2013). Listeria fleischmannii sp. nov., isolated from cheese. *International journal of systematic and evolutionary microbiology*. 63(Pt 2). p. 526–32.

BESSE, N.G., BARRE, L., BUHARIWALLA, C., VIGNAUD, M.L., KHAMISSI, E., DECOURSEULLES, E., NIRSIMLOO, M., CHELLY, M. & KALMOKOFF, M. (2010). The overgrowth of Listeria monocytogenes by other Listeria spp. in food samples undergoing enrichment cultivation has a nutritional basis. *International journal of food microbiology*. 136(3). p. 345–51.

BHUNIA, A.K., BALL, P.H., FUAD, A.T., KURZ, B.W., EMERSON, J.W. & JOHNSON, M.G. (1991). Development and characterization of a monoclonal antibody specific for Listeria monocytogenes and Listeria innocua. *Infection and immunity*. 59(9). p. 3176–84.

BLIKSTAD, C. & IVARSSON, Y. (2015). High-throughput methods for identification of

protein-protein interactions involving short linear motifs. *Cell Communication and Signaling*. 13(1). p. 1–9.

BOEDEKER, C., SCHÜLER, M., REINTJES, G., JESKE, O., VAN TEESELING, M.C.F., JOGLER, M., RAST, P., BORCHERT, D., DEVOS, D.P., KUCKLICK, M., SCHAFFER, M., KOLTER, R., VAN NIFTRIK, L., ENGELMANN, S., AMANN, R., ROHDE, M., ENGELHARDT, H. & JOGLER, C. (2017). Determining the bacterial cell biology of Planctomycetes. *Nature Communications*. 8.

BRADBURY, A.R.M., SIDHU, S., DÜBEL, S. & MCCAFFERTY, J. (2011). Beyond natural antibodies: the power of in vitro display technologies. *Nature Biotechnology*. 29(3). p. 245–254.

BRAUN, L., DRAMSI, S., DEHOUX, P., BIERNE, H., LINDAHL, G. & COSSART, P. (1997). InlB: an invasion protein of Listeria monocytogenes with a novel type of surface association. *Molecular microbiology*. 25(2). p. 285–94.

BREITLING, F., DÜBEL, S., SEEHAUS, T., KLEWINGHAUS, I. & LITTLE, M. (1991). A surface expression vector for antibody screening. *Gene*. 104(2). p. 147–153.

BRINKMANN, U. & KONTERMANN, R.E. (2017). The making of bispecific antibodies. *mAbs*. 9(2). p. 182–212.

BRYK, R., ARANGO, N., MAKSYMIUK, C., BALAKRISHNAN, A., WU, Y.T., WONG, C.H., MASQUELIN, T., HIPSKIND, P., LIMA, C.D. & NATHAN, C. (2013). Lipoamide channel-binding sulfonamides selectively inhibit mycobacterial lipoamide dehydrogenase. *Biochemistry*. 52(51). p. 9375–9384.

BRYK, R., ARANGO, N., VENUGOPAL, A., DAVID WARREN, J., PARK, Y.H., PATEL, M.S., LIMA, C.D. & NATHAN, C. (2010). Triazaspirodimethoxybenzoyls as selective inhibitors of mycobacterial lipoamide dehydrogenase. *Biochemistry*. 49(8). p. 1616–1627.

CARICCIO, V.L., DOMINA, M., BENFATTO, S., VENZA, M., VENZA, I., FALERI, A., BRUTTINI, M., BARTOLINI, E., GIULIANI, M.M., SANTINI, L., BRUNELLI, B., NORAIS, N., BORGOGNI, E., MIDIRI, A., GALBO, R., ROMEO, L., BIONDO, C., MASIGNANI, V., TETI, G., ET AL. (2016). Phage display revisited: Epitope mapping of a monoclonal antibody directed against Neisseria meningitidis adhesin A using the PROFILER technology. *mAbs*. 8(4). p. 741–50.

CHEN, Y.-T., GURE, A.O. & SCANLAN, M.J. (2005). Serological analysis of expression cDNA libraries (SEREX): an immunoscreening technique for identifying immunogenic tumor antigens. *Methods in molecular medicine*. 103. p. 207–16.

CHIARA, M., CARUSO, M., ERCHIA, A.M.D., MANZARI, C., FRACCALVIERI, R., GOFFREDO, E., LATORRE, L., MICCOLUPO, A., PADALINO, I., SANTAGADA, G., CHIOCCO, D., PESOLE, G., HORNER, D.S. & PARISI, A. (2015). Comparative Genomics of Listeria Sensu Lato : Genus-Wide through Lateral Gene Transfer. *Genome Biology and Evolution*. 7(8). p. 2154–2172.

CHIKAEV, A.N., BAKULINA, A.Y., BURDICK, R.C., KARPENKO, L.I., PATHAK, V.K. & ILYICHEV, A.A. (2015). Selection of Peptide Mimics of HIV-1 Epitope Recognized by Neutralizing Antibody VRC01 N. J. Mantis (ed.). *PLOS ONE*. 10(3). p. E0120847.

CHIU, M.L. & GILLILAND, G.L. (2016). Engineering antibody therapeutics. *Current Opinion in Structural Biology*. 38. p. 163–173.

CHO, I.-H., BHUNIA, A. & IRUDAYARAJ, J. (2015). Rapid pathogen detection by lateral-flow immunochromatographic assay with gold nanoparticle-assisted enzyme signal amplification. *International Journal of Food Microbiology*. 206. p. 60–66.

CONNOR, D.O., ZANTOW, J., HUST, M., BIER, F.F. & VON NICKISCH-ROSENEGK, M. (2016). Identification of Novel Immunogenic Proteins of Neisseria gonorrhoeae by Phage Display. *PloS one*. 11(2). p. E0148986.

CRUZ, C.D. & FLETCHER, G.C. (2011). Prevalence and biofilm-forming ability of Listeria monocytogenes in New Zealand mussel (Perna canaliculus) processing plants. *Food Microbiology*. 28(7). p. 1387–1393.

D'ANGELO, S., FERRARA, F., NARANJO, L., ERASMUS, M.F., HRABER, P. & BRADBURY, A.R.M. (2018). Many Routes to an Antibody Heavy-Chain CDR3: Necessary, Yet Insufficient, for Specific Binding. *Frontiers in Immunology*. 9. p. 395.

DAFFIS, S., KONTERMANN, R.E., KORIMBOCUS, J., ZELLER, H., KLENK, H.D. & TER MEULEN, J. (2005). Antibody responses against wild-type yellow fever virus and the 17D vaccine strain: Characterization with human monoclonal antibody fragments and neutralization escape variants. *Virology*. 337(2). p. 262–272.

DALLO, S.F., KANNAN, T.R., BLAYLOCK, M.W. & BASEMAN, J.B. (2002). Elongation factor Tu and E1 β subunit of pyruvate dehydrogenase complex act as fibronectin binding proteins in Mycoplasma pneumoniae. *Molecular Microbiology*. 46(4). p. 1041–1051.

DAVIDSON, E. & DORANZ, B.J. (2014). A high-throughput shotgun mutagenesis approach to mapping B-cell antibody epitopes. *Immunology*. 143(1). p. 13–20.

DEBS, B. EL, UTHARALA, R., BALYASNIKOVA, I. V., GRIFFITHS, A.D. & MERTEN, C.A. (2012). Functional single-cell hybridoma screening using droplet-based microfluidics. *Proceedings of the National Academy of Sciences*. 109(29). p. 11570–11575.

DELVECCHIO, V.G., CONNOLLY, J.P., ALEFANTIS, T.G., WALZ, A., QUAN, M.A., PATRA, G., ASHTON, J.M., WHITTINGTON, J.T., CHAFIN, R.D., LIANG, X., GREWAL, P., KHAN, A.S. & MUJER, C. V. (2006). Proteomic Profiling and Identification of Immunodominant Spore Antigens of Bacillus anthracis, Bacillus cereus, and Bacillus thuringiensis. *Applied and Environmental Microbiology*. 72(9). p. 6355–6363.

DEVASUNDARAM, S. & RAJA, A. (2017). Dihydrolipoamide dehydrogenase-Lpd (Rv0462)-specific T cell recall responses are higher in healthy household contacts of TB: a novel immunodominant antigen from *M. tuberculosis*. *Journal of Leukocyte Biology*. 102(1). p. 135–151.

DOIJAD, S.P., POHARKAR, K. V., KALE, S.B., KERKAR, S., KALOREY, D.R., KURKURE, N. V., RAWOOL, D.B., MALIK, S.V.S., AHMAD, R.Y., HUDEL, M., CHAUDHARI, S.P., ABT, B., OVERMANN, J., WEIGEL, M., HAIN, T., BARBUDDHE, S.B. & CHAKRABORTY, T. (2018). Listeria goaensis sp. nov. *International Journal of Systematic and Evolutionary Microbiology*. 68(10). p. 3285–3291.

DOMINA, M., LANZA CARICCIO, V., BENFATTO, S., D'ALIBERTI, D., VENZA, M., BORGOGNI,

E., CASTELLINO, F., BIONDO, C., D'ANDREA, D., GRASSI, L., TRAMONTANO, A., TETI, G., FELICI, F. & BENINATI, C. (2014). Rapid Profiling of the Antigen Regions Recognized by Serum Antibodies Using Massively Parallel Sequencing of Antigen-Specific Libraries M. Isalan (ed.). *PLoS ONE*. 9(12). p. E114159.

DROLIA, R., TENGURIA, S., DURKES, A.C., TURNER, J.R. & BHUNIA, A.K. (2018). Listeria Adhesion Protein Induces Intestinal Epithelial Barrier Dysfunction for Bacterial Translocation. *Cell Host and Microbe*. 23(4). p. 470–484.E7.

DU, X., ZANG, Y., LIU, H., LI, P. & WANG, S. (2018). Recombinase Polymerase Amplification Combined with Lateral Flow Strip for *Listeria monocytogenes* Detection in Food. *Journal of Food Science*. 83(4). p. 1041–1047.

EC REGULATIONS (2005). Commission Regulation (EC) Nº 2073/2005 of 15th November 2005 on microbiological criteria for foodstuffs. *Official Journal of the European Union*. p. L338, 1–26.

ELGUNDI, Z., RESLAN, M., CRUZ, E., SIFNIOTIS, V. & KAYSER, V. (2017). The state-of-play and future of antibody therapeutics. *Advanced Drug Delivery Reviews*. 122. p. 2–19.

ELIYAHU, S., SHARABI, O., ELMEDVI, S., TIMOR, R., DAVIDOVICH, A., VIGNEAULT, F., CLOUSER, C., HOPE, R., NIMER, A., BRAUN, M., WEISS, Y.Y., POLAK, P., YAARI, G. & GAL-TANAMY, M. (2018). Antibody Repertoire Analysis of Hepatitis C Virus Infections Identifies Immune Signatures Associated With Spontaneous Clearance. *Frontiers in Immunology*. 9(December). p. 1–17.

FACK, F., HÜGLE-DÖRR, B., SONG, D., QUEITSCH, I., PETERSEN, G. & BAUTZ, E.K. (1997). Epitope mapping by phage display: random versus gene-fragment libraries. *Journal of immunological methods*. 206(1–2). p. 43–52.

FRANZ, C.M.A.P., HOLZAPFEL, W.H. & STILES, M.E. (1999). Enterococci at the crossroads of food safety? *International Journal of Food Microbiology*. 47. p. 1–24.

FRENZEL, A., KÜGLER, J., HELMSING, S., MEIER, D., SCHIRRMANN, T., HUST, M. & DÜBEL, S. (2017). Designing Human Antibodies by Phage Display. *Transfusion Medicine and Hemotherapy*. 44(5). p. 312–318.

FRENZEL, A., SCHIRRMANN, T. & HUST, M. (2016). Phage display-derived human antibodies in clinical development and therapy. *mAbs*. 8(7). p. 1177–1194.

FÜHNER, V., HEINE, P.A., HELMSING, S., GOY, S., HEIDEPRIEM, J., LOEFFLER, F.F., DÜBEL, S., GERHARD, R. & HUST, M. (2018). Development of Neutralizing and Non-neutralizing Antibodies Targeting Known and Novel Epitopes of TcdB of Clostridioides difficile. *Frontiers in Microbiology*. 9(December). p. 2908.

FÜHNER, V., HEINE, P.A., ZILKENS, K.J.C., MEIER, D., ROTH, K.D.R., MOREIRA, G.M.S.G., HUST, M. & RUSSO, G. (2019). Epitope Mapping via Phage Display from Single-Gene Libraries. In *Methods in molecular biology (Clifton, N.J.)*. p. 353–375.

GALÁN, A., COMOR, L., HORVATIĆ, A., KULEŠ, J., GUILLEMIN, N., MRLJAK, V. & BHIDE, M. (2016). Library-based display technologies: Where do we stand? *Molecular BioSystems*. 12(8). p. 2342–2358.

GAZARIAN, K.G., PALACIOS-RODRÍGUEZ, Y., GAZARIAN, T.G. & HUERTA, L. (2013). HIV-1

V3 loop crown epitope-focused mimotope selection by patient serum from random phage display libraries: Implications for the epitope structural features. *Molecular Immunology*. 54(2). p. 148–156.

GENG, T., HAHM, B.-K. & BHUNIA, A.K. (2006). Selective enrichment media affect the antibody-based detection of stress-exposed Listeria monocytogenes due to differential expression of antibody-reactive antigens identified by protein sequencing. *Journal of food protection*. 69(8). p. 1879–86.

GUILLET, C., JOIN-LAMBERT, O., LE MONNIER, A., LECLERCQ, A., MECHAÏ, F., MAMZER-BRUNEEL, M.F., BIELECKA, M.K., SCORTTI, M., DISSON, O., BERCHE, P., VAZQUEZ-BOLAND, J., LORTHOLARY, O. & LECUIT, M. (2010). Human listeriosis caused by Listeria ivanovii. *Emerging infectious diseases*. 16(1). p. 136–8.

GUPTA, S., ANSARI, H.R., GAUTAM, A., OPEN SOURCE DRUG DISCOVERY CONSORTIUM & RAGHAVA, G.P.S. (2013). Identification of B-cell epitopes in an antigen for inducing specific class of antibodies. *Biology direct*. 8. p. 27.

HAGER-BRAUN, C. & TOMER, K.B. (2005). Determination of protein-derived epitopes by mass spectrometry. *Expert Review of Proteomics*. 2(5). p. 745–756.

HAHM, B.-K., KIM, H., SINGH, A.K. & BHUNIA, A.K. (2015). Pathogen enrichment device (PED) enables one-step growth, enrichment and separation of pathogen from food matrices for detection using bioanalytical platforms. *Journal of Microbiological Methods*. 117. p. 64–73.

HAIN, T., STEINWEG, C. & CHAKRABORTY, T. (2006). Comparative and functional genomics of Listeria spp . *Journal of Biotechnology*. 126. p. 37–51.

HENDERSON, B. & MARTIN, A. (2011). Bacterial Moonlighting Proteins and Bacterial Virulence. In *Current topics in microbiology and immunology*. p. 155–213.

HOOFNAGLE, A.N., WHITEAKER, J.R., CARR, S.A., KUHN, E., LIU, T., MASSONI, S.A., THOMAS, S.N., TOWNSEND, R.R., ZIMMERMAN, L.J., BOJA, E., CHEN, J., CRIMMINS, D.L., DAVIES, S.R., GAO, Y., HILTKE, T.R., KETCHUM, K.A., KINSINGER, C.R., MESRI, M., MEYER, M.R., ET AL. (2017). Recommendations for the generation, quantification, storage and handling of peptides used for mass spectrometry-based assays. *Clinical Chemistry*. 19(2). p. 65–73.

HUST, M., MEYSING, M., SCHIRRMANN, T., SELKE, M., MEENS, J., GERLACH, G.-F. & DÜBEL, S. (2006). Enrichment of open reading frames presented on bacteriophage M13 using Hyperphage. *BioTechniques*. 41(3). p. 335–342.

IZARD, T., AEVARSSON, A., ALLEN, M., WESTPHAL, A., PERHAM, R., DE KOK, A. & HOL, W.G.J. (1999). Principles of quasi-equivalence and Euclidean geometry govern the assembly of cubic and dodecahedral cores of pyruvate dehydrogenase complexes. *Proceedings of the National Academy of Sciences of the United States of America*. 96. p. 1240–1245.

JADHAV, S., BHAVE, M. & PALOMBO, E.A. (2012). Methods used for the detection and subtyping of Listeria monocytogenes. *Journal of microbiological methods*. 88(3). p. 327–41.

JAGADEESAN, B., BASTIC SCHMID, V., KUPSKI, B., MCMAHON, W. & KLIJN, A. (2019). Detection of Listeria spp. and L. monocytogenes in pooled test portion samples

of processed dairy products. *International Journal of Food Microbiology*. 289(July 2018). p. 30–39.

JAGADEESAN, B., FLEISHMAN LITTLEJOHN, A.E., AMALARADJOU, M.A.R., SINGH, A.K., MISHRA, K.K., LA, D., KIHARA, D. & BHUNIA, A.K. (2011). N-Terminal Gly224–Gly411 Domain in Listeria Adhesion Protein Interacts with Host Receptor Hsp60 D. M. Ojcius (ed.). *PLoS ONE*. 6(6). p. E20694.

JÄGER, V., BÜSSOW, K., WAGNER, A., WEBER, S., HUST, M., FRENZEL, A. & SCHIRRMANN, T. (2013). High level transient production of recombinant antibodies and antibody fusion proteins in HEK293 cells. *BMC biotechnology*. 13(1). p. 52.

JALILZADEH-RAZIN, S., MANTEGI, M., TOHIDKIA, M.R. & PAZHANG, Y. (2019). Phage antibody library screening for the selection of novel high-affinity human single-chain variable fragment against gastrin receptor : an in silico and in vitro study. *DARU Journal of Pharmaceutical Sciences*.

JAMES, L.C., ROVERSI, P. & TAWFIK, D.S. (2003). Mediated by Conformational Diversity. *Science*. 299(February). p. 1362–1368.

JAMES, L.C. & TAWFIK, D.S. (2003). The specificity of cross-reactivity: Promiscuous antibody binding involves specific hydrogen bonds rather than nonspecific hydrophobic stickiness. *Protein Science*. 12. p. 2183–2193.

JANZTEN, M.M., NAVAS, J., CORUJO, A., MORENO, R., LÓPEZ, V. & MARTÍNEZ-SUAREZ, V.J. (2006). Specific detection of Listeria monocytogenes in foods using commercial methods: from chromogenic media to real-time PCR. *Spanish Journal of Agricultural Research*. 4(3). p. 235–247.

JEFFERY, C. (2018). Intracellular proteins moonlighting as bacterial adhesion factors. *AIMS Microbiology*. 4(2). p. 362–376.

JEFFERY, C.J. (2016). What is Protein Moonlighting and Why is it Important? *Moonlighting Proteins: Novel Virulence Factors in Bacterial Infections*. (figure 1). p. 1–19.

JOSTOCK, T., VANHOVE, M., BREPOELS, E., VAN GOOL, R., DAUKANDT, M., WEHNERT, A., VAN HEGELSOM, R., DRANSFIELD, D., SEXTON, D., DEVLIN, M., LEY, A. & MÜLLBERG, J. (2004). Rapid generation of functional human IgG antibodies derived from Fab-on-phage display libraries. *Journal of Immunological Methods*. 289(1–2). p. 65–80.

KIM, H. & BHUNIA, A.K. (2008). SEL, a selective enrichment broth for simultaneous growth of Salmonella enterica, Escherichia coli O157:H7, and Listeria monocytogenes. *Applied and environmental microbiology*. 74(15). p. 4853–66.

KIM, S.-H., PARK, M.-K., KIM, J.-Y., CHUONG, P.D., LEE, Y.-S., YOON, B.-S., HWANG, K.-K. & LIM, Y.-K. (2005). Development of a sandwich ELISA for the detection of Listeria spp. using specific flagella antibodies. *Journal of veterinary science*. 6(1). p. 41–6.

KREBBER, A., BURMESTER, J. & PLÜCKTHUN, A. (1996). Inclusion of an upstream transcriptional terminator in phage display vectors abolishes background expression of toxic fusions with coat protein g3p. *Gene*. 178(1–2). p. 71–74.

KÜGLER, J., TOMSZAK, F., FRENZEL, A. & HUST, M. (2018). Construction of Human

Immune and Naive scFv Libraries. In *Methods in molecular biology (Clifton, N.J.)*. p. 3–24.

KÜGLER, J., WILKE, S., MEIER, D., TOMSZAK, F., FRENZEL, A., SCHIRRMANN, T., DÜBEL, S., GARRITSEN, H., HOCK, B., TOLEIKIS, L., SCHÜTTE, M. & HUST, M. (2015). Generation and analysis of the improved human HAL9/10 antibody phage display libraries. *BMC Biotechnology*. 15(1). p. 1–15.

KÜGLER, J., ZANTOW, J., MEYER, T. & HUST, M. (2013). Oligopeptide m13 phage display in pathogen research. *Viruses*. 5(10). p. 2531–45.

KUHN, P., THIEM, S., STEINERT, M., PURVIS, D., LUGMAYR, V., TREUTLEIN, U., PLOBNER, L., LEISER, R.M., HUST, M. & DÜBEL, S. (2017). Human Anti-Lipopolysaccharid (LPS) antibodies against Legionella with high species specificity. *Human Antibodies*. 26(1). p. 29–38.

KUHN, P., FÜHNER, V., UNKAUF, T., MOREIRA, G.M.S.G., FRENZEL, A., MIETHE, S. & HUST, M. (2016). Recombinant antibodies for diagnostics and therapy against pathogens and toxins generated by phage display. *Proteomics. Clinical applications*. 10(9–10). p. 922–948.

KUMAR, R., PARRAY, H.A., SHRIVASTAVA, T., SINHA, S. & LUTHRA, K. (2019). Phage display antibody libraries: A robust approach for generation of recombinant human monoclonal antibodies. *International Journal of Biological Macromolecules*. 135. p. 907–918.

LALONDE, M.-E. & DUROCHER, Y. (2017). Therapeutic glycoprotein production in mammalian cells. *Journal of Biotechnology*. 251. p. 128–140.

LANG HALTER, E., NEUHAUS, K. & SCHERER, S. (2013). Listeria weihenstephanensis sp. nov., isolated from the water plant Lemna trisulca taken from a freshwater pond. *International journal of systematic and evolutionary microbiology*. 63(Pt 2). p. 641–7.

LECLERCQ, A., MOURA, A., VALES, G., TESSAUD-RITA, N., AGUILHON, C. & LECUIT, M. (2019). Listeria thailandensis sp. nov. *International journal of systematic and evolutionary microbiology*. 69(1). p. 74–81.

LEDSGAARD, L., KILSTRUP, M., KARATT-VELLATT, A., MCCAFFERTY, J. & LAUSTSEN, A. (2018). Basics of Antibody Phage Display Technology. *Toxins*. 10(6). p. 236.

LETUNIC, I. & BORK, P. (2018). 20 years of the SMART protein domain annotation resource. *Nucleic Acids Research*. 46(D1). p. D493–D496.

LI, F., LI, F., LUO, D., LAI, W., XIONG, Y. & XU, H. (2018). Biotin-exposure-based immunomagnetic separation coupled with nucleic acid lateral flow biosensor for visibly detecting viable Listeria monocytogenes. *Analytica Chimica Acta*. 1017. p. 48–56.

LI, W., COWLEY, A., ULUDAG, M., GUR, T., MCWILLIAM, H., SQUIZZATO, S., PARK, Y.M., BUSO, N. & LOPEZ, R. (2015). The EMBL-EBI bioinformatics web and programmatic tools framework. *Nucleic acids research*. 43(W1). p. W580-4.

LIU, G.-Y., MEI, X.-J., HU, M.-J., YANG, Y., LIU, M., LI, M.-S., ZHANG, M.-L., CAO, M.-J. & LIU, G.-M. (2018). Analysis of the Allergenic Epitopes of Tropomyosin from Mud Crab Using Phage Display and Site-Directed Mutagenesis. *Journal of*

Agricultural and Food Chemistry. 66(34). p. 9127–9137.

LIU, H., DU, X., ZANG, Y.-X., LI, P. & WANG, S. (2017). SERS-Based Lateral Flow Strip Biosensor for Simultaneous Detection of *Listeria monocytogenes* and *Salmonella enterica* Serotype Enteritidis. *Journal of Agricultural and Food Chemistry*. 65(47). p. 10290–10299.

LIU, J.L., SHRIVER-LAKE, L.C., ZABETAKIS, D., ANDERSON, G.P. & GOLDMAN, E.R. (2019). Selection and characterization of protective anti-chikungunya virus single domain antibodies. *Molecular Immunology*. 105(November 2018). p. 190–197.

LODES, M.J., CONG, Y., ELSON, C.O., MOHAMATH, R., LANDERS, C.J., TARGAN, S.R., FORT, M. & HERSHBERG, R.M. (2004). Bacterial flagellin is a dominant antigen in Crohn disease. *The Journal of clinical investigation*. 113(9). p. 1296–306.

MACKENZIE, C.R., ARBABI-GHAHROUDI, M., GENE, R.W., VAN FAASSEN, H., AROCHE, C., HALL, J.C. & KUMARAN, J. (2014). High affinity anti-Internalin B VHH antibody fragments isolated from naturally and artificially immunized repertoires. *Journal of Immunological Methods*. 416. p. 29–39.

MALAVOLTA, L., PINTO, M.R.S., CUVERO, J.H. & NAKAIE, C.R. (2006). Interpretation of the dissolution of insoluble peptide sequences based on the acid-base properties of the solvent. *Protein Science*. 15(6). p. 1476–1488.

MALITO, E., CARFI, A. & BOTTOMLEY, M.J. (2015). Protein Crystallography in Vaccine Research and Development. *International journal of molecular sciences*. 16(6). p. 13106–40.

MARIUZZA, R.A. (2006). Multiple Paths to Multispecificity. *Immunity*. 24(4). p. 359–361.

MCCAFFERTY, J., GRIFFITHS, A.D., WINTER, G. & CHISWELL, D.J. (1990). Phage antibodies: filamentous phage displaying antibody variable domains. *Nature*. 348(6301). p. 552–554.

MEENS, J., SELKE, M. & GERLACH, G.-F. (2006). Identification and immunological characterization of conserved Mycoplasma hyopneumoniae lipoproteins Mhp378 and Mhp651. *Veterinary Microbiology*. 116(1–3). p. 85–95.

MENDONÇA, M., MOREIRA, G.M.S.G., CONCEIÇÃO, F.R., HUST, M., MENDONÇA, K.S., MOREIRA, Â.N., FRANÇA, R.C., DA SILVA, W.P., BHUNIA, A.K. & ALEIXO, J.A.G. (2016). Fructose 1,6-Bisphosphate Aldolase, a Novel Immunogenic Surface Protein on Listeria Species D. F. Hozbor (ed.). *PLOS ONE*. 11(8). p. E0160544.

MENDONÇA, M., CONRAD, N.L., CONCEIÇÃO, F.R., MOREIRA, A.N., DA SILVA, W.P., ALEIXO, J.A. & BHUNIA, A.K. (2012). Highly specific fiber optic immunosensor coupled with immunomagnetic separation for detection of low levels of Listeria monocytogenes and L. ivanovii. *BMC microbiology*. 12(1). p. 275.

MIETHE, S., RASETTI-ESCARGUEIL, C., LIU, Y., CHAHBOUN, S., PELAT, T., AVRIL, A., FRENZEL, A., SCHIRRMANN, T., THULLIER, P., SESARDIC, D. & HUST, M. (2014). Development of neutralizing scFv-Fc against botulinum neurotoxin A light chain from a macaque immune library. *mAbs*. 6(2). p. 446–59.

MINENKOVA, O., PUCCI, A., PAVONI, E., DE TOMASSI, A., FORTUGNO, P., GARGANO, N., CIANFRIGLIA, M., BARCA, S., DE PLACIDO, S., MARTIGNETTI, A., FELICI, F., CORTESE,

R. & MONACI, P. (2003). Identification of tumor-associated antigens by screening phage-displayed human cDNA libraries with sera from tumor patients. *International Journal of Cancer*. 106(4). p. 534–544.

MISHRA, K.K., MENDONCA, M., AROONNUAL, A., BURKHOLDER, K.M. & BHUNIA, A.K. (2011). Genetic organization and molecular characterization of secA2 locus in Listeria species. *Gene*. 489(2). p. 76–85.

MOEZI, P., KARGAR, M., DOOSTI, A. & KHOSHNEVISZADEH, M. (2019). Multiplex touchdown PCR assay to enhance specificity and sensitivity for concurrent detection of four foodborne pathogens in raw milk. *Journal of Applied Microbiology*. 127(1). p. 262–273.

MOORHEAD, S.M. & DYKES, G.A. (2004). Influence of the sigB gene on the cold stress survival and subsequent recovery of two Listeria monocytogenes serotypes. *International Journal of Food Microbiology*. 91(1). p. 63–72.

MOREIRA, G., MOREIRA, C., DA CUNHA, C.E.P., MENDONÇA, M. & CONCEIÇÃO, F.R. (2016). Recombinant Botulinum Toxoids: A Practical Guide for Production. In *Methods in molecular biology (Clifton, N.J.)*. p. 621–632.

MOREIRA, G., FÜHNER, V. & HUST, M. (2018). Epitope Mapping by Phage Display. In *Methods in molecular biology (Clifton, N.J.)*. p. 497–518.

MOREIRA, G.M.S.G., FÜHNER, V. & HUST, M. (2018). *Epitope mapping by phage display*,

MORELAND, N.J., SUSANTO, P., LIM, E., TAY, M.Y.F., RAJAMANONMANI, R., HANSON, B.J. & VASUDEVAN, S.G. (2012). Phage display approaches for the isolation of monoclonal antibodies against dengue virus envelope domain III from human and mouse derived libraries. *International journal of molecular sciences*. 13(3). p. 2618–35.

MORTON, J., KAROONUTHAISIRI, N., CHARLERMROJ, R., STEWART, L.D., ELLIOTT, C.T. & GRANT, I.R. (2013). Phage display-derived binders able to distinguish Listeria monocytogenes from other Listeria species. *PloS one*. 8(9). p. E74312.

MURPHY, K.M., TRAVERS, P. & WALPORT, M. (2007). *Janeway's Immunobiology* 7th ed., New York and London: Gargland Science.

NANDURI, V., BHUNIA, A.K., TU, S.I., PAOLI, G.C. & BREWSTER, J.D. (2007). SPR biosensor for the detection of L. monocytogenes using phage-displayed antibody. *Biosensors and Bioelectronics*. 23(2). p. 248–252.

NGUYEN, X.-H., TRINH, T.-L., VU, T.-B.-H., LE, Q.-H. & TO, K.-A. (2018). Isolation of phage-display library-derived scFv antibody specific to *Listeria monocytogenes* by a novel immobilized method. *Journal of Applied Microbiology*. 124(2). p. 591–597.

DI NIRO, R., SULIC, A.M., MIGNONE, F., D'ANGELO, S., BORDONI, R., IACONO, M., MARZARI, R., GAIOTTO, T., LAVRIC, M., BRADBURY, A.R.M., BIANCONE, L., ZEVIN-SONKIN, D., DE BELLIS, G., SANTORO, C. & SBLATTERO, D. (2010). Rapid interactome profiling by massive sequencing. *Nucleic Acids Research*. 38(9). p. 1–10.

NIXON, A.E., SEXTON, D.J. & LADNER, R.C. (2014). Drugs derived from phage display

from candidate identification to clinical practice. *mAbs*. 6(1). p. 73–85.

NOORDHOUT, C.M. DE, DEVLEESSCHAUWER, B., ANGULO, F.J., HAAGSMA, J., KIRK, M., HAVELAAR, A. & SPEYBROECK, N. (2015). The global burden of listeriosis: a systematic review and meta- analysis. *Lancet Infectious Diseases*. 14(11). p. 1073–1082.

NÚÑEZ-MONTERO, K., LECLERCQ, A., MOURA, A., VALES, G., PERAZA, J., PIZARRO-CERDÁ, J. & LECUIT, M. (2018). Listeria costaricensis sp. nov. *International Journal of Systematic and Evolutionary Microbiology*. 68(3). p. 844–850.

OHK, S.H., KOO, O.K., SEN, T., YAMAMOTO, C.M. & BHUNIA, A.K. (2010). Antibody-aptamer functionalized fibre-optic biosensor for specific detection of Listeria monocytogenes from food. *Journal of Applied Microbiology*. 109(3). p. 808–817.

OPUNI, K.F.M., AL-MAJDOUB, M., YEFREMOVA, Y., EL-KASED, R.F., KOY, C. & GLOCKER, M.O. (2018). Mass spectrometric epitope mapping. *Mass Spectrometry Reviews*. 37(2). p. 229–241.

ORAVCOVÁ, K., TRNCÍKOVÁ, T., KUCHTA, T. & KACLÍKOVÁ, E. (2008). Limitation in the detection of Listeria monocytogenes in food in the presence of competing Listeria innocua. *Journal of applied microbiology*. 104(2). p. 429–37.

ORSI, R.H., DEN BAKKER, H.C. & WIEDMANN, M. (2011). Listeria monocytogenes lineages: Genomics, evolution, ecology, and phenotypic characteristics. *International journal of medical microbiology : IJMM*. 301(2). p. 79–96.

ORSI, R.H. & WIEDMANN, M. (2016). Characteristics and distribution of Listeria spp., including Listeria species newly described since 2009. *Applied Microbiology and Biotechnology*. 100. p. 5273–5287.

PANG, E., TIEN-LIN, C., SELVARAJ, M., CHANG, J. & KWANG, J. (2011). Deletion of the aceEgene (encoding a component of pyruvate dehydrogenase) attenuates Salmonella enterica serovar Enteritidis. *FEMS Immunology and Medical Microbiology*. 63(1). p. 108–118.

PAOLI, G.C., CHEN, C.Y. & BREWSTER, J.D. (2004). Single-chain Fv antibody with specificity for Listeria monocytogenes. *Journal of Immunological Methods*. 289(1–2). p. 147–155.

PASCHKE, M. & HÖHNE, W. (2005). A twin-arginine translocation (Tat)-mediated phage display system. *Gene*. 350(1). p. 79–88.

PATEL, M.S., NEMERIA, N.S. & FUREY, W. (2014). The Pyruvate Dehydrogenase Complexes: Structure-based Function and Regulation. *The Journal of Biological Chemistry*. 289(24). p. 16615–16623.

PIZARRO-CERDÁ, J. & COSSART, P. (2018). Listeria monocytogenes: cell biology of invasion and intracellular growth. *Microbiology Spectrum*. 6(6). p. 1–16.

PIZARRO-CERDÁ, J., KÜHBACHER, A. & COSSART, P. (2012). Entry of listeria monocytogenes in mammalian epithelial cells: An updated view. *Cold Spring Harbor Perspectives in Medicine*. 2(11).

PONSEL, D., NEUGEBAUER, J., LADETZKI-BAEHS, K. & TISSOT, K. (2011). High affinity, developability and functional size: the holy grail of combinatorial antibody library

generation. *Molecules (Basel, Switzerland)*. 16(5). p. 3675–700.

QUEREDA, J.J., GARCÍA-DEL PORTILLO, F. & PUCCIARELLI, M.G. (2016). Listeria monocytogenes remodels the cell surface in the blood-stage. *Environmental Microbiology Reports*. 8(5). p. 641–648.

RAHMAN, K.S., CHOWDHURY, E.U., SACHSE, K. & KALTENBOECK, B. (2016). Inadequate Reference Datasets Biased toward Short Non-epitopes Confound B-cell Epitope Prediction. *The Journal of biological chemistry*. 291(28). p. 14585–99.

RAMLI, S.R., MOREIRA, G.M.S.G., ZANTOW, J., GORIS, M.G.A., NGUYEN, V.K., NOVOSELOVA, N., PESSLER, F. & HUST, M. (2019). Discovery of Leptospira spp. seroreactive peptides using ORFeome phage display J. Coburn (ed.). *PLOS Neglected Tropical Diseases*. 13(1). p. E0007131.

RAMNATH, M., RECHINGER, K.B., JÄNSCH, L., HASTINGS, J.W., KNØCHEL, S. & GRAVESEN, A. (2003). Development of a Listeria monocytogenes EGDe partial proteome reference map and comparison with the protein profiles of food isolates. *Applied and environmental microbiology*. 69(6). p. 3368–76.

RANGNOI, K., JARUSERANEE, N., O'KENNEDY, R., PANSRI, P. & YAMABHAI, M. (2011). One-step detection of aflatoxin-B 1 using scFv-alkaline phosphatase-fusion selected from human phage display antibody library. *Molecular Biotechnology*. 49(3). p. 240–249.

ROJAS, G., CARMENATE, T., SANTO-TOMÁS, J.F., VALIENTE, P.A., BECKER, M., PÉREZ-RIVERÓN, A., TUNDIDOR, Y., ORTIZ, Y., FERNANDEZ DE COSSIO-DIAZ, J., GRAÇA, L., DÜBEL, S. & LEÓN, K. (2019). Directed evolution of super-secreted variants from phage-displayed human Interleukin-2. *Scientific Reports*. 9(1). p. 1–13.

ROJAS, G., TUNDIDOR, Y. & INFANTE, Y.C. (2014). High throughput functional epitope mapping: Revisiting phage display platform to scan target antigen surface. *mAbs*. 6(6). p. 1368–1378.

RONDOT, S., KOCH, J., BREITLING, F. & DÜBEL, S. (2001). A helper phage to improve single-chain antibody presentation in phage display. *Nature biotechnology*. 19(1). p. 75–78.

RUSSO, G., MEIER, D., HELMSING, S., WENZEL, E., OBERLE, F., FRENZEL, A. & HUST, M. (2018). Parallelized Antibody Selection in Microtiter Plates. *Methods in molecular biology (Clifton, N.J.)*. 1701. p. 273–284.

SCHIRRMANN, T., MEYER, T., SCHÜTTE, M., FRENZEL, A. & HUST, M. (2011). Phage display for the generation of antibodies for proteome research, diagnostics and therapy. *Molecules (Basel, Switzerland)*. 16(1). p. 412–26.

SCHIRWITZ, C., LOEFFLER, F.F., FELGENHAUER, T., STADLER, V., BREITLING, F. & BISCHOFF, F.R. (2012). Sensing Immune Responses with Customized Peptide Microarrays. *Biointerphases*. 7(1). p. 47.

SCHROEDER, H.W., CAVACINI, L. & CAVACINI, L. (2010). Structure and function of immunoglobulins. *The Journal of allergy and clinical immunology*. 125(2 Suppl 2). p. S41-52.

SEELIGER, H.P.R., ROCOURT, J., SCHRETTENBRUNNER, A., GRIMONT, P.A.D. & JONES, D. (1984). Listeria ivanovii sp. nov. *International Journal of Systematic Bacteriology*.

34(3). p. 336–337.

SHAMS, F., OLDFIELD, N.J., WOOLDRIDGE, K.G. & TURNER, D.P.J. (2014). Fructose-1,6-bisphosphate aldolase (FBA)-A conserved glycolytic enzyme with virulence functions in bacteria: “Ill met by moonlight.” *Biochemical Society Transactions*. 42(6). p. 1792–1795.

SHI, L., WU, F., WEN, Y., ZHAO, F., XIANG, J. & MA, L. (2015). A novel method to detect Listeria monocytogenes via superparamagnetic lateral flow immunoassay. *Analytical and Bioanalytical Chemistry*. 407(2). p. 529–535.

SHI, L., WU, F., WEN, Y., ZHAO, F., XIANG, J. & MA, L. (2014). A novel method to detect Listeria monocytogenes via superparamagnetic lateral flow immunoassay. *Analytical and Bioanalytical Chemistry*. 407(2). p. 529–535.

SINGH, V.K., SIROBHUSHANAM, S., RING, R.P., SINGH, S., GATTO, C. & WILKINSON, B.J. (2018). Roles of pyruvate dehydrogenase and branched-chain α-keto acid dehydrogenase in branched-chain membrane fatty acid levels and associated functions in Staphylococcus aureus. *Journal of Medical Microbiology*. 67(4). p. 570–578.

SKERRA, A. & PLUCKTHUN, A. (1988). Assembly of a functional immunoglobulin Fv fragment in Escherichia coli. *Science*. 240(4855). p. 1038–1041.

SMITH, G.P. (1985). Filamentous fusion phage: novel expression vectors that display cloned antigens on the virion surface. *Science (New York, N.Y.)*. 228(4705). p. 1315–7.

SOLTES, G., HUST, M., NG, K.K.Y., BANSAL, A., FIELD, J., STEWART, D.I.H., DÜBEL, S., CHA, S. & WIERSMA, E.J. (2007). On the influence of vector design on antibody phage display. *Journal of biotechnology*. 127(4). p. 626–37.

SOON LIM, T. & KHIM CHAN, S. (2017). Immune Antibody Libraries: Manipulating The Diverse Immune Repertoire for Antibody Discovery. *Current Pharmaceutical Design*. 22(43). p. 6480–6489.

STROHL, W.R. (2018). Current progress in innovative engineered antibodies. *Protein & cell*. 9(1). p. 86–120.

SUN, J., XU, T., WANG, S., LI, G., WU, D. & CAO, Z. (2011). Does difference exist between epitope and non-epitope residues? Analysis of the physicochemical and structural properties on conformational epitopes from B-cell protein antigens. *Immunome Research*. 7(3). p. 1–11.

SUN, Z., FU, P., WEI, K., ZHANG, H., ZHANG, Y., XU, J., JIANG, F., LIU, X., XU, W. & WU, W. (2014). Identification of novel immunogenic proteins from Mycoplasma bovis and establishment of an indirect ELISA based on recombinant E1 beta subunit of the pyruvate dehydrogenase complex. *PLoS ONE*. 9(2).

SUNDELL, G.N. & IVARSSON, Y. (2014). Interaction Analysis through Proteomic Phage Display. *BioMed Research International*. 2014.

TULLY, E., HEARTY, S., LEONARD, P. & O’KENNEDY, R. (2006). The development of rapid fluorescence-based immunoassays, using quantum dot-labelled antibodies for the detection of Listeria monocytogenes cell surface proteins. *International Journal of Biological Macromolecules*. 39(1–3). p. 127–134.

VAUGHAN, T.J., WILLIAMS, A.J., PRITCHARD, K., OSBOURN, J.K., POPE, A.R., EARNSHAW, J.C., MCCAFFERTY, J., HODITS, R.A., WILTON, J. & JOHNSON, K.S. (1996). Human Antibodies with Sub-nanomolar Affinities Isolated from a Large Non-immunized Phage Display Library. *Nature Biotechnology*. 14(3). p. 309–314.

VERNET, T., CHOULIER, L., NOMINÉ, Y., BELLARD, L., BALTZINGER, M., TRAVÉ, G. & ALTSCHUH, D. (2015). Spot peptide arrays and SPR measurements: throughput and quantification in antibody selectivity studies. *Journal of Molecular Recognition*. 28(10). p. 635–644.

WANG, G., XIA, Y., CUI, J., GU, Z., SONG, Y., CHEN, Y.Q., CHEN, H., ZHANG, H. & CHEN, W. (2014). The Roles of Moonlighting Proteins in Bacteria. *Current issues in molecular biology*. 16. p. 15–22.

YU, K.-Y., NOH, Y., CHUNG, M., PARK, H.-J., LEE, N., YOUN, M., JUNG, B.Y. & YOUN, B.-S. (2004). Use of monoclonal antibodies that recognize p60 for identification of Listeria monocytogenes. *Clinical and diagnostic laboratory immunology*. 11(3). p. 446–51.

ZANTOW, J., JUST, S., LAGKOUVARDOS, I., KISLING, S., DÜBEL, S., LEPAGE, P., CLAVEL, T. & HUST, M. (2016). Mining gut microbiome oligopeptides by functional metaproteome display. *Scientific Reports*. 6(1). p. 34337.

ZANTOW, J., MOREIRA, G.M.S.G., DÜBEL, S. & HUST, M. (2018). ORFeome Phage Display. In *Methods in molecular biology (Clifton, N.J.)*. p. 477–495.

ZHANG, F., CHEN, Y., KE, Y., ZHANG, L., ZHANG, B., YANG, L., ZHU, J., ZHANG, F., CHEN, Y., KE, Y., ZHANG, L., ZHANG, B., YANG, L. & ZHU, J. (2019). Single Chain Fragment Variable (scFv) Antibodies Targeting the Spike Protein of Porcine Epidemic Diarrhea Virus Provide Protection against Viral Infection in Piglets. *Viruses*. 11(1). p. 58.

ZHANG, H., CUI, W. & GROSS, M.L. (2014). Mass spectrometry for the biophysical characterization of therapeutic monoclonal antibodies. *FEBS Letters*. 588(2). p. 308–317.

ZHANG, Q., FENG, Y., DENG, L., FENG, F., WANG, L., ZHOU, Q. & LUO, Q. (2011). SigB plays a major role in Listeria monocytogenes tolerance to bile stress. *International Journal of Food Microbiology*. 145(1). p. 238–243.

8 CURRICULUM VITAE

Personal information

Name	**Gustavo Marçal Schmidt Garcia Moreira**
E-mail	moreira.gmsg@gmail.com
Date of birth	21/10/1991
Place of birth	Pelotas – RS, Brazil

Education

Since 2015	PhD in Antibody Engineering and Phage Display.
	Technische Universität Braunschweig, Institute for Biotechnology, Braunschweig, Germany
	Project: Use of phage display for the identification of novel biomarkers and generation of recombinant antibodies for *Listeria* spp. detection
	Supervisor: Prof. Dr. Michael Hust
2013 – 2015	Master of Science in Biotechnology.
	Universidade Federal de Pelotas, UFPel, Pelotas, Brazil
	Thesis: Test of a recombinant trivalent vaccine against *Clostridium perfringens* in ruminants
	Supervisor: Prof. Dr. Fabricio Rochedo Conceição
2009 – 2012	Bachelor Degree in Biotechnology.
	Universidade Federal de Pelotas, UFPel, Pelotas, Brazil
	Thesis: Characterization of recombinant proteins and monoclonal antibodies for the development of vaccines and diagnostic tests
	Supervisor: Prof. Dr. Fabricio Rochedo Conceição
2006 – 2008	High School.
	Colégio São José – Pelotas (CSJ-Pel), Brazil
1998 – 2005	Elementary School.
	Colégio São José – Pelotas (CSJ-Pel), Brazil

International and event experiences

Apr/2014 – Jun/2014	Guest Master Student at Purdue University, IN, USA.
	Activity: Production of recombinant proteins and use of different methods for microbiological characterization of *Listeria* spp.

Supervisor: Prof. Dr. Arun K. Bhunia

Feb/2017 Guest PhD Researcher at Queen's University Belfast, UK.

Activity: Test of recombinant antibodies against environment and food isolates of *Listeria* spp. for the development of an ELISA detection.

Supervisor: Prof. Dr. Linda Stewart

Jun/2016 Speaker at "The TB Congress 2016" (London, UK)

Presentation: A vaccine pipeline: phage display for identification of vaccine candidates, and generation of human antibodies for diagnostic and therapy.

Oct/2017 Speaker at "National Symposium on Zoonoses Research 2017" (Berlin, Germany)

Presentation: Identification of biomarkers of zoonotic pathogens by ORFeome phage display.

Nov/2017 Speaker at "Vaccines R&D 2017" (Washington D.C., USA).

Presentation: A vaccine pipeline: phage display for identification of vaccine candidates, and generation of human antibodies for diagnostic and therapy.

Language skills

Portuguese native speaker

English fluent

Spanish good listening, speaking, and writing

German good listening, average speaking and writing

Publications

Ramli, R.S., **Moreira, G.M.S.G.**, Zantow, J., Goris, M.G.A., Nguyen, V.K., Novoselova, N., Pessler, F. and Hust, M. (2019). Discovery of Leptospira spp. seroreactive peptides using ORFeome Phage Display. PLOS Neglected Tropical Diseases 13:e0007131

Fühner, V., Heine, P.A., Zilkens, K., Meier, D., Roth, K.D.R., **Moreira, G.M.S.G.**, Hust, M. and Russo, G. (2019). Epitope Mapping via Phage Display from single gene libraries. Methods Molecular Biology 1904: 353-375

Moreira, G. & Dübel, S. (2018) Recombinant Antibodies and Phage Display. In: An Introduction to Molecular Biotechnology, 3rd ed., Ed.: Wink, M. Wiley-VCH, in press

Moreira, G.M.S.G., Fühner, V. and Hust, M. (2018). Epitope Mapping by Phage Display. Phage display, Ed: Lim, T.S. and Hust, M., Methods Molecular Biology 1701: 497-518

Zantow, J., **Moreira, G.M.S.G.**, Dübel, S. and Hust, M. (2018). ORFeome Phage Display. Phage display, Ed: Lim, T.S. and Hust, M., Methods Molecular Biology 1701: 477-495

Silveira, MM, Conceição, FR, Mendonça, M, Cunha, CE, **Moreira, GM**, Conrad, N, Oliveira, PD, Hartwig, D, de Leon, P, Moreira, AN. (2016). Saccharomyces boulardii improves humoral immune response to DNA vaccines against leptospirosis. 66(2):184-190 Journal of Medical Microbiology

Ferreira, MR, **Moreira, GM**, Cunha, CE, Mendonça, M, Salvarani, FM, Moreira, AN, Conceição, FR. (2016). Recombinant Alpha, Beta, and Epsilon Toxins of Clostridium perfringens: Production Strategies and Applications as Veterinary Vaccines. 21;8(11) Toxins

Klafke, GB, **Moreira, GM**, Pereira, JL, Oliveira, PD, Conceição, FR, Lund, RG, Grassmann, AA, Dellagostin, OA, Pinto, LS. (2016). Lectin I from Bauhinia variegata (BVL-I) expressed by Pichia pastoris inhibits initial adhesion of oral bacteria in vitro. 93(Pt A):913-918 International Journal of Biological Macromolecules

Mendonça M, **Moreira, GM**, Conceição, FR, Hust, M, Mendonça, KS, Moreira, AN, França, RC, Silva, WP, Bhunia, AK, Aleixo, JA. (2016). Fructose 1,6-bisphosphate aldolase, a novel immunogenic surface protein on Listeria species. 11(8):e0160544 PLoS One

Moreira Jr., C, Cunha CE, **Moreira, GM**, Mendonça, M, Salvarani, FM, Moreira, AN, Conceição, FR. (2016). Protective potential of recombinant non-purified botulinum neurotoxins serotypes C and D. 40:58-62 Anaerobe

Kuhn, P, Fühner, V, Unkauf, T, **Moreira, GM**, Frenzel, A, Miethe, S and Hust, M. (2016). Recombinant Antibodies for Diagnostics and Therapy against Pathogens and Toxins generated by Phage Display. 10(9-10):922-948 Proteomics - Clinical Applications

Moreira GM, Moreira Jr. C, Cunha CE, Mendonça M, Conceição FR. (2016). Recombinant botulinum toxoids: a practical guide for production. 1404:621-32 Methods in Molecular Biology

Moreira GM, Salvarani FM, Cunha CE, Mendonça M, Moreira AN, Gonçalves LA, Pires PS, Lobato FC, Conceição FR. (2016). Immunogenicity of a trivalent recombinant vaccine against Clostridium perfringens alpha, beta, and epsilon toxins in farm ruminants. 6:22816 Scientific Reports

Moreira GM, Telmo P de L, Mendonça M, Moreira AN, McBride AJ, Scaini CJ, Conceição FR. (2014). Human toxocariasis: current advances in diagnostics, treatment, and interventions. 30(9):456-64 Trends in Parasitology

Moreira GM, Cunha CE, Salvarani FM, Gonçalves LA, Pires PS, Conceição FR, Lobato FC. (2014). Production of recombinant botulism antigens: a review of expression systems. 28:130-6 Anaerobe

Cunha CE, **Moreira GM**, Salvarani FM, Neves MS, Lobato FC, Dellagostin OA, Conceição FR. (2014). Vaccination of cattle with a recombinant bivalent toxoid against botulism serotypes C and D. 32(2):214-6 Vaccine

Moreira GM, Conceição FR, McBride AJ, Pinto L da S. (2013) Structure predictions of two Bauhinia variegata lectins reveal patterns of C-terminal properties in single chain legume lectins. 8(11):e81338 PLoS One

Gil LA, da Cunha CE, **Moreira GM**, Salvarani FM, Assis RA, Lobato FC, Mendonça M, Dellagostin OA, Conceição FR. (2013) Production and evaluation of a recombinant chimeric vaccine against clostridium botulinum neurotoxin types C and D. 8(7):e69692 PLoS One

Salvarani FM, Conceição FR, Cunha CE, **Moreira GM**, Pires PS, Silva RO, Alves GG, Lobato FC. (2013) Vaccination with recombinant Clostridium perfringens toxoids α and β promotes elevated antepartum and passive humoral immunity in swine. 31(38):4152-5 Vaccine

Klafke GB, **Moreira GM**, Monte LG, Pereira JL, Brandolt TM, Xavier MO, Santi-Gadelha T, Dellagostin OA, Pinto L da S. Assessment of plant lectin antifungal potential against yeasts of major importance in medical mycology. 175(1-2):147-51 Mycopathologia

Patents

"Simplified production process of recombinant vaccines for veterinary botulism control, and obtained vaccines". Registration number: BR1020150134908. INPI - Instituto Nacional da Propriedade Industrial, Brazil.

"Simplified production process of recombinant veterinary vaccines against Clostridium perfringens toxins alpha, beta, and epsilon, and obtained vaccines". Registration number: BR1020170115607. INPI - Instituto Nacional da Propriedade Industrial, Brazil.